AD-A052 937 AIR FORCE INST OF TECH WRIGHT-PATTERSON AFB OHIO SCH--ETC F/G 17/5
MULTICHANNEL INFRARED RECEIVER PERFORMANCE.(U)
DEC 77 S J DUNNING

UNCLASSIFIED AFIT/GE/EE/77-15 NL

1 OF 2
AD A052937

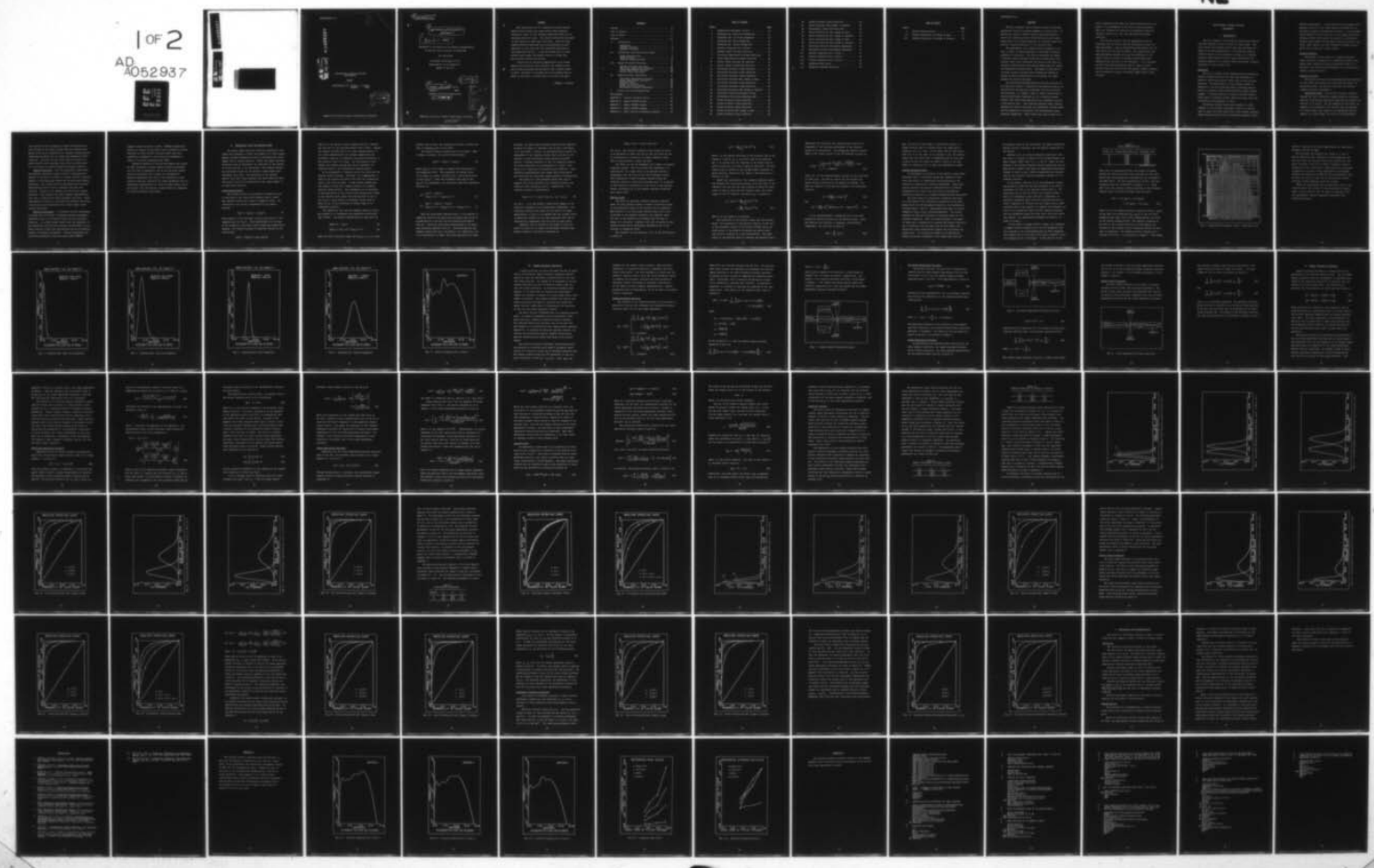

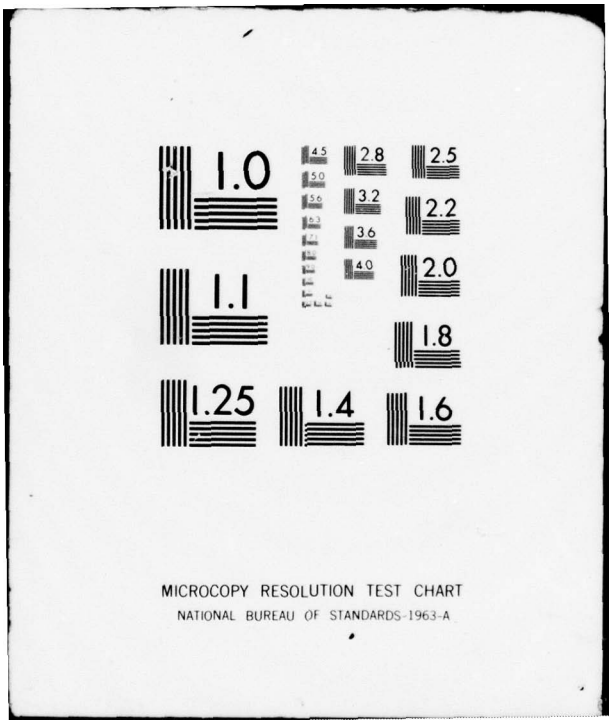
1.0
1.1
1.25
1.4
1.6
1.8
2.0
2.2
2.5
2.8
3.2
3.6
4.0
4.5
5.0
5.6
MICROCOPY RESOLUTION TEST CHART
NATIONAL BUREAU OF STANDARDS-1963-A

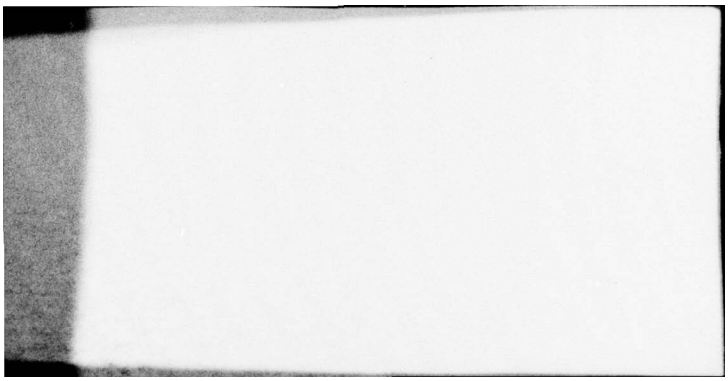

AFIT/GE/EE/77-15

(1)

MULTICHANNEL INFRARED RECEIVER PERFORMANCE

THESIS

AFIT/GE/EE/77-15 Stephen J. Dunning
Captain USAF

Approved for public release; distribution unlimited

(14) AFIT/GE/EE/77-15

(6) MULTICHANNEL INFRARED RECEIVER PERFORMANCE •

(9) Master's THESIS

Presented to the Faculty of the School of Engineering

of the Air Force Institute of Technology

Air University

in Partial Fulfillment of the

Requirements for the Degree of

Master of Science

(12) 111 p.

by

(10) Stephen J. Dunning B.S.E.E.

Captain USAF

Graduate Electrical Engineering

(11) December 1977

14 73

Approved for public release; distribution unlimited

012225

B

Preface

This thesis grew out of a study done by AFIT faculty members Stan Robinson and Jurgen Gobien which proposed a statistical model for the infrared background field and the resulting detector output. The receiver structures developed in this thesis are based upon this model. There are many complex problems associated with the performance problem addressed by this study and time constaints prevented me from examining them all. I hope this study will at least provide some insight and possibly serve as a base from which further studies can develop.

I would like to express my appreciation to my thesis advisor and instructor, Stan Robinson, who taught me more about random processes and statistics than I really wanted to know. Although I've learned alot in my studies here at AFIT, at this point I am glad that it is now in the past.

Stephen J. Dunning

Contents

List of Figures

List of Tables

Abstract

The use of passive electro-optical sensors in military systems has received increased emphasis in recent years. In particular, passive infrared sensors could potentially be used in an infrared airborne threat warning receiver which would detect the infrared signature of a hostile threat and provide a warning indication to the aircraft crew.

The performance of an optical receiver designed to detect a target by taking advantage of the target's spectral signature is presented. The receiver processes the signal in several narrow frequency bands and is based upon a statistical model which represents the field in each band as a Gaussian random process whose moments depend upon the target and background characteristics. The signal is detected by an array of power detectors whose outputs are modeled as random variables characterized by non-central chi square probability density functions.

The optimal Bayes/Neyman-Pearson receiver structure for an M spectral channel, N sequential look scanning receiver is presented and two practical suboptimal receiver structures are developed. An attempt is made to obtain closed form analytical performance expressions, but it quickly becomes evident that closed form expressions are obtainable only for a few special cases. Thus numerical methods using a digital computer are used to calculate the probability of false alarm and the probability of detection for each processor using identical parameters. These results are used to plot a re-

ceiver operating curve (ROC) for each processor and are compared to the performance of two ad-hoc linear processors. ROC's are obtained for variations in parameters (mean and variance) and for one, two, and three spectral channel receivers.

The results indicate that the approximate receiver structures and the ad-hoc receiver structures all have the same performance. This is demonstrated analytically for the case where only the mean is varied. The results also show that performance depends only upon the difference in the square roots of the mean to variance ratios under each hypothesis and the ratio of the variances. It is concluded by this study that performance equal to that of either receiver structure derived from the general optimal processor can be obtained by using a relatively simple ad-hoc linear receiver.

MULTICHANNEL INFRARED RECEIVER PERFORMANCE

I. Introduction

The use of passive electro-optical sensors has received increased emphasis by the Air Force in recent years. Passive optical and infrared sensors have been developed for a number of military applications. In particular, passive infrared sensors could potentially be used in an infrared airborne threat warning receiver which would detect the infrared signature of a hostile threat and provide a warning indication to the aircraft crew.

Background

The use of airborne threat warning receivers employing scanned infrared detectors has often been proposed as a method of detecting airborne threats such as anti-aircraft missiles. The practicality of such scanning systems is supported by the well developed sensor technology aquired during the Forward Looking Infrared Receiver (FLIR) system program. A warning receiver on board an aircraft ideally would detect a launched airborne threat and cause some form of defensive countermeasure to occur.

As avionics systems become more automatic in their response to the aircraft environment, there is a obvious need to reduce the false alarm rate of any eventual airborne threat warning receiver while maintaining acceptable threat

detection performance. A large number of false alarms would generate distrust in the human operator and would also unnecessarily expend countermeasure resources. A well designed threat warning receiver would have to use signal processing techniques which would enable the receiver to distinguish between valid targets and phenomenon such as sun glint, open fires, smoke stacks, and other non-hostile thermal sources which could contribute to false alarms.

Problem Statement

The purpose of this thesis is to apply statistical signal detection techniques to a statistical infrared background model proposed by Gobien and Robinson (Ref 11) to determine the structure and performance of an optimal multichannel infrared receiver.

Approach and Scope

The receiver structure and performance problem addressed by this thesis was divided into three distinct areas; the statistical model, the receiver structure, and receiver (signal processor) performance.

Statistical Model. Any receiver structure obtained through the use of statistical signal detection techniques requires a statistical model which describes the signals the receiver is to detect. For the purposes of this study, the signals to be processed by the receiver were the presence of a valid target (the target or one hypothesis) and the absence of a valid target (the null or zero hypothesis).

The statistical model proposed by Gobien and Robinson and used throughout this thesis states that the infrared background field may be represented by a Gaussian random process whose moments depend upon the target and background characteristics. The model further states that the output of a power detector that intercepts this field is characterized by a non-central chi-square probability density function.

Receiver Structure. Once the statistical signal model was assumed, statistical signal detection techniques were applied to the model to arrive at a binary receiver structure capable of distinguishing between the two previously defined hypotheses. The likelihood ratio was formed and an optimal Bayes/Neyman-Pearson receiver processor structure was obtained. Because of the complex structure of the optimal processor, large argument and small argument approximations were used to simplify the signal processor structure. These approximations resulted in two practical processor structures, a non-linear receiver processor and a small signal linear receiver processor.

Receiver Performance. To determine receiver performance, an attempt was first made to determine analytic performance expressions such as the Chernoff bound for each processor structure. It quickly became evident that the complexity of the mathematics involved would prevent the derivation of any useful analytic results and necessitated the use of numerical methods to determine performance. Receiver performance was calculated numerically using the Control Data CYBER-74

computer system available to AFIT. FORTRAN programs were written to compute the processor output probability density functions for each receiver structure which were then numerically integrated to yield receiver performance in terms of a receiver operating curve (ROC).

Numerical analysis of receiver performance was limited by time constaints to single channel receiver performance for five sets of parameters, and to two and three channel receiver performance for a single set of parameters. Identical parameters were used in the evaluation of each receiver structure, and while the chosen parameters were not necessarily representative of those one might obtain from a real system, they did provide a common basis for comparison of receiver processor performance.

II. Statistical Field and Detector Model

The binary signal detection receivers presented in this thesis were designed to detect the presence of a valid target against infrared background clutter by processing the output signal from an optical detector. Before the signal processor structure could be determined, the statistics of the signals to be detected had to be ascertained. This chapter presents the statistical model for the detector output signal used throughout this study. The statistics of the observed optical field were first examined, and these statistics were then used to derive the statistics for the output signal of an ideal power detector.

Field Representation

The incident field to be detected at a position $\underline{r}$ can be described by the scalar field quantity $u(\underline{r},t)$, which may represent either the electric or magnetic field. For convenience, this field is represented by its complex envelope

$$U(\underline{r},t) = U_R(\underline{r},t) + jU_I(\underline{r},t) \tag{1}$$

where $U_R(\underline{r},t)$ is the real part of $U(\underline{r},t)$ and $U_I(\underline{r},t)$ is the imaginary part of $U(\underline{r},t)$. This representation is the same as the quadrature field model used in radar and communication systems. The complex envelope is implicitly defined by the relationship

$$u(\underline{r},t) = \mathrm{Re}\left[U(\underline{r},t)\ \exp(-j2\pi f_o t)\right] \tag{2}$$

where f_o is the optical center frequency and Re(·) denotes the real part of the enclosed quantity (Ref 3:1810). Because the complex envelope $U(\underline{r},t)$ is a time varying quantity, it is a valid representation for extremes ranging from the incoherent light due to naturally occurring illumination, to the coherent output of a laser. For the purpose of this thesis, the complex envelope was used to represent the received fields in the intermediate infrared region.

It is unreasonable to assume a priori the field that the detector would intercept. Therefore, it is appropriate to think of the complex envelope of the field as a random process in both time and space. It was further assumed that the complex envelope was a sample function of a complex Gaussian random process. This assumption can be justified by the application of the central limit theorem (Ref 10:266) to the received field, where the received field is due to the sum of a large number of individual fields, each of which is due to the scattering of natural light by an independent particle.

For simplicity, the real and imaginary parts of $U(\underline{r},t)$ are assumed to be independent and identically distributed (Ref 3:1849). The complete specification is then given by

$$E\left[U(\underline{r},t)\right] = m(\underline{r},t) \tag{3}$$

$$E\left[U(\underline{r},t)\ U^*(\underline{r}',t')\right] = R(\underline{r},\underline{r}',t,t') \tag{4}$$

where the above conditions imply that $R(\underline{r},\underline{r}',t,t')$ is a real

function and is twice the correlation function of either the real or imaginary part of the field.

The optical detection problem can now be stated. When a target is present, the received field becomes

$$U(\underline{r},t) = U_s(\underline{r},t) + U_b(\underline{r},t) \tag{5}$$

where $U_s(\underline{r},t)$ is the signal or target field and $U_b(\underline{r},t)$ is the background field. This hypothesis is denoted by H_1. If no target is present, denoted by H_0 , the received field is only $U_b(\underline{r},t)$. Under the assumption that $U_s(\underline{r},t)$ and $U_b(\underline{r},t)$ are independent, the statistics under each hypothesis are given by

$$H_0: \quad \begin{aligned} m(\underline{r},t) &= m_b(\underline{r},t) \\ R(\underline{r},\underline{r}',t,t') &= R_b(\underline{r},\underline{r}',t,t') \end{aligned} \tag{6}$$

$$H_1: \quad \begin{aligned} m(\underline{r},t) &= m_s(\underline{r},t) + m_b(\underline{r},t) \\ R(\underline{r},\underline{r}',t,t') &= R_s(\underline{r},\underline{r}',t,t') + R_b(\underline{r},\underline{r}',t,t') \end{aligned} \tag{7}$$

With the field model described above, it is possible to completely describe the space-time processing that should be accomplished by a receiver and the resulting performance (Ref 13). There are three major disadvantages to the space-time processing approach (Ref 11). The processing and performance depend upon $m(\underline{r},t)$ and $R(\underline{r},\underline{r}',t,t')$ explicitly, and it is unreasonable to expect that these quantities are known.

Secondly, the space-time processing required would typically be much too complex to implement even if $m(\underline{r},t)$ and $R(\underline{r},\underline{r}', t,t')$ were known. Finally, the processing would require the measurement of the complex envelope $U(\underline{r},t)$ and this is not possible at most wavelengths using currently available devices. Although equations (6) and (7) completely specify the field statistics, the determination of $m(\underline{r},t)$ and $R(\underline{r},\underline{r}',t,t')$ explicitly is generally quite difficult. Thus, reasonable approximations were sought which would permit more practical and realizable signal processor configurations.

Two simple but crude parameters which were used to simplify the field statistics were coherence distance and coherence time, denoted D_c and T_c , respectively. The coherence distance is described by

$$R(\underline{r},\underline{r}',t,t\ ) = m(\underline{r},t)\ m(\underline{r}',t)\ ;\ |\underline{r} - \underline{r}'| > D_c \qquad (8)$$

for all t. It is the distance beyond which samples of the field are considered to be statistically independent. The resulting coherence cell model for the field is a simple approximation in which it is assumed that the incident field is spatially constant over an area (coherence cell) and is statistically independent from the field in other cells.

Coherence time is defined as the length of time over which the field can be broken into piecewise constant independent samples in time and is described by

$$R(\underline{r},\underline{r},t,t+T_c) = m(\underline{r},t)\, m(\underline{r},t+T_c) \qquad (9)$$

for all $\underline{r}$. The coherence time/cell model allows the field to be decimated in space and time so that the field can now be considered as a collection of random variables rather than a random process in space and time.

The field can also be separated into a number of disjoint frequency windows. Since the fields are considered to be uncorrelated, the output field in any spectral window is independent from the field in any other frequency window. This independence between frequency windows allows the coherence time/cell field model developed above to be applied to the statistical description of the field in each spectral window, differing only in the moments required to describe each output field.

Detector Model

Utilizing the piecewise constant coherence time/cell model for each spectral window, an array of detectors placed in the measurement plane of the receiver can be considered. Each detector is an ideal power detector whose active area is matched to the smallest coherence cell expected, where the size of the coherence cell depends upon the type of target to be detected. Coherence cell size in excess of that required would lead to performance degradation due to the increase in background noise.

The intensity or rate function, $\lambda(t)$, of the j^{th} detector is given by

$$\lambda_j(t) = \frac{\eta}{hf_o} \int_{A_j} |U(\underline{r},t)|^2 \, d\underline{r} \qquad (10)$$

where η is the quantum efficiency of the detector, hf_o is the energy of a photon, A_j is the active area of the detector, and it is assumed that the intensity of the scalar field in units of power per unit area is given by $|U(\underline{r},t)|^2$. The rate function may be defined as the average number (ensemble) of photo-electrons observed at the output of the detector as a function of time.

Within the constraints of the coherence time/cell model and assuming that the detector area A_j is on the order of the coherence cell and that the time interval in which the observation is made is less than the coherence time, the current output of the j^{th} detector, centered at $\underline{r}_j$, is given by

$$y_j = q\lambda_j(t) = \frac{q\eta}{hf_o} \int_{A_j} |U(\underline{r},t)|^2 \, d\underline{r}$$

$$\approx \frac{q\eta}{hf_o} |U(\underline{r}_j,t)|^2 A_j \qquad (11)$$

where q is the charge of an electron.

The statistics of the detector output can now be determined. The randomness of the detector output y_j is due only to the stochastic nature of the received fields, since the ideal nature of the detector eliminates any device noise that would be inherent in a real photodetector. The ideal nature of the detector serves to simplify the analysis and is

based upon the contention that detector noise need not be considered if the noiseless performance of the receiver proved to be unacceptable. The probability density function (pdf) of the output current of the j^{th} detector is given by

$$f_j(y_j) = \begin{cases} \frac{1}{2\sigma_j^2} \exp\left[-\frac{y_j + m_j}{2\sigma_j^2}\right] I_o\left[\frac{\sqrt{y_j\, m_j}}{\sigma_j^2}\right] ; & y_j \geq 0 \\ 0 \quad ; \text{ elsewhere} \end{cases} \tag{12}$$

where $I_o(\cdot)$ is the modified Bessel function of the first kind of order zero. This pdf is know as the non-central chi-square density function with two degrees of freedom. The mean and variance of this pdf are related to the field quantities by

$$m_j = 2\left[\frac{q\eta}{hf_o} A_j\, m(\underline{r}_j, t)\right]^2 \tag{13}$$

and

$$\sigma_j^2 = \left(\frac{q\eta}{hf_o} A_j\right)^2 \left[\tfrac{1}{2}R(\underline{r}_j, \underline{r}_j, t, t) - (m(\underline{r}_j, t))^2\right] \tag{14}$$

It is straightforward to extend Eq (12) to the joint probability density function for the detector array. Since the detectors are disjoint in frequency, and therefore independent, the joint pdf is given by

$$f(\underline{y}) = \prod_{j=1}^{M} f_j(y_j) \tag{15}$$

Eqs (12) and (15) also apply to the detector output of a single detector which is scanned across the image plane a coherence cell at a time. If the frame time for each coherence cell is on the order of the coherence time, the detector output for each frame time is independent and the joint pdf is given by Eq (15), where the index j refers to the time frame (or coherence cell) in which the measurement is made.

Infrared Background Data

To investigate the validity of the detector output model developed above, a literature search was conducted to discover any sources of experimental data pertaining to the statistical properties of infrared backgrounds. While many sources relating the spectral characteristics of infrared backgrounds were found, only two sources concerning the statistical properties of infrared backgrounds were discovered.

The first source of statistical information was found in a 1974 paper titled "Statistical Properties of the Background Noise for the Atmospheric Windows in the Intermediate Infrared Region" (Ref 4). Measurements were made of various background types using a scanning radiometer. The authors analyzed the data and developed a statistical model for the infrared background. While the model proposed in the paper is based upon a combination of Gaussian and Poisson statistics and is different from the model used in this thesis, the statistical data presented does support the non-central chi-square model. The distinctive shapes of the probability density functions illustrated in the report (Ref 4:28) are

all possible forms of the non-central chi square probability density function, dependent upon the specific parameters of the density.

Another source of infrared background statistical data was found in a series of reports by the Lockheed Missile and Space Company (LMSC) (Refs 5; 6; 7; and 8). Under the sponsorship of the Advanced Research Projects Agency and the U.S. Army Missile Command, LMSC began the Background Measurements Program in which natural infrared backgrounds were measured from the air using an infrared radiometer mounted in a U-2 research aircraft.

In one report, data for one of the measurement flights was analyzed by LMSC and the data presented in the form of histograms for each of six spectral filters (Ref 5). The characteristics of the six filters are listed in Table I. While the histograms contain data for a combination of different background types that were overflown by the aircraft, comparison of the data with the flight track by LMSC indicated that it was possible to separate the histograms for each of four background types from the combined histogram. The four background types were high cloud, low cloud, water, and terrain. The experimental histogram for filter 1 is shown in Figure 1.

If the number of sample points is large, the histogram or sample relative frequency plot for each background type will converge to the corresponding pdf for that background. The weighted sum of these pdf's will yield a cumulative relative frequency plot or histogram. To test the fit of the

Table I
Filter Characteristics

Filter No.	Center Wavelength (μm)	Bandwidth (μm)
1	4.50	0.202
6	4.48	0.157
5	4.45	0.124
4	4.44	0.097
3	4.42	0.074
2	4.41	0.055

(From Ref 5:1-1)

model with the experimental data, non-central chi-square probability density functions were generated for each background type using parameters estimated from the histogram in the LMSC report. The pdf's generated for filter 1 for each background type are illustrated in Figures 2 - 5. These pdf's were then linearly combined according to the following equation which was derived through trial and error:

$$f(x) = 0.08\, f_{HC}(x) + 0.14\, f_{LC}(x) + 0.26\, f_{W}(x) + 0.52\, f_{T}(x) \qquad (16)$$

where $f(x)$ is the combined relative frequency function, $f_{HC}(x)$ is the high cloud background pdf, $f_{LC}(x)$ is the low cloud background pdf, $f_{W}(x)$ is the water background pdf, and $f_{T}(x)$ is the terrain background pdf. The numerical constants in Eq (16) are the estimated fraction of total samples contributed to the combined relative frequency function by each type of background. The combined relative frequency plot obtained for filter 1 is illustrated in Figure 6. This sample

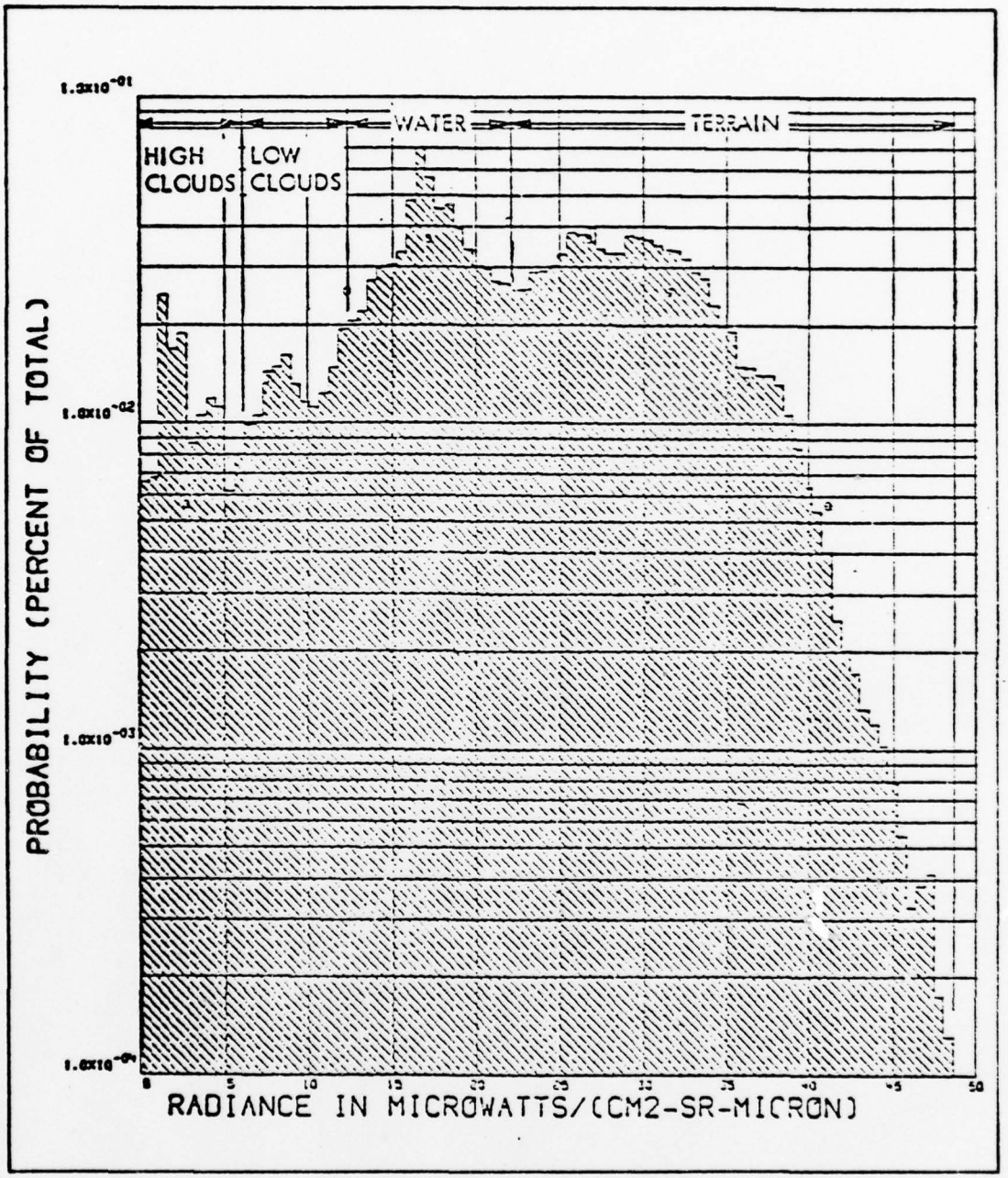

Fig. 1. Experimental Histogram, Filter 1 (From Ref 5:4-2)

relative frequency plot closely approximates the experimental histogram obtained by LMSC.

This procedure was repeated for filters 4, 5, and 6. Density parameters were estimated for each background type for each filter and the pdf's which were obtained were combined according to Eq (16) to obtain a cumulative relative frequency plot for each filter. These plots are illustrated in Appendix A and also closely approximate the histograms obtained experimentally by LMSC for the corresponding filter. The data for filters 2 and 3 was so uniform that reliable estimates of pdf parameters could not be made.

While the experimental data reviewed here does not conclusively prove the validity of the non-central chi-square model, it does indicate that the model is consistent with the experimental infrared background statistical data currently available.

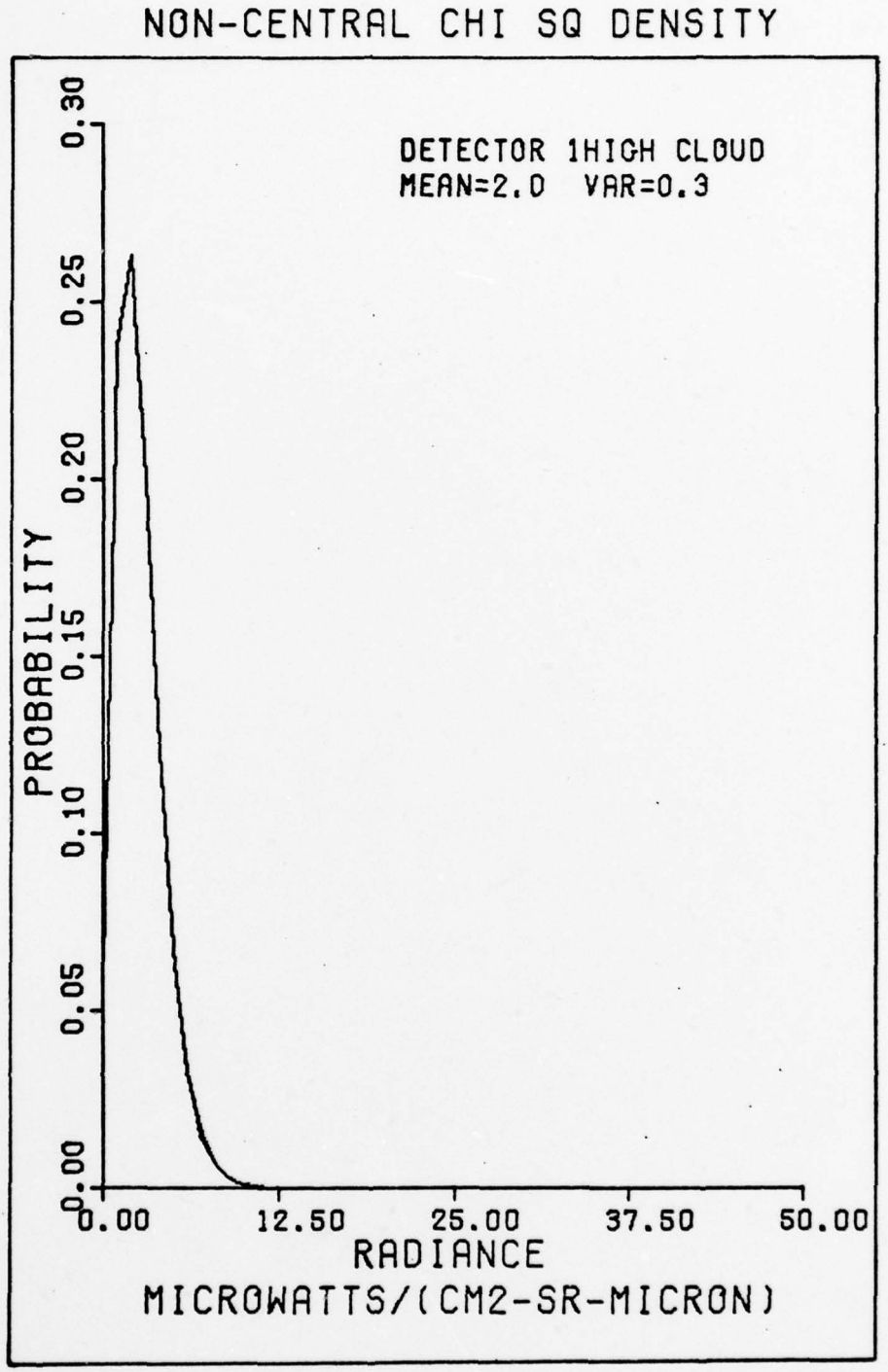

Fig. 2. Estimated pdf, High Cloud Background

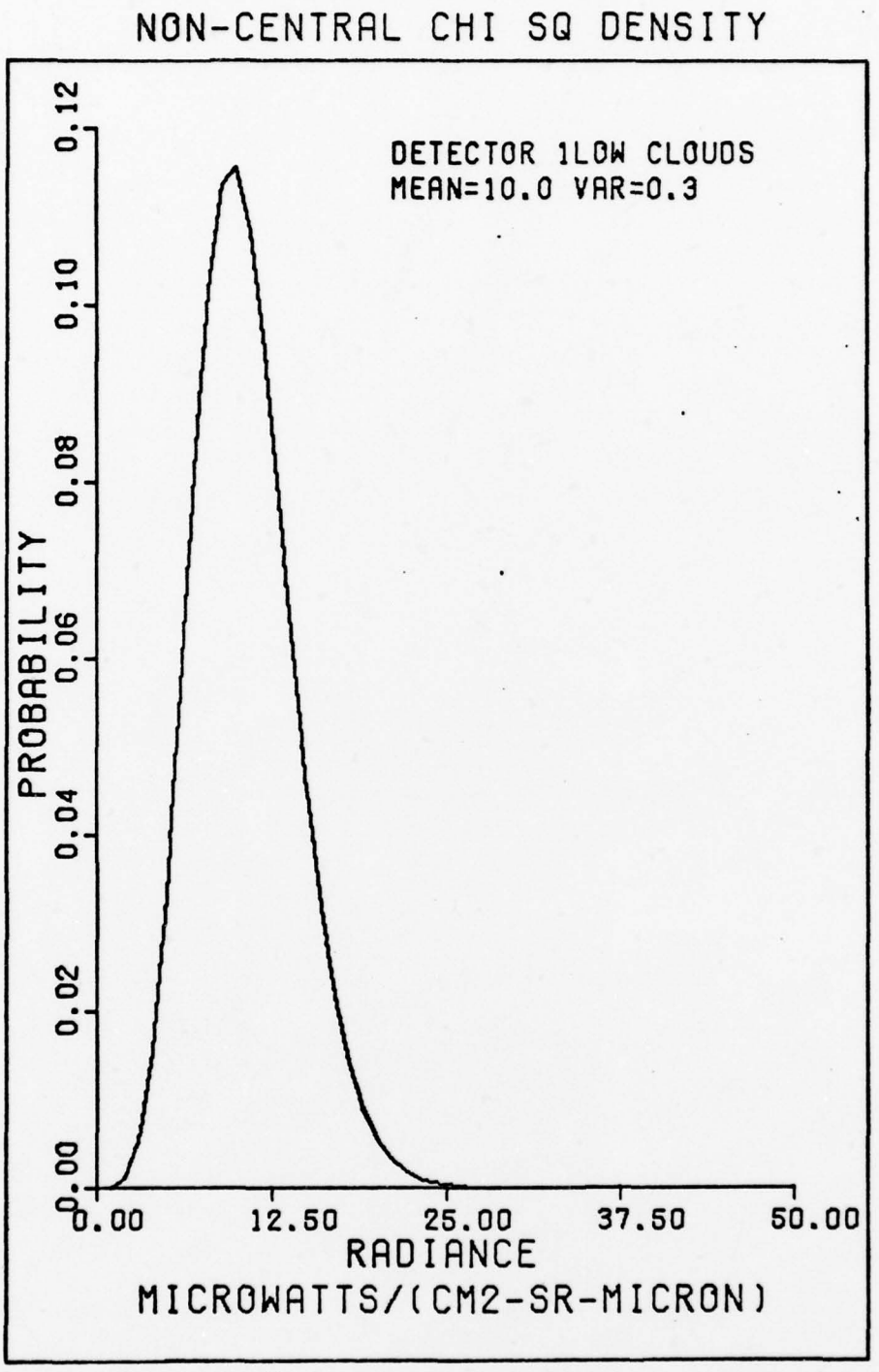

Fig. 3. Estimated pdf, Low Cloud Background

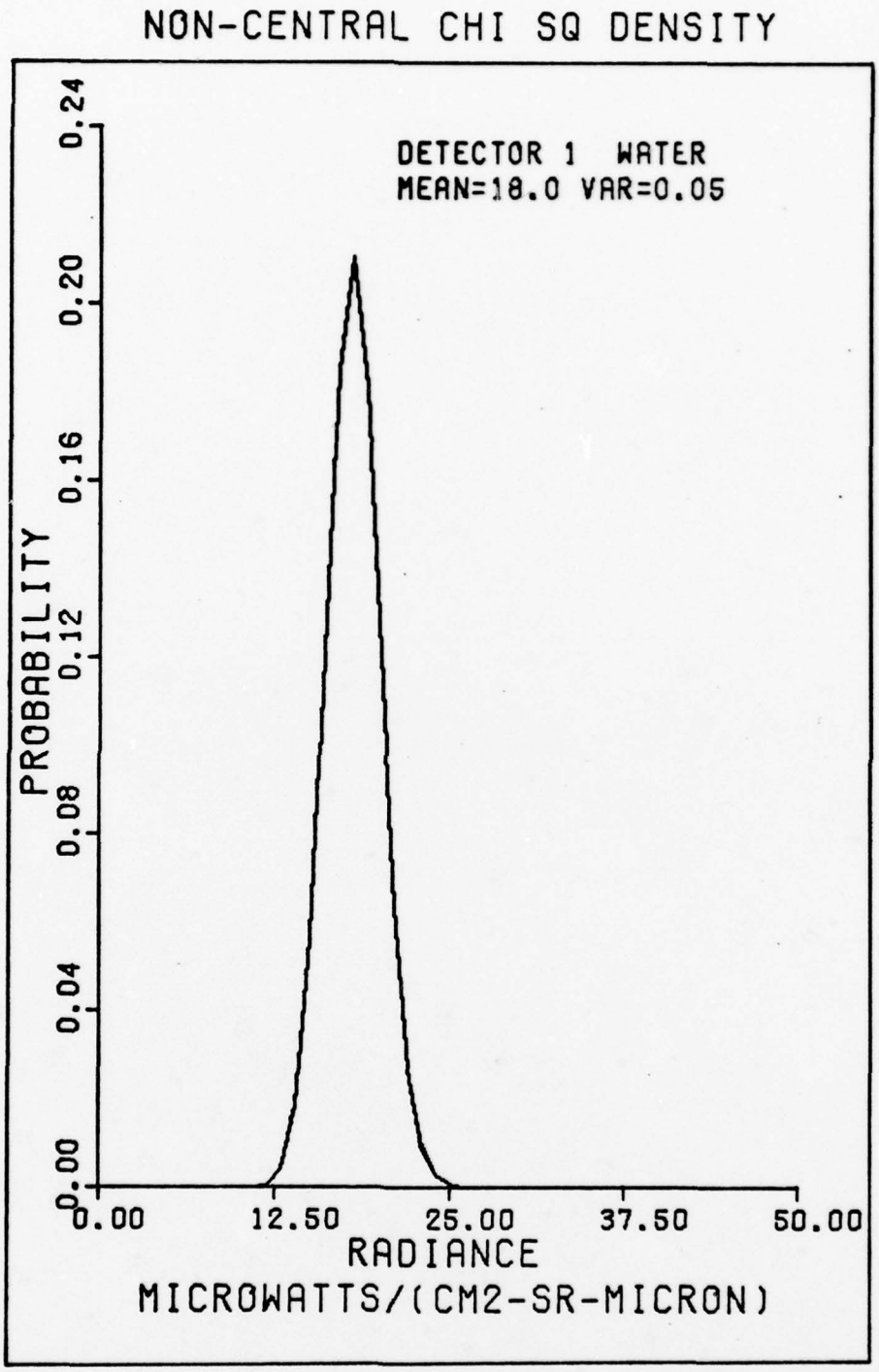

Fig. 4. Estimated pdf, Water Background

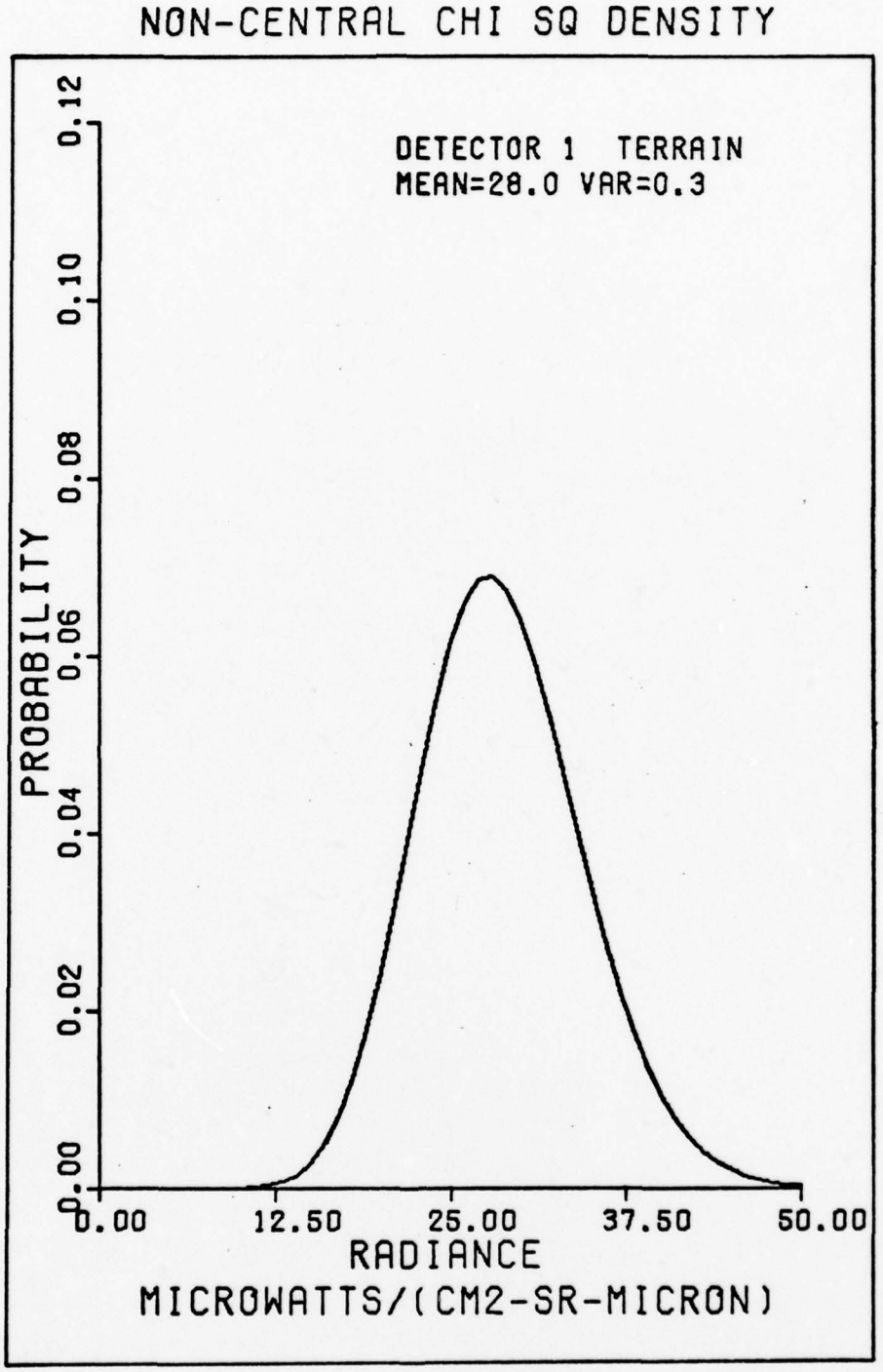

Fig. 5. Estimated pdf, Terrain Background

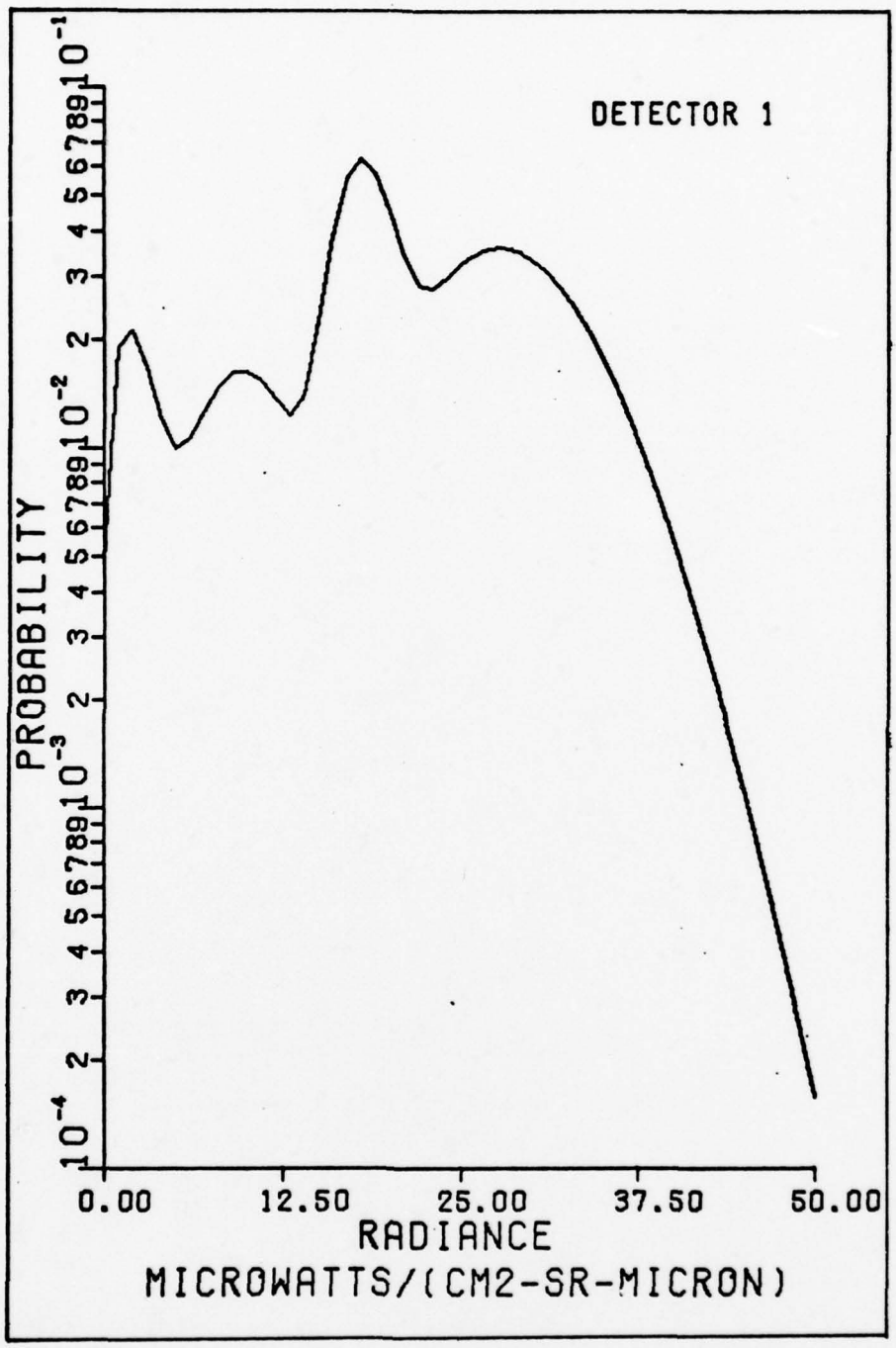

Fig. 6. Relative Frequency Plot, Filter 1

III. Signal Processor Structures

A signal processor structure developed through the application of statistical signal detection techniques depends explicitly upon the statistical characteristics of the signals being detected. The signals to be processed by the processors developed here are the detector outputs under the null and target hypotheses. By correctly processing these signals, it is hoped that the receiver will distinguish between the presence or absence of a valid target with a high degree of accuracy. This chapter presents the receiver processor structures developed by using the non-central chi-square detector output model to characterize the statistics of the null and target hypothesis signals.

The basic receiver considered here is a scanning receiver which , by means of narrowband filters and parallel ideal power detectors, observes M frequency disjoint channels. The reasoning behind this structure lies in the fact that most targets to be detected will have characteristic spectral signatures. By properly choosing the spectral channels, the receiver can discriminate against unwanted sources whose spectral characteristics differ from those of the desired target.

The receiver processor development and following analysis pertains to a receiver which makes N successive observations of M detector outputs for an arbitrary coherence cell. The channel outputs during the i^{th} observation of the cell would constitute a vector $\underline{y}_i = y_{i1}, y_{i2}, \ldots, y_{iM}$ where the

elements are the channel output currents. Each successive observation is assumed statistically independent and identically distributed. The first assumption is based upon the coherence time/cell model, while the second assumption serves to simplify the processor structure and later analysis by excluding temporal processing of successive observations. If the target has known temporal characteristics, temporal processing would be advantageous, but at the cost of increased receiver complexity.

Optimal Processor Structure

The totality of all observations made by the receiver is denoted by $\vec{y}$ and has the following joint probability density functions under the null and target hypotheses:

$$H_0: \quad f_0(\vec{y}) = \begin{cases} \prod_{k=1}^{N} \prod_{i=1}^{M} \frac{1}{2\sigma_{i0}^2} \exp\left[-\frac{1}{2\sigma_{i0}^2}(y_{ki}+m_{i0})\right] \\ \qquad \times I_o\left[\frac{1}{\sigma_{i0}^2}\sqrt{y_{ki}\, m_{i0}}\right] ; \; y_{ki} \geq 0 \\ 0 \; ; \text{ elsewhere} \end{cases} \tag{17}$$

$$H_1: \quad f_1(\vec{y}) = \begin{cases} \prod_{k=1}^{N} \prod_{i=1}^{M} \frac{1}{2\sigma_{i1}^2} \exp\left[-\frac{1}{2\sigma_{i1}^2}(y_{ki}+m_{i1})\right] \\ \qquad \times I_o\left[\frac{1}{\sigma_{i1}^2}\sqrt{y_{ki}\, m_{i1}}\right] ; \; y_{ki} \geq 0 \\ 0 \; ; \text{ elsewhere} \end{cases} \tag{18}$$

These pdf's are obtained from Eqs (12) and (15). The receiver must choose between the hypotheses by processing the received signal described by the above probability density functions. An optimal decision is made by comparing the likelihood ratio, $\Lambda(\vec{y}) = f_1(\vec{y})/f_0(\vec{y})$, with a threshold and declaring a target if the threshold is exceeded (Ref 12:19-46). An equivalent expression is obtained by computing the logarithm of the likelihood ratio. This results in the statistic $z(\vec{y})$, which is defined by

$$z(\vec{y}) = \ln \Lambda(\vec{y}) = \sum_{k=1}^{N} \sum_{i=1}^{M} \left[a_i + b_i y_{ki} + \ln I_o(c_i\sqrt{y_{ki}}) - \ln I_o(e_i\sqrt{y_{ki}}) \right] \quad (19)$$

where

$$a_i = 2 \ln(\sigma_{i0}/\sigma_{i1}) + \tfrac{1}{2}\left[(m_{i0}/\sigma_{i0}^2) - (m_{i1}/\sigma_{i1}^2)\right]$$

$$b_i = \tfrac{1}{2}(1/\sigma_{i0}^2 - 1/\sigma_{i1}^2)$$

$$c_i = \sqrt{m_{i1}}/\sigma_{i1}^2$$

$$e_i = \sqrt{m_{i0}}/\sigma_{i0}^2$$

If the threshold is v, then the optimal signal processor algorithm is given by

$$\sum_{k=1}^{N} \sum_{i=1}^{M} \left[b_i y_{ki} + \ln I_o(c_i\sqrt{y_{ki}}) - \ln I_o(e_i\sqrt{y_{ki}}) \right] \underset{D_0}{\overset{D_1}{\gtrless}} w \quad (20)$$

where $w = \ln(v) - \sum_{i=1}^{M} N a_i$

and D_1 and D_0 represent the decisions "a valid target is present" and "no target is present," respectively. One channel of the required processor structure is illustrated in Figure 7. The complex processing required makes this structure impractical for a real time system and also makes performance analysis extremely difficult.

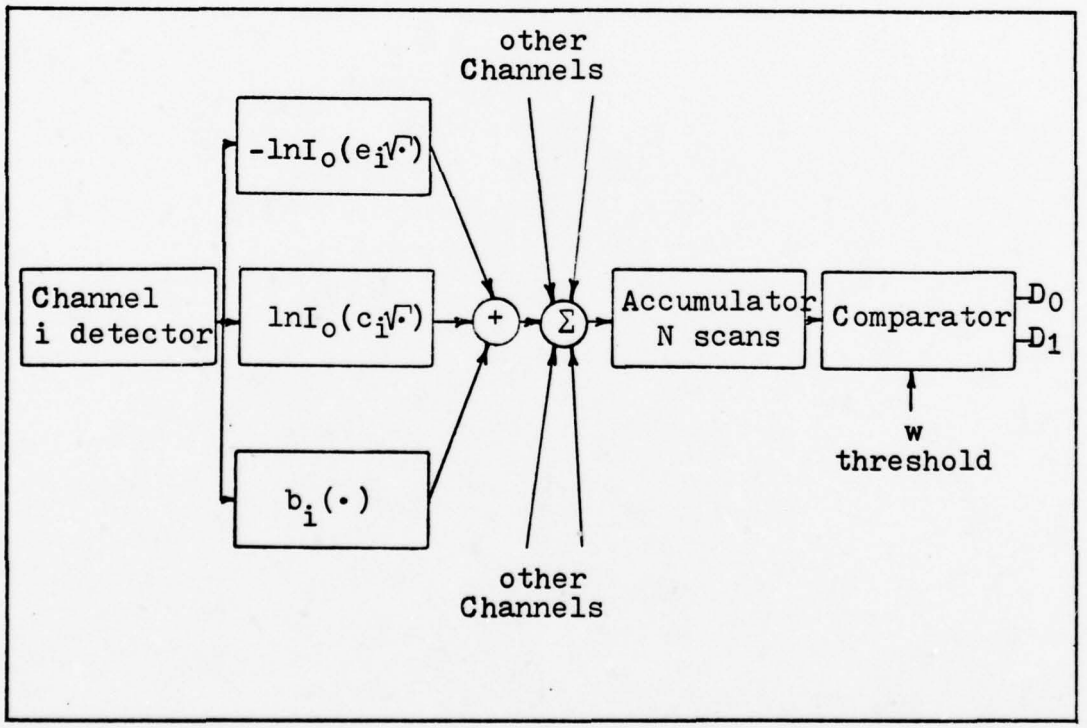

Fig. 7. Optimal Signal Processor Structure

Non-Linear Approximate Processor

The optimal processor structure may be simplified by substituting the large argument approximation for the modified Bessel function into the optimal signal processor algorithm given in Eq (20). This approximation is given by

$$I_o(x) \approx e^x/\sqrt{2\pi x} \quad ; \; x>1 \tag{21}$$

Substituting this approximation into the processor algorithm and reducing the expression, the new signal processor algorithm becomes

$$\sum_{k=1}^{N} \sum_{i=1}^{M} b_i \, y_{ki} + (c_i - e_i)\sqrt{y_{ki}} \underset{D_0}{\overset{D_1}{\gtrless}} w \tag{22}$$

where $w = \ln(v) - N \sum_{i=1}^{M} a_i + \frac{1}{2} \ln(e_i/c_i)$

The processing required by this structure is less complex than that required by the optimal processor and is much more practical to implement. One channel of the non-linear processor structure is illustrated in Figure 8.

Linear Approximate Processor

By approximating the modified Bessel function with its small argument equivalent, the signal processor structure can be further simplified. The small argument approximation for the modified Bessel function is given by

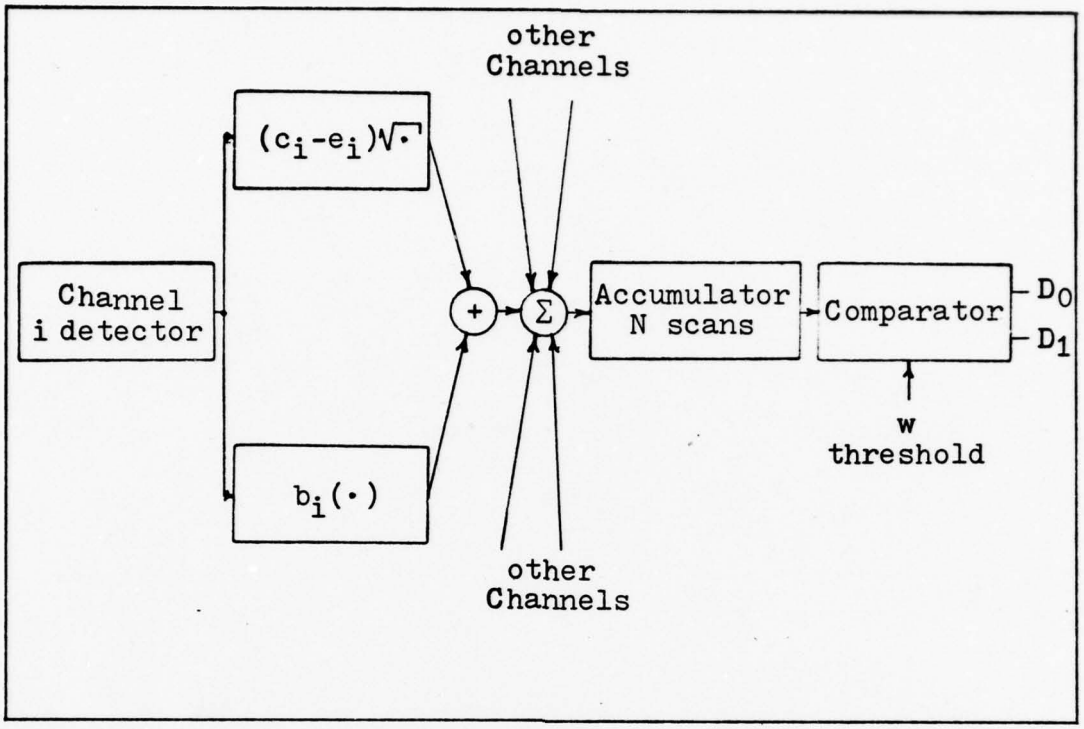

Fig. 8. Non-Linear Approximate Processor Structure

$$I_o(x) \approx x^2/4 \; ; \; x<1 \tag{23}$$

Substituting this expression into the optimal processor algorithm and reducing terms, the processor algorithm becomes

$$\sum_{k=1}^{N} \sum_{i=1}^{M} \left[b_i + \tfrac{1}{4}(c_i^2 - e_i^2)\right] y_{ki} \underset{D_0}{\overset{D_1}{\gtrless}} w \tag{24}$$

where $w = \ln(v) - N \sum_{i=1}^{M} a_i$

This linear signal processor structure is simpler than either

the optimal processor or the non-linear approximate processor and is one of the most elementary signal processor structures possible. One channel of the necessary processing is illustrated in Figure 9.

Ad-hoc Linear Processors

An ad-hoc signal processor is one which is obtained through intuition rather than analytical procedures. Two ad-hoc linear signal processors are presented here and will be used for later performance comparison with the non-linear approximate processor and the linear approximate processor.

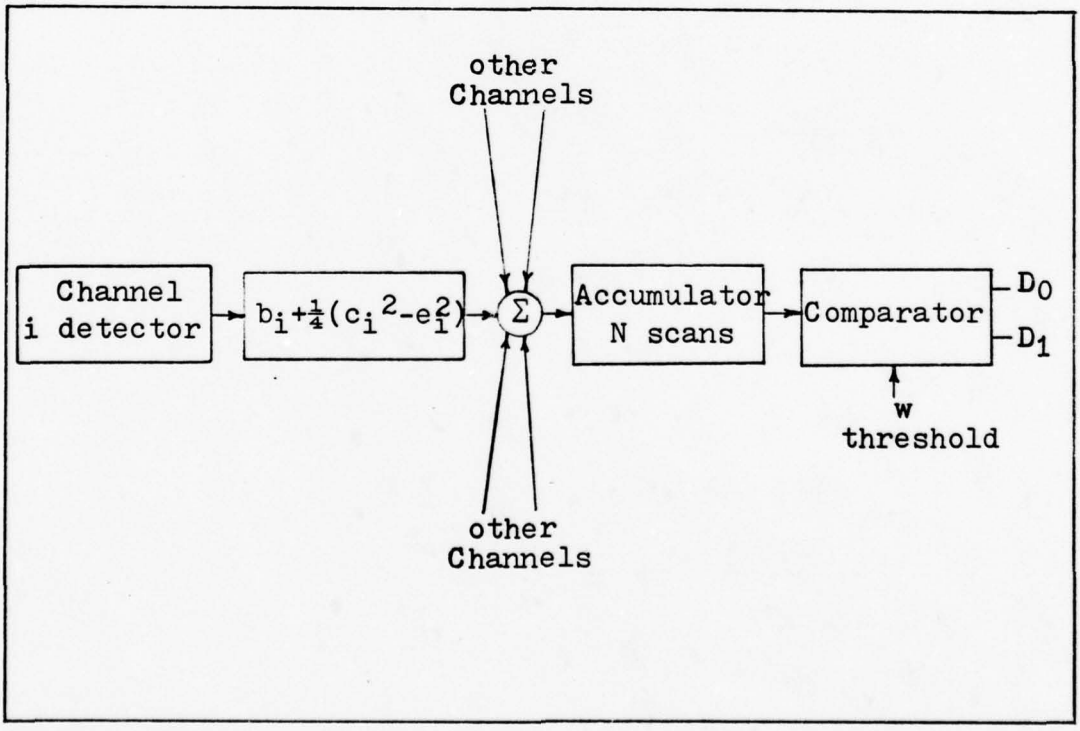

Fig. 9. Linear Approximate Processor Structure

The processor constants used here are proportional to the signal mean and inverse to signal fluctuation. The algorithms for the two ad-hoc processors are given by

$$\sum_{k=1}^{N} \sum_{i=1}^{M} (m_{i1}/\sigma_{i1}^{4} - m_{i0}/\sigma_{i0}^{4})\, y_{ki} \underset{D_0}{\overset{D_1}{\gtrless}} w \qquad (25)$$

and

$$\sum_{k=1}^{N} \sum_{i=1}^{M} (m_{i1}/\sigma_{i1}^{2} - m_{i0}/\sigma_{i0}^{2})\, y_{ki} \underset{D_0}{\overset{D_1}{\gtrless}} w \qquad (26)$$

where w is an arbitrary threshold. The processor described by Eq (25) will be referred to as the ad-hoc linear processor #1 and the other processor will be designated as the ad-hoc linear processor #2. One channel of the processor structure for each ad-hoc processor is illustrated in Figures 10 and 11.

IV. Signal Processor Performance

Signal processor performance is characterized by the probability of the receiver making an error. For the Neyman-Pearson processor structure, performance is completely specified by the quantities probability of detection (P_D) and probability of false alarm (P_{FA}). The probability of detection and the probability of false alarm are defined by

$$P_D = P(D_1|H_1) = P\left[z(\vec{y}) > w|H_1\right] \tag{27}$$

$$P_{FA} = P(D_1|H_0) = P\left[z(\vec{y}) > w|H_0\right] \tag{28}$$

These quantities are functions of the threshold w and are normally plotted as a *performance curve*, P_D vs P_{FA}, known as the receiver operating characteristic or receiver operating curve (ROC). The exact computation of the probability of detection and the probability of false alarm requires that the probability density function (or distibution function) for the log likelihood ratio, $z(\vec{y})$, be known under both hypotheses.

This chapter presents the performance characteristics of the non-linear approximate processor and the linear approximate processor only, as the complexity of the optimal signal processor makes the computation of its output probability density function unrealistic. An attempt is made to derive analytic performance expressions by first determining the joint pdf for the output of each signal processor. This

impossible except for a special case of the linear approximate processor. A general expression for the Chernoff bound on P_D and P_{FA} for the linear approximate processor is derived, but other analytic expressions could not be obtained.

The difficulty in obtaining analytic performance expressions for either the non-linear or linear processor necessitated the use of numerical methods to determine processor performance. Using a digital computer, conditional processor output pdf's were calculated and receiver operating curves for each processor structure were generated. While numerical methods cannot yield absolute measures of performance unless the exact "real world" density parameters are known, by using identical parameters in the performance calculations for each processor, the relative performance of each processor can be determined. Performance curves are generated for changes in mean, changes in variance, and for one, two, and three channel receivers.

Non-Linear Approximate Processor

Starting with the non-linear processor algorithm given by Eq (22), the processor output function, $z(\vec{y})$, for a single channel "i" is given by

$$z(y) = b_i\, y + (c_i - e_i)\sqrt{y} \qquad (29)$$

Since the detector output y is modeled by a non-central chi-square random variable, through transformation of variables the processor output probability density function can be derived. For any given values of b_i, c_i, and e_i there is a

one-to-one correspondence between y and z(y), where $y \geq 0$. Completing the square and solving for y in terms of z yields

$$y(z) = \frac{\left(\sqrt{(c_i-e_i)^2/b_i + z} - (c_i-e_i)/b_i\right)^2}{b_i} \qquad (30)$$

from which the Jacobian of the transformation is found. The Jacobian is given by

$$J = \left|\frac{\partial y(z)}{\partial z}\right| = \left|\frac{1}{b_i} - \frac{(c_i-e_i)}{b_i\sqrt{(c_i-e_i)^2 + b_i z}}\right| \qquad (31)$$

where $|\cdot|$ indicates the magnitude of the expression. The unconditional single channel processor output probability density function can now be expressed by

$$f_z(z) = Jf_y(\, y(z)\,)$$

$$= \frac{J}{2\sigma_i^2}\exp\left[-\frac{\left(\sqrt{z + \frac{(c_i-e_i)^2}{b_i}} - \frac{(c_i-e_i)}{\sqrt{b_i}}\right)^2}{2\sigma_i{}^2 b_i} - \frac{m_i}{2\sigma_i{}^2}\right]$$

$$\times\, I_o\left[\frac{\sqrt{z + \frac{(c_i-e_i)^2}{b_i}} - \frac{(c_i-e_i)}{\sqrt{b_i}}}{\sigma_i{}^2}\sqrt{\frac{m_i}{b_i}}\right] \qquad (32)$$

where m_i and $\sigma_i{}^2$ are hypothesis dependent channel parameters and the range of z depends upon the constants b_i, c_i, and e_i. Since each channel of a multichannel receiver is disjoint in frequency and independent, the joint processor output pdf can

be derived from the product of the characteristic functions for each channel.

The characteristic function, $\Phi(u)$, is a special case of the Fourier transform given by the relationship

$$\Phi(u) = F(-u/2\pi) \tag{33}$$

where $F(\cdot)$ is the Fourier transform of the processor output density function. The direct computation of the transform of the expression given by Eq (32) is a mathematical exercise beyond the scope of this thesis. A search of the Campbell and Foster transform table (Ref 1) failed to identify the necessary transform pair, which may indicate that a general transform for the probability density function given in Eq (32) does not exist. The lack of a suitable transform with which to obtain the non-linear approximate processor output characteristic function means that analytic performance expressions for the general non-linear approximate processor cannot be derived. Single channel performance expressions can be defined by

$$P_D = \int_w^\infty f_z(z|H_1)\, dz \tag{34}$$

$$P_{FA} = \int_w^\infty f_z(z|H_0)\, dz \tag{35}$$

but the required integration is very complex and its computation viewed as of little real value.

If it is assumed that the conditional detector output variances are equal, then $b_i = 0$ and the single channel

processor output density function is then given by

$$f_z(z) = \frac{|z|}{(c_i-e_i)^2\,\sigma_i^2} \exp\left[-\frac{\frac{z^2}{(c_i-e_i)^2}+m_i}{2\sigma_i^2}\right] \times I_o\left[\frac{z\sqrt{m_i}}{(c_i-e_i)\,\sigma_i^2}\right] \qquad (36)$$

While this expression is less complex than that given by Eq (32), a general Fourier transform pair still could not be found and the direct integration of the expression remains overly complex. Here again the complexity of the necessary mathematics prevents the acquisition of analytic performance expressions for the non-linear approximate processor. The attempt to find analytic performance expressions is next directed at the simpler case of the linear approximate processor.

Linear Approximate Processor

Beginning with the linear approximate processor algorithm given by Eq (24), the processor output function for a single channel "i" is given by

$$z(y) = \left[b_i + \tfrac{1}{4}(c_i^2-e_i^2)\right] y \qquad (37)$$

Through transformation of variables, the unconditional single channel processor output probability density function is expressed by

$$f_z(z) = \frac{1}{2|K_i|\sigma_i^2} \exp\left[-\frac{z/K_i + m_i}{2\sigma_i^2}\right] I_o\left(\sqrt{\frac{zm_i}{K_i\sigma_i^4}}\right) \qquad (38)$$

the range of z depending upon K_i, where $K_i = b_i + \frac{1}{4}(c_i^2 - e_i^2)$.

Using transform pair 655.1 from the Campbell and Foster transform table (Ref 1), the Fourier transform for an M channel, N look linear approximate processor is given by

$$F(f) = \left(\prod_{i=1}^{M} \frac{\exp\left[-\frac{m_i}{2\sigma_i^2}\right] \exp\left[\frac{m_i}{2\sigma_i^2(1+j4\pi K_i\sigma_i^2 f)}\right]}{(1+j4\pi K_i\sigma_i^2 f)} \right)^N \qquad (39)$$

where j is the imaginary unit $\sqrt{-1}$. Unfortunately, an inverse transform for Eq (39), which would yield an expression for the general multichannel linear approximate processor output joint density function, could not be found except for the special case where each channel is assumed to be identically distributed. Under this assumption Eq (39) can be reduced to

$$F(f) = \frac{\exp\left[-N\,M\,\frac{m}{2\sigma^2}\right] \exp\left[\frac{N\,M\,m}{2\sigma^2(1+j4\pi K\sigma^2 f)}\right]}{(1+j4\pi K\sigma^2 f)} \qquad (40)$$

where the density parameters are no longer channel dependent. Using transform pair 650.0 from the Campbell and Foster table, the processor output joint density function for M identically distributed channels is given by

$$f_z(z) = \frac{1}{(2K\sigma^2)^{MN}} \exp\left[-\frac{M\cdot N\cdot m}{2\sigma^2} - \frac{z}{2K\sigma^2}\right]\left(\frac{4K\sigma^4 z}{M\cdot N\cdot m}\right)^{\frac{M\cdot N}{2} - \frac{1}{2}}$$

$$I_{(M\cdot N)-1}\left[\sqrt{\frac{M\cdot N\cdot m\cdot z}{K\sigma^4}}\right] \qquad (41)$$

While the joint density function is in analytic form, the calculation of the performance parameters P_D and P_{FA} requires that this pdf be integrated according to Eqs (34) and (35). This integration is prohibitively complex and a search of available integral tables failed to yield an integral of the required form. Even for the simpler structure of the linear approximate processor, the derivation of exact performance expressions remains prohibitively cumbersome. When exact performance calculations are impossible, it is often useful to determine bounds on error probabilities.

Chernoff Bound

An exponetially tight bound on the probability of false alarm and the probability of detection is the Chernoff bound (Refs 2:126; 12:121). This bound is obtained from the moment generating function, $\mu(s)$, which is derived from the conditional characteristic function $\Phi(\mu|H_0)$. The moment generating function and the resultant bounds on the probability of false alarm and the probability of detection are given by

$$\mu(s) = \ln\left[E(e^{sz}|H_0)\right] = \ln \Phi(-js|H_0) \qquad (42)$$

$$P_D \geq 1-\exp\left[\mu(s) + (1-s)\dot{\mu}(s)\right] \tag{43}$$

$$P_{FA} \leq \exp\left[\mu(s) - s\dot{\mu}(s)\right] \tag{44}$$

where $E(\cdot)$ indicates expected value and $\dot{\mu}(s) = \partial\mu(s)/\partial s$. Using Eqs (33) and (39), the characteristic function for the linear approximate processor can be derived. Because no transform for the non-linear approximate processor output density function exists, neither the moment generating function or the Chernoff bound for the non-linear approximate processor can be obtained.

The conditional characteristic function for the linear approximate processor output is given by

$$\Phi(\mu|H_0) = \left[\prod_{i=1}^{M} \frac{\exp\left(-\frac{m_{i0}}{2\sigma_{i0}^2}\right)\exp\left(\frac{m_{i0}}{2\sigma_{i0}^2(1-j2K_i\sigma_{i0}^2\mu)}\right)}{(1-j2K_i\sigma_{i0}^2\mu)}\right]^N \tag{45}$$

for μ real, from which the moment generating function

$$\mu(s) = N\sum_{i=1}^{M}\left[\frac{m_{i0}}{2\sigma_{i0}^2}\left(\frac{1}{1-2K_i\sigma_{i0}^2 s} - 1\right) - \ln(1-2K_i\sigma_{i0}^2 s)\right] \tag{46}$$

is obtained. The partial derivative, $\dot{\mu}(s)$, is found to be

$$\dot{\mu}(s) = N\sum_{i=1}^{M}\left[\frac{2K_i\sigma_{i0}^2}{1-2K_i\sigma_{i0}^2 s} + \frac{m_{i0}K_i}{(1-2K_i\sigma_{i0}^2 s)^2}\right] \tag{47}$$

The bounds on P_D and P_{FA} are now defined by Eqs (43) and (44), where the optimal value of s is the solution to the equation

$$\dot{\mu}(s) = w$$

where w is the previously defined threshold.

The use of the bounds in general require that a polynomial be solved to obtain the optimal value of s. In all but the most simple cases, this can be quite cumbersome. For the single channel, one look case, the optimal value of s was determined to be

$$s = \frac{(w-K_i\sigma_{i0}^2) + \sqrt{K_i^2\sigma_{i0}^4+m_{i0}K_iw}}{2K_i\sigma_{i0}^2w} \qquad (49)$$

Assuming for simplicity that $m_{i0} = 0$ and that the variances under each hypothesis are equal, $s = 2/\eta_1$ where $\eta_1 = m_{i1}/\sigma_{i1}^2$ and the bound on the probability of false alarm is given by

$$P_{FA} \leq \exp\left[-\frac{2\ln(v)+\eta_1}{\eta_1}\right] \qquad (50)$$

where v is the linear threshold. The limit of this bound as η_1 increases without bound is

$$P_{FA} \leq 1/e = 0.37 \qquad (51)$$

Intuitively, one would expect the bound on P_{FA} to approach zero as η_1 increased without bound, since the conditional

processor output density functions separate as η_1 increases. The loose bound on P_{FA} of 0.37 indicates that the Chernoff bound obtained is valid only for small values of η_1, a result consistent with the small argument assumption originally used in the derivation of the linear approximate processor.

Numerical Analysis

The lack of analytic expressions with which to compare between signal processors necessitated the use of numerical methods to achieve a common basis for comparison. The procedure used here was to write a FORTRAN computer program which directly computed the conditional processor output densities of each processor for a given set of parameters. These densities were then numerically integrated over a range of threshold values to generate an array of values for the probability of detection and the probability of false alarm. These values were in turn plotted as a receiver operating curve (ROC).

The computation of joint density functions for multichannel receiver performance evaluation made use of a fast Fourier transform (FFT) algorithm to compute the transforms of the conditional processor output densities for each channel. The product of the individual channel transforms was then inverse transformed to obtain the conditional joint processor output density functions. These joint density functions were then numerically integrated as above to obtain values for P_D and P_{FA} which were plotted as a receiver operating curve.

The conditional output density functions for the nonlinear approximate processor and the linear approximate processor were derived from Eqs (32), (36), and (38) and were expressed in terms of the parameters $\eta_0 = m_{i0}/\sigma_{i0}^2$, $\eta_1 = m_{i1}/\sigma_{i1}^2$, and $\rho = \sigma_{i1}^2/\sigma_{i0}^2$. Single channel processor performance was calculated for changes in target hypothesis mean and for changes in target hypothesis variance. The parameters used in this analysis were chosen primarily for convienience in computation and are scaled versions of the parameters estimated from the Lockheed Background Measurements Program data discussed in Chapter II. Since the values of m_{i0} and σ_{i0}^2 estimated from the Lockheed data are linearly related to the detector output voltage (Ref 6:3-27), it was asserted that the ratio of detector output mean to variance (η_0) could effectively be set for a given value through proper selection of processor components. The parameters used to observe the effects of changes in mean upon processor performance are listed in Table II. The parameters used to observe the effects of changes in variance upon processor performance are listed in Table III.

Table II
Channel Parameters for Change in Mean

η_0	η_1	ρ
8.0	16.0	1.0
8.0	24.0	1.0
8.0	32.0	1.0

Table III
Channel Parameters for Change in Variance

η_0	η_1	ρ
8.0	24.0	1.0
8.0	24.0	1.5
8.0	24.0	2.0

Typical non-linear processor output densities for change in mean are illustrated in Figures 12- 14. It is easily observed that the conditional processor output density functions separate as the target hypothesis mean increases. The resulting receiver performance curves are shown in Figure 15. For a probability of false alarm equal to 0.10, the probability of detection increases from 0.45 to 0.96 as η_1 goes from 16.0 to 32.0 with η_0 equal to 8.0 . Typical non-linear processor output densities for change in target hypothesis variance are illustrated in Figures 16 and 17. The resulting performance curves are shown in Figure 18. As the target hypothesis variance increases to twice the null hypothesis variance with constant mean to variance ratios, the probability of detection goes from 0.80 to 0.99 for a probability of false alarm of 0.10 . The observed changes in performance indicate that the receiver is more sensitive to changes in mean than to changes in variance. A representative FORTRAN program used to generate the ROC's for the non-linear approximate processor is listed in Appendix B.

To determine the effect of multiple channels upon receiver performance, performance curves were generated for one,

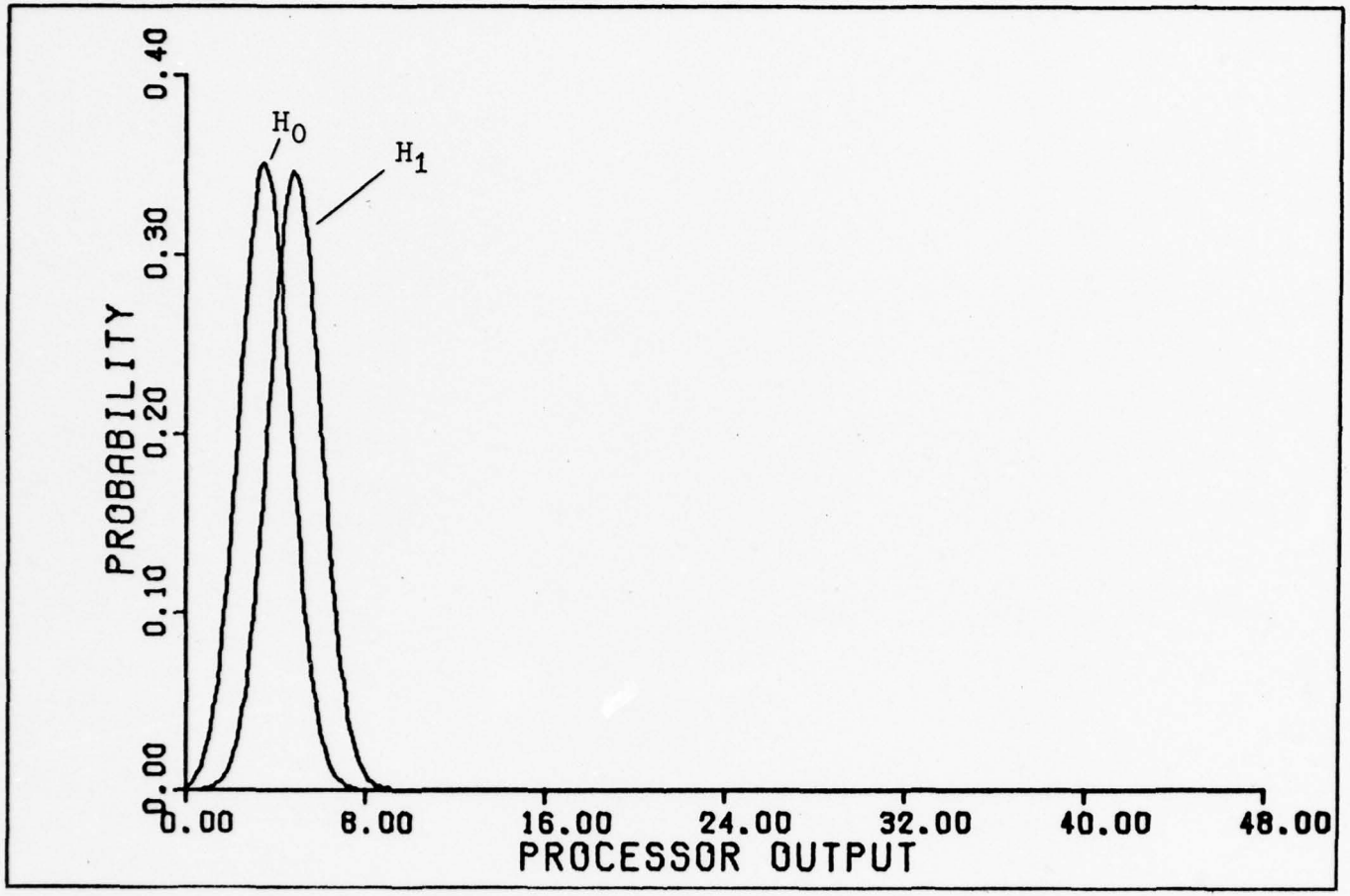

Fig.12. Non-linear Processor Output Densities: η_0=8.0, η_1=16.0, ρ=1.0

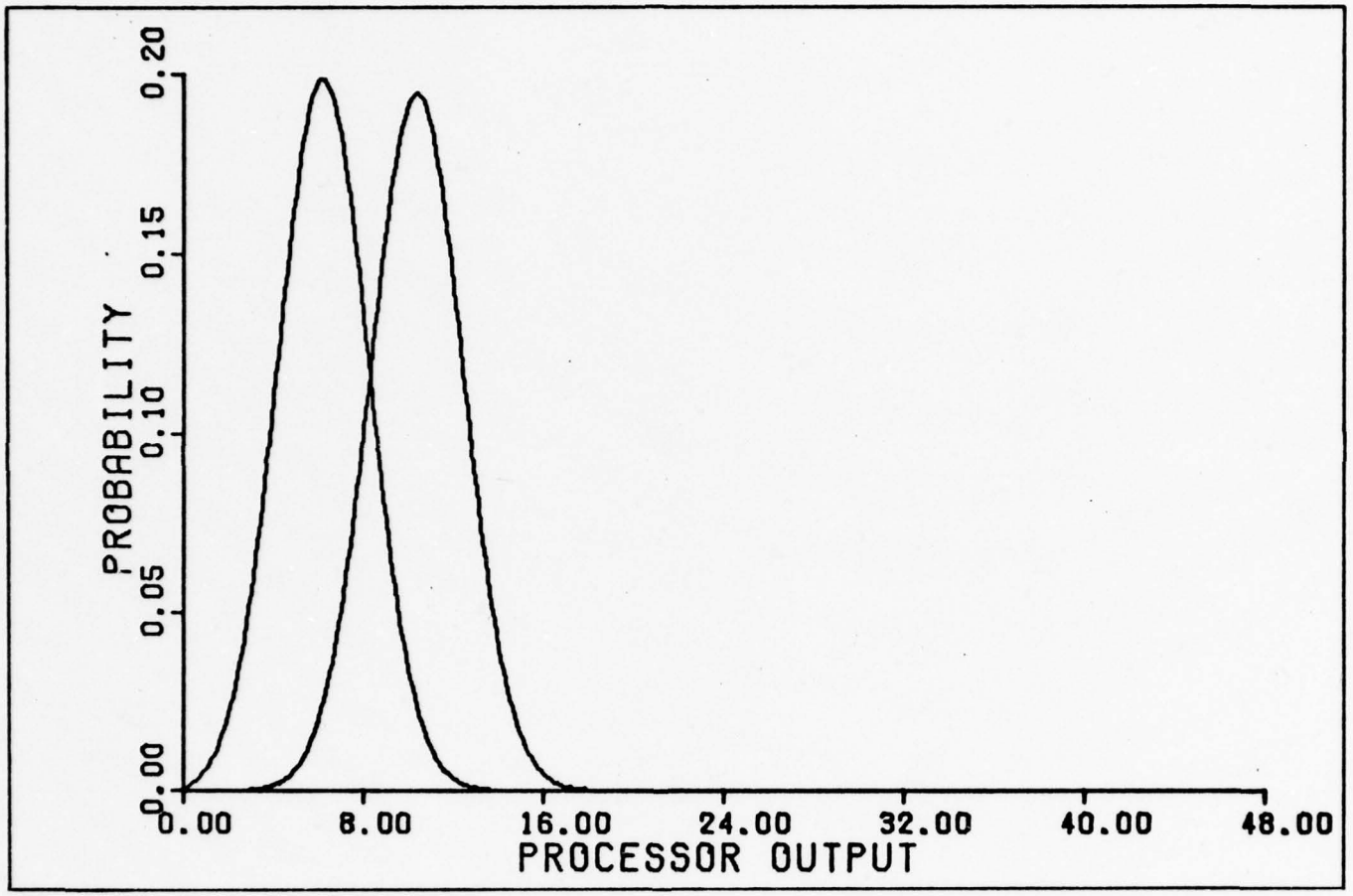

Fig.13. Non-linear Processor Output Densities: η_0=8.0, η_1=24.0, ρ=1.0

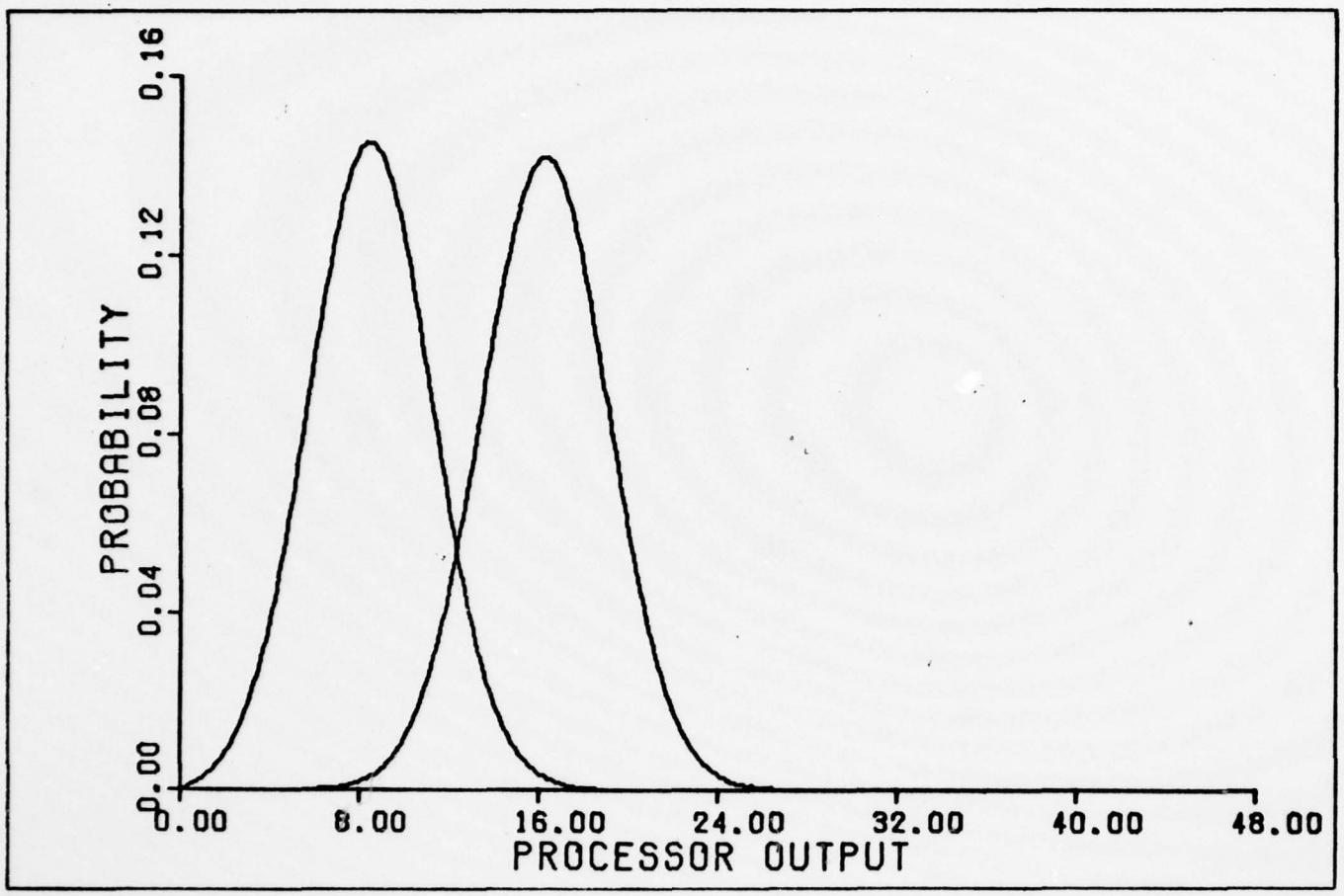

Fig. 14. Non-linear Processor Output Densities: $\eta_0=8.0$, $\eta_1=32.0$, $\rho=1.0$

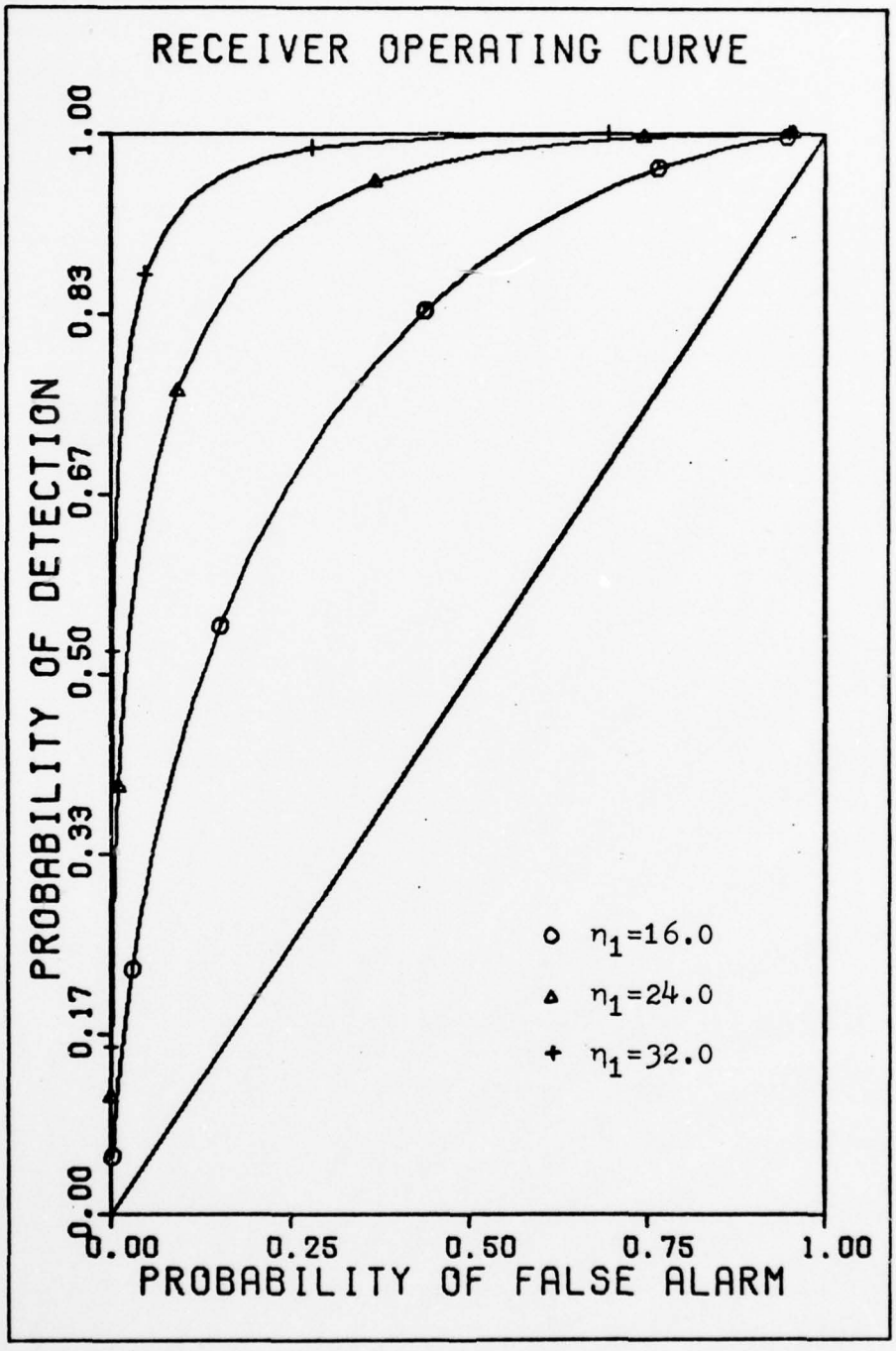

Fig. 15. Non-linear Processor ROC, Change in Mean

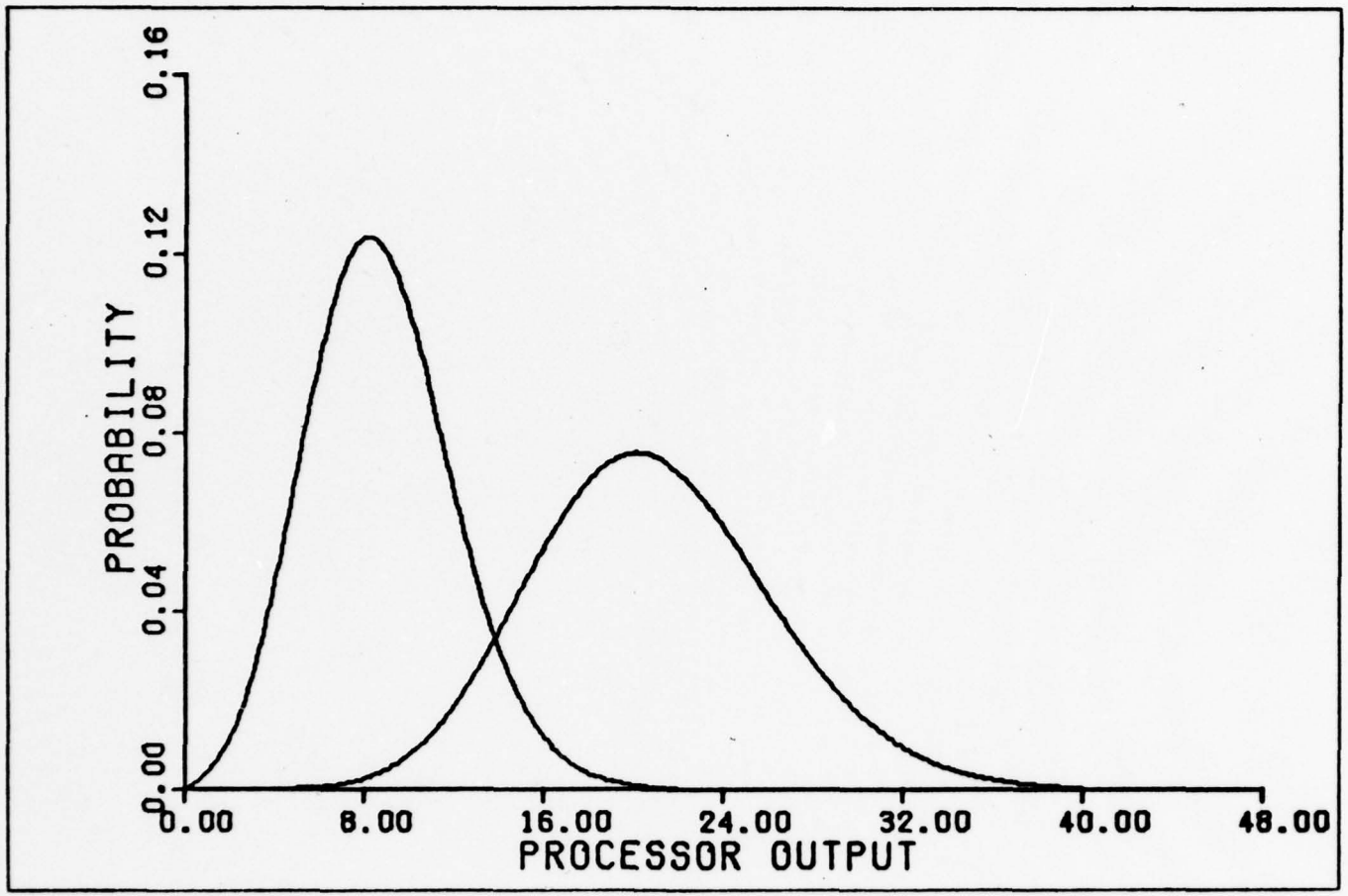

Fig. 16. Non-linear Processor Output Densities: η_0=8.0, η_1=24.0, ρ=1.5

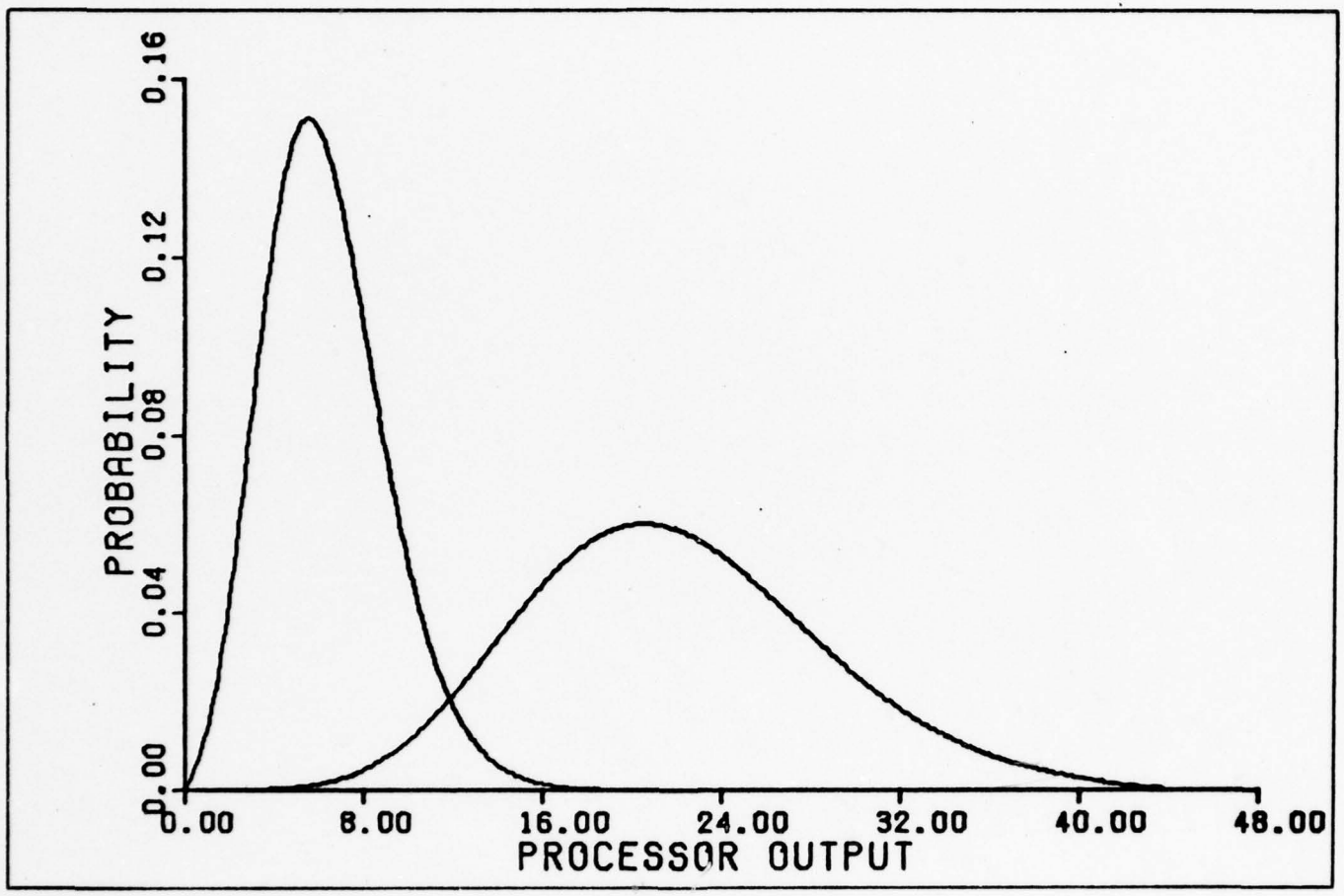

Fig. 17. Non-linear Processor Output Densities: η_0=8.0, η_1=24.0, ρ=2.0

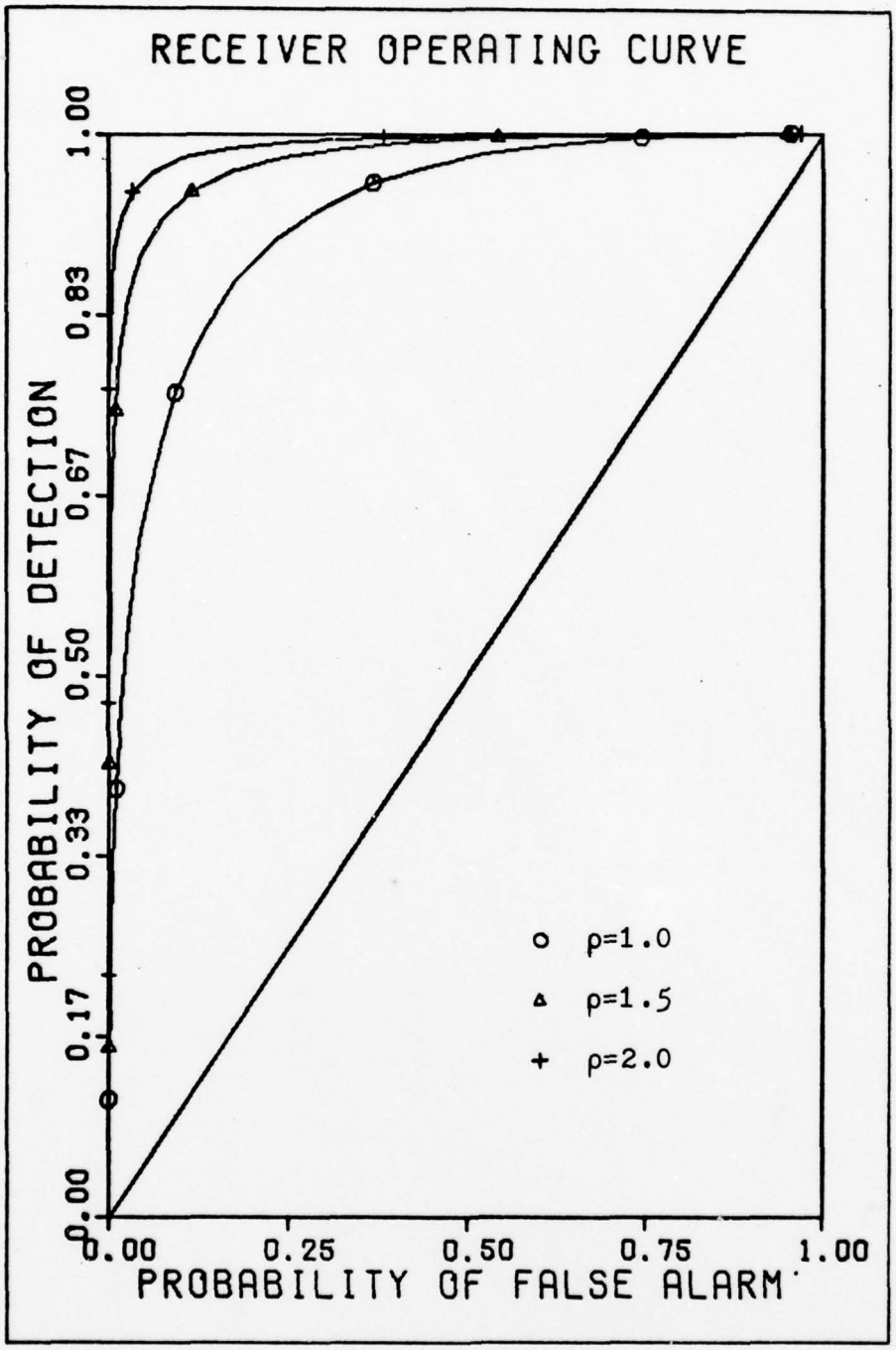

Fig. 18. Non-linear Processor ROC, Change in Variance

two, and three channel receivers. Three nearly identical channels were used; the channel parameters are listed in Table IV. The performance curves for the individual channels are plotted in Figure 19. For a probability of false alarm of 0.10, each of the individual channels has a probability of detection of approximately 0.49. Multichannel receiver performance curves for the non-linear approximate processor are shown in Figure 20. The probability of detection increases to 0.66 for two channels and to 0.82 for three channels, an improvement of 67% over single channel performance. Since a similar joint density function would be obtained for a multi-look receiver, by extension of the multichannel results, one would also expect receiver performance to improve for a multi-look receiver. A representative FORTRAN program used to generate multichannel ROC's is listed in Appendix C.

The same procedures were applied to the linear approximate processor using identical parameters. Typical linear processor output densities for change in mean are illustrated in Figures 21 - 23. The resulting receiver performance curves are shown in Figure 24. The observed performance is identi-

Table IV
Multichannel Parameters

Channel	η_0	η_1	ρ
1	8.0	16.0	1.0
2	9.0	18.0	1.0
3	10.0	20.0	1.0

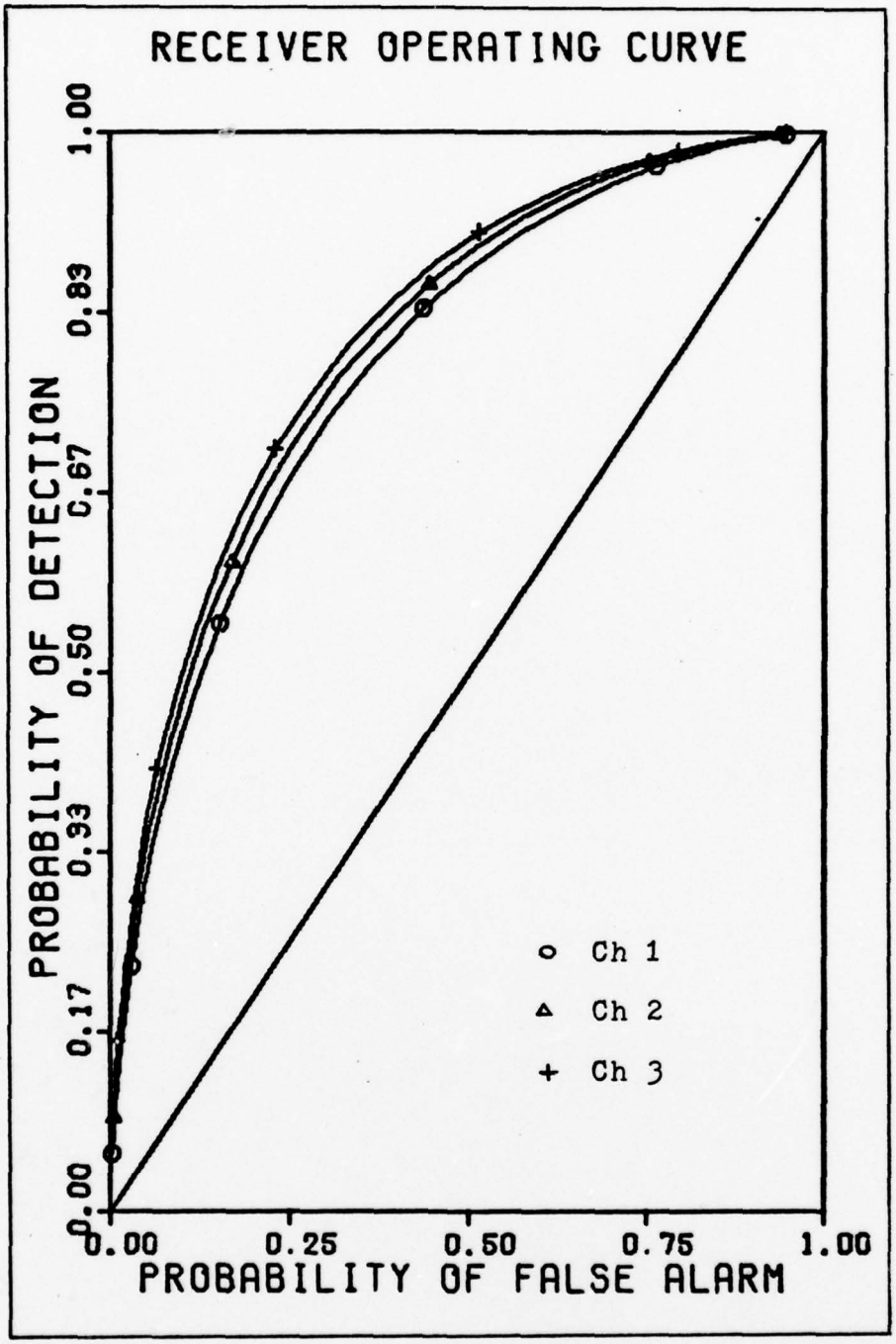

Fig. 19. Individual Channel Performance Curves

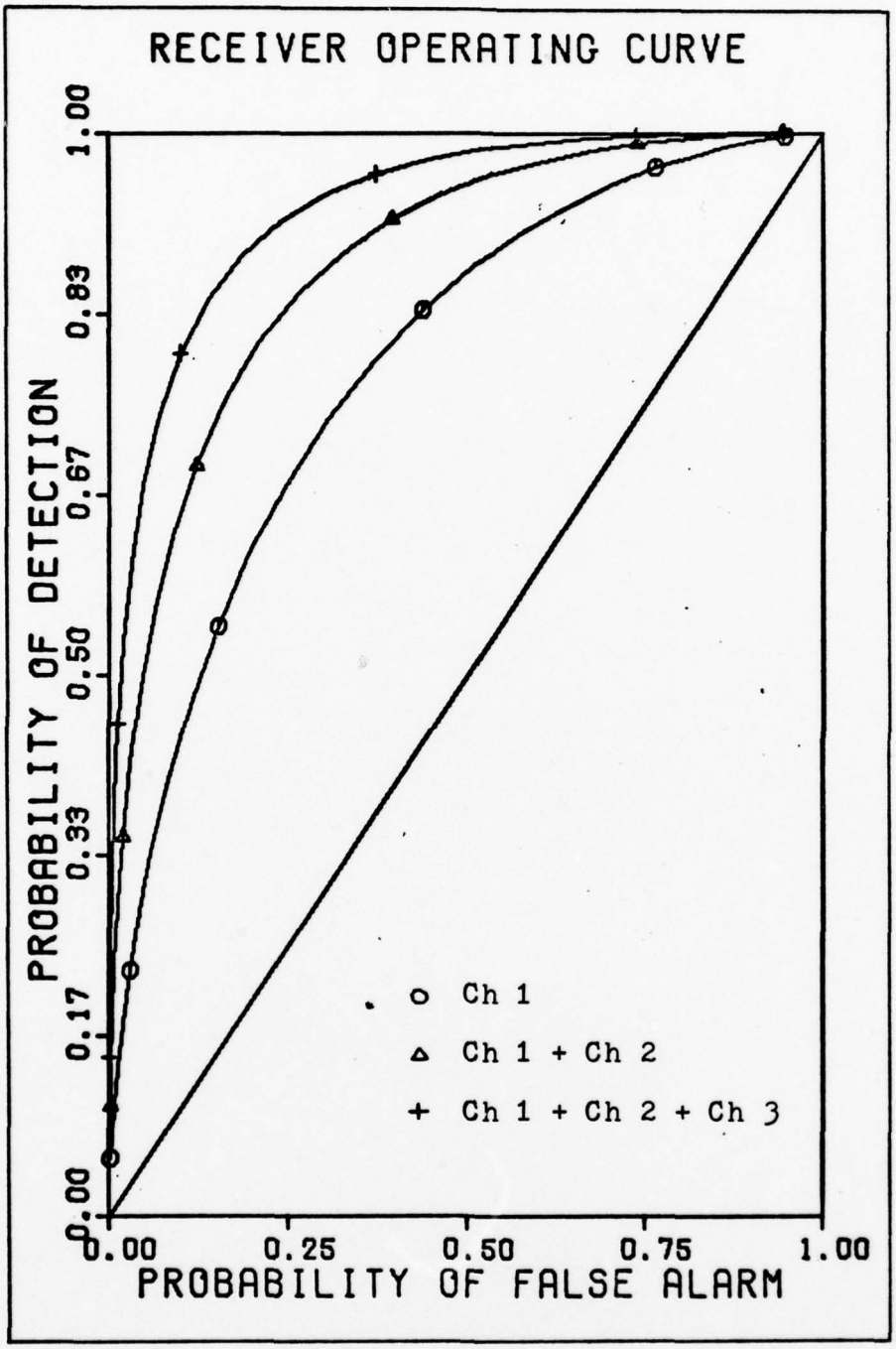

Fig. 20. Multichannel Non-linear Processor ROCs

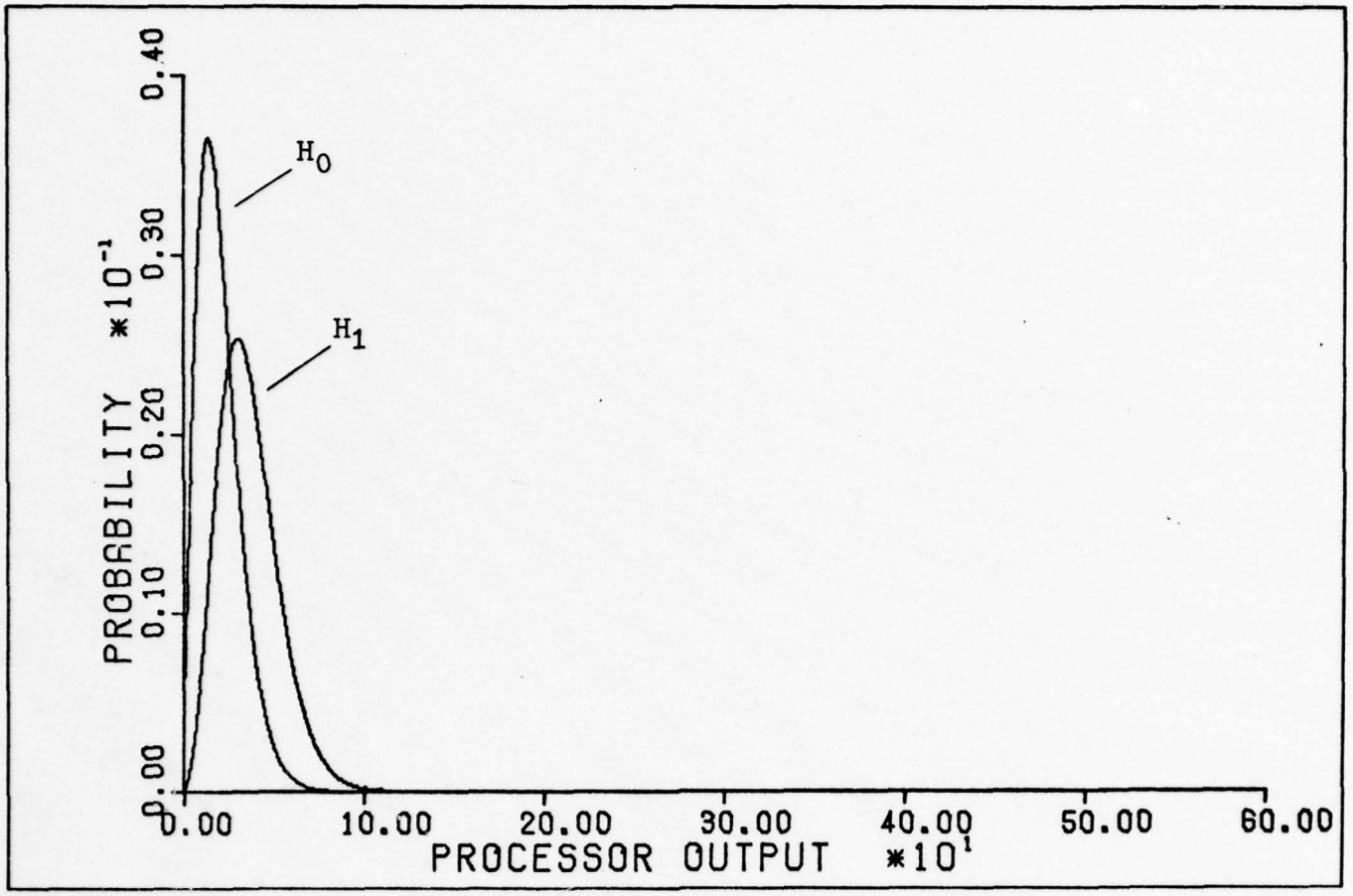

Fig. 21. Linear Processor Output Densities: η_0=8.0, η_1=16.0, ρ=1.0

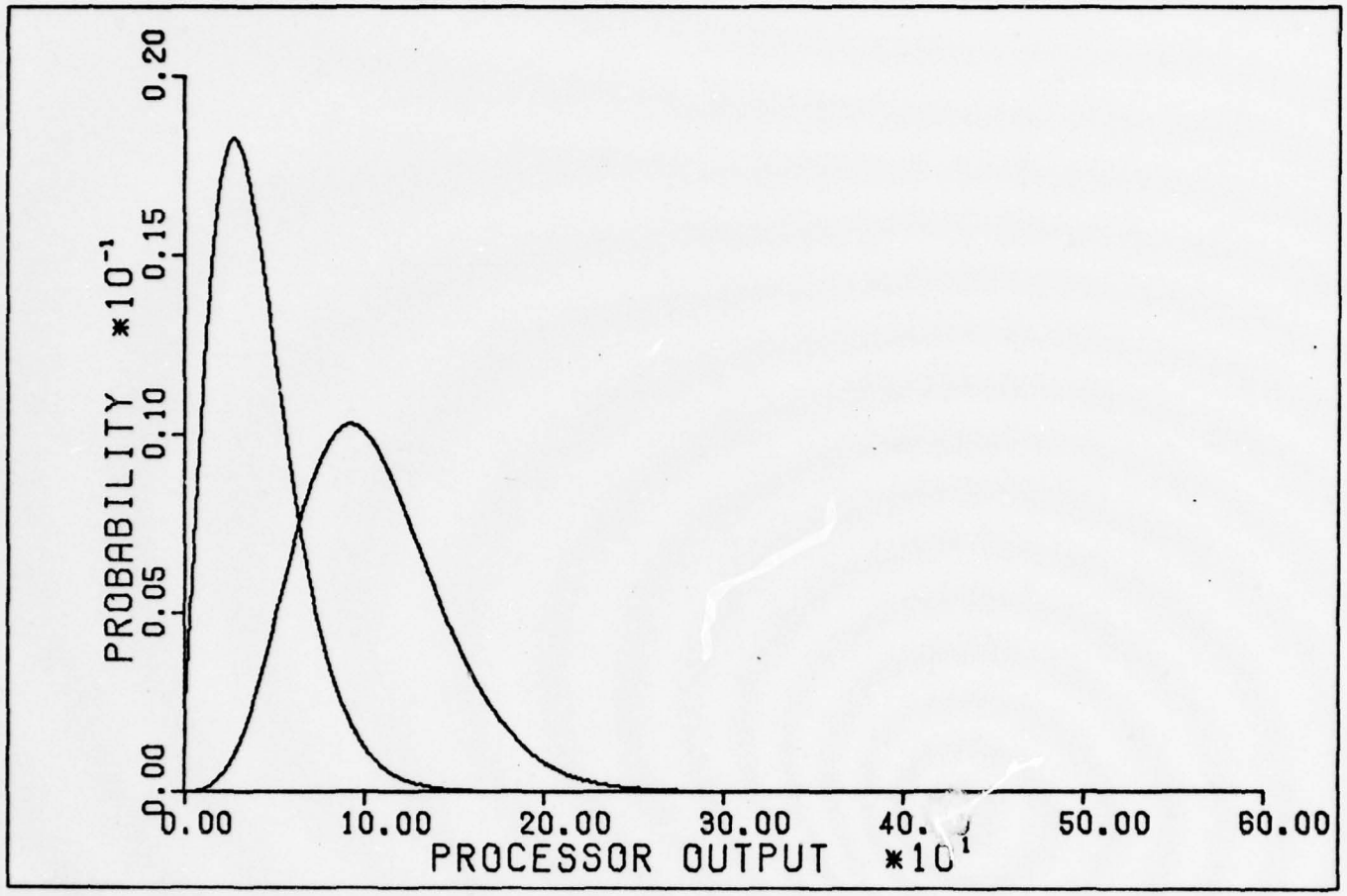

Fig. 22. Linear Processor Output Densities: η_0=8.0, η_1=24.0, ρ=1.0

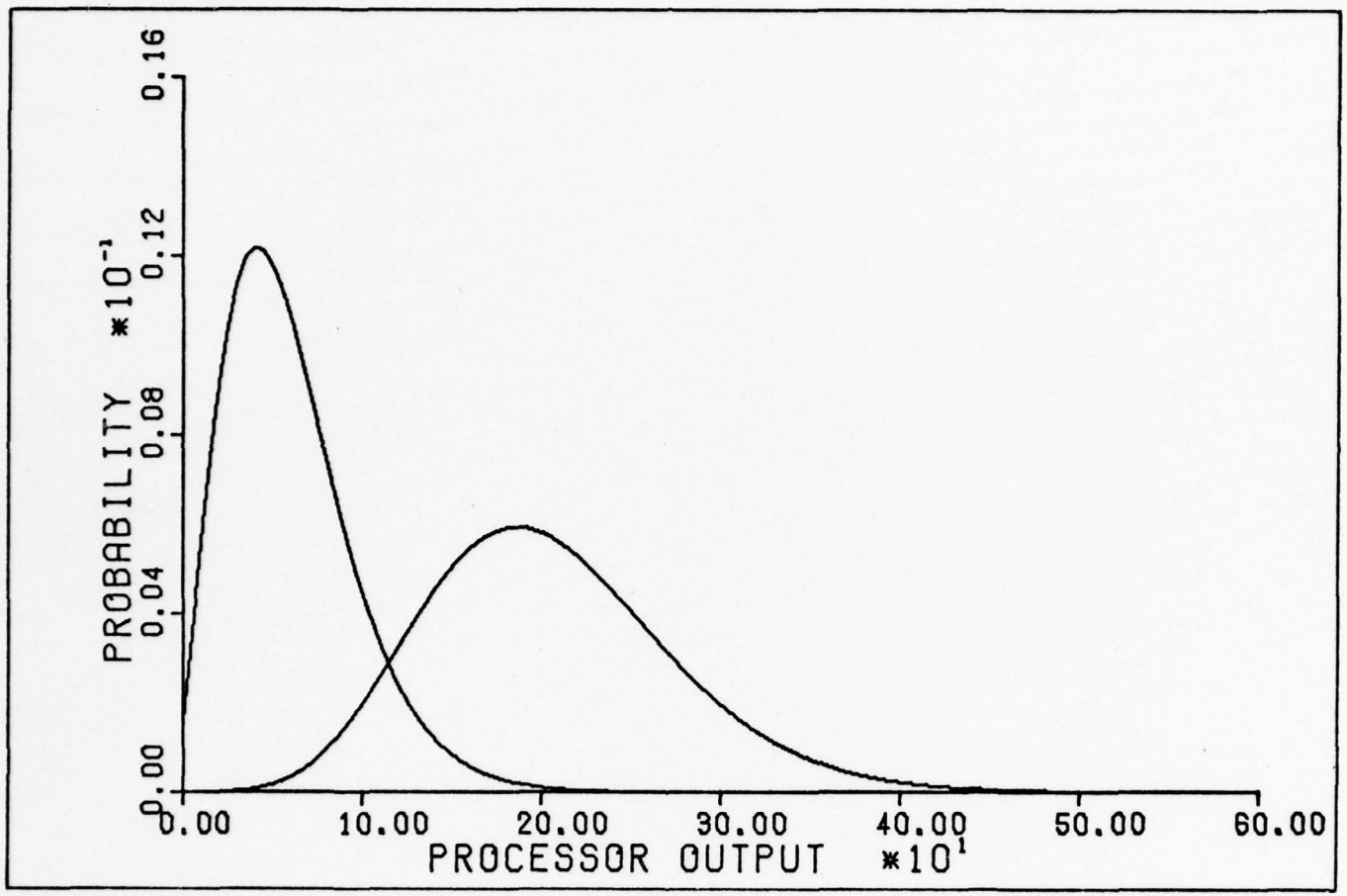

Fig. 23. Linear Processor Output Densities: η_0=8.0, η_1=32.0, ρ=1.0

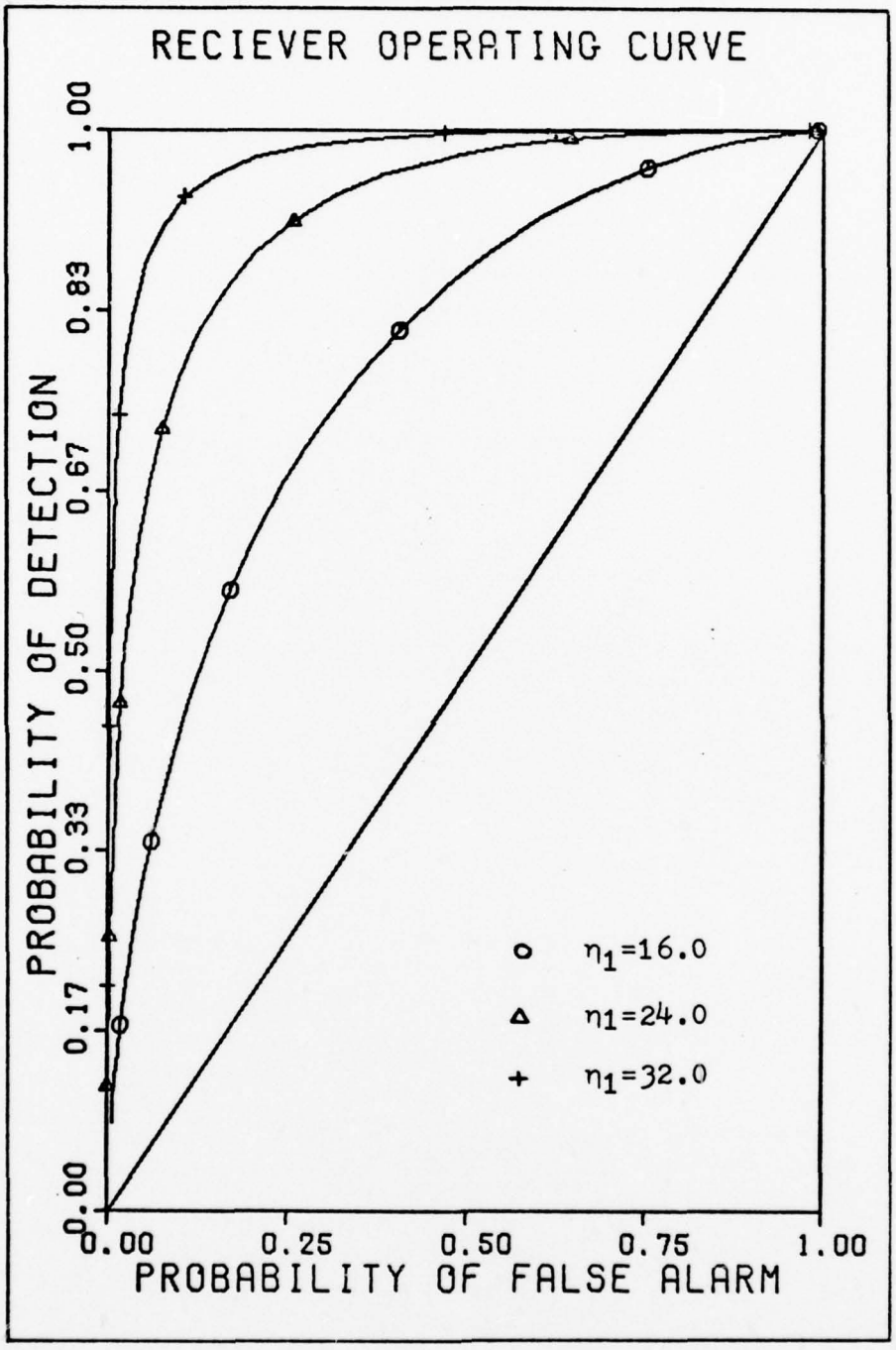

Fig. 24. Linear Processor ROC, Change in Mean

cal to that of the non-linear approximate processor. Typical linear processor output densities for change in variance are illustrated in Figures 25 and 26. The resulting performance curves are shown in Figure 27. Again, the performance of the linear approximate processor is identical to the performance of the non-linear approximate processor. A representative FORTRAN program used to generate the ROC's for the linear approximate processor is listed in Appendix D. Multichannel receiver performance durves for the linear approximate processor are shown in Figure 28. Linear and non-linear processor multichannel performance is also identical. The equal performance result is proven analytically for the single channel case in Appendix E.

Ad-hoc Linear Processors

An ad-hoc signal processor is a processor whose structure is based upon engineering intuition rather than statistical analysis. The ad-hoc linear processors presented in Chapter III are used here to compare the relatively simple ad-hoc processor structure with the performance of the non-linear and linear approximate processors derived from signal statistics.

The conditional processor output density functions for the ad-hoc linear processor #1 are obtained from the processor algorithm given by Eq (25) through transformation of variables. The resulting single channel conditional processor output density functions are given by

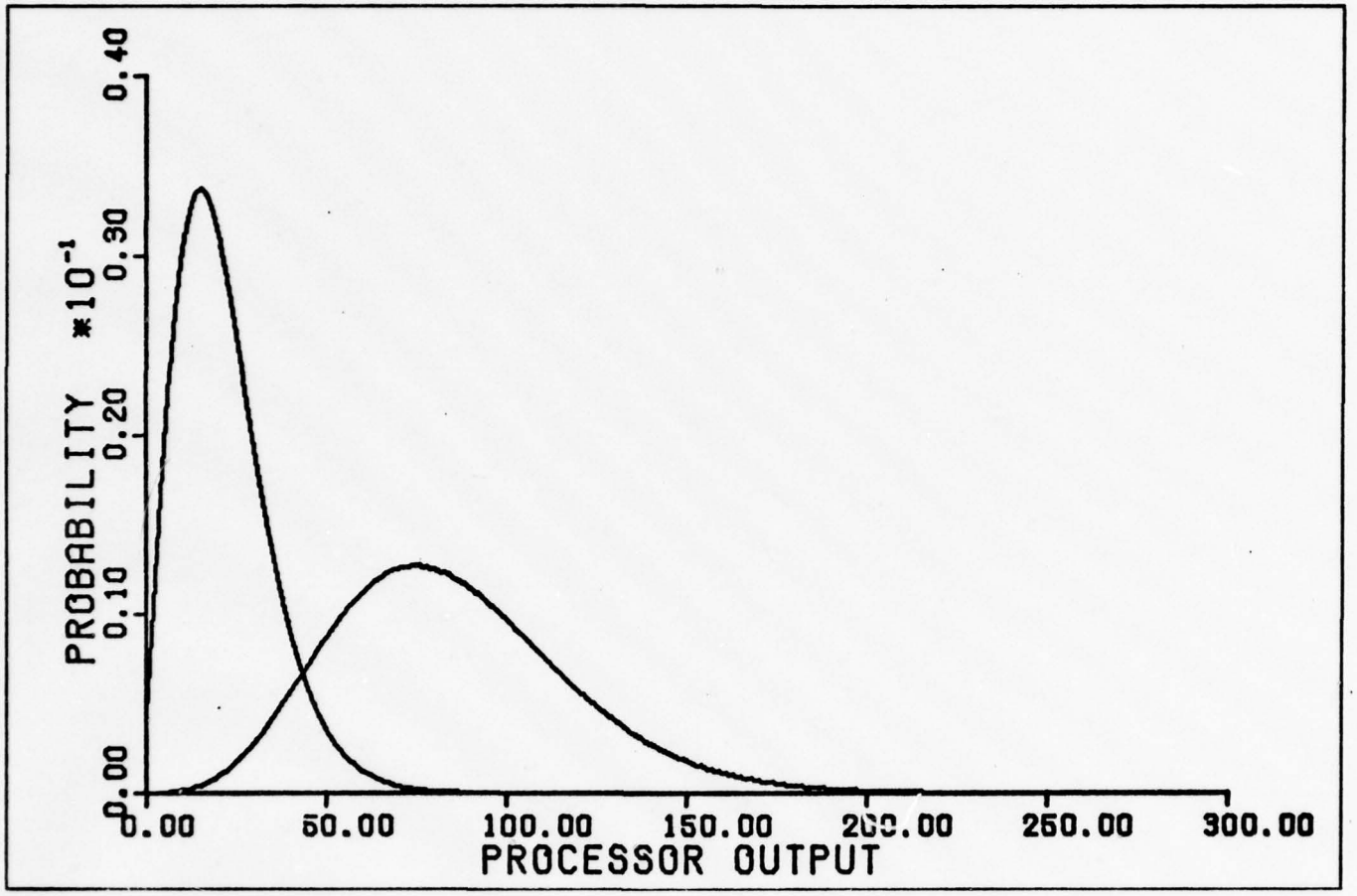

Fig. 25. Linear Processor Output Densities: η_0=8.0, η_1=24.0, ρ=1.5

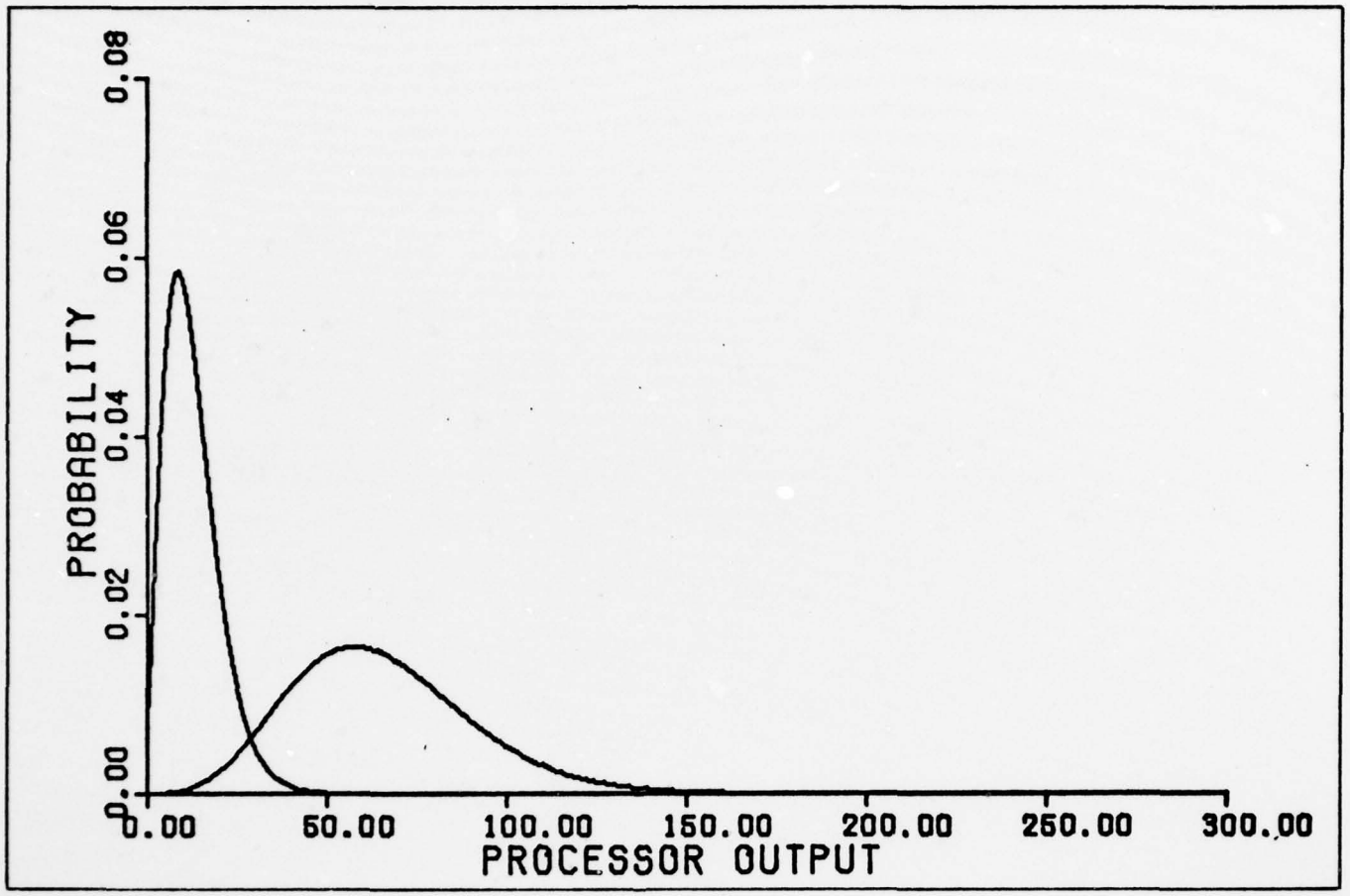

Fig. 26. Linear Processor Output Densities: η_0=8.0, η_1=24.0, ρ=2.0

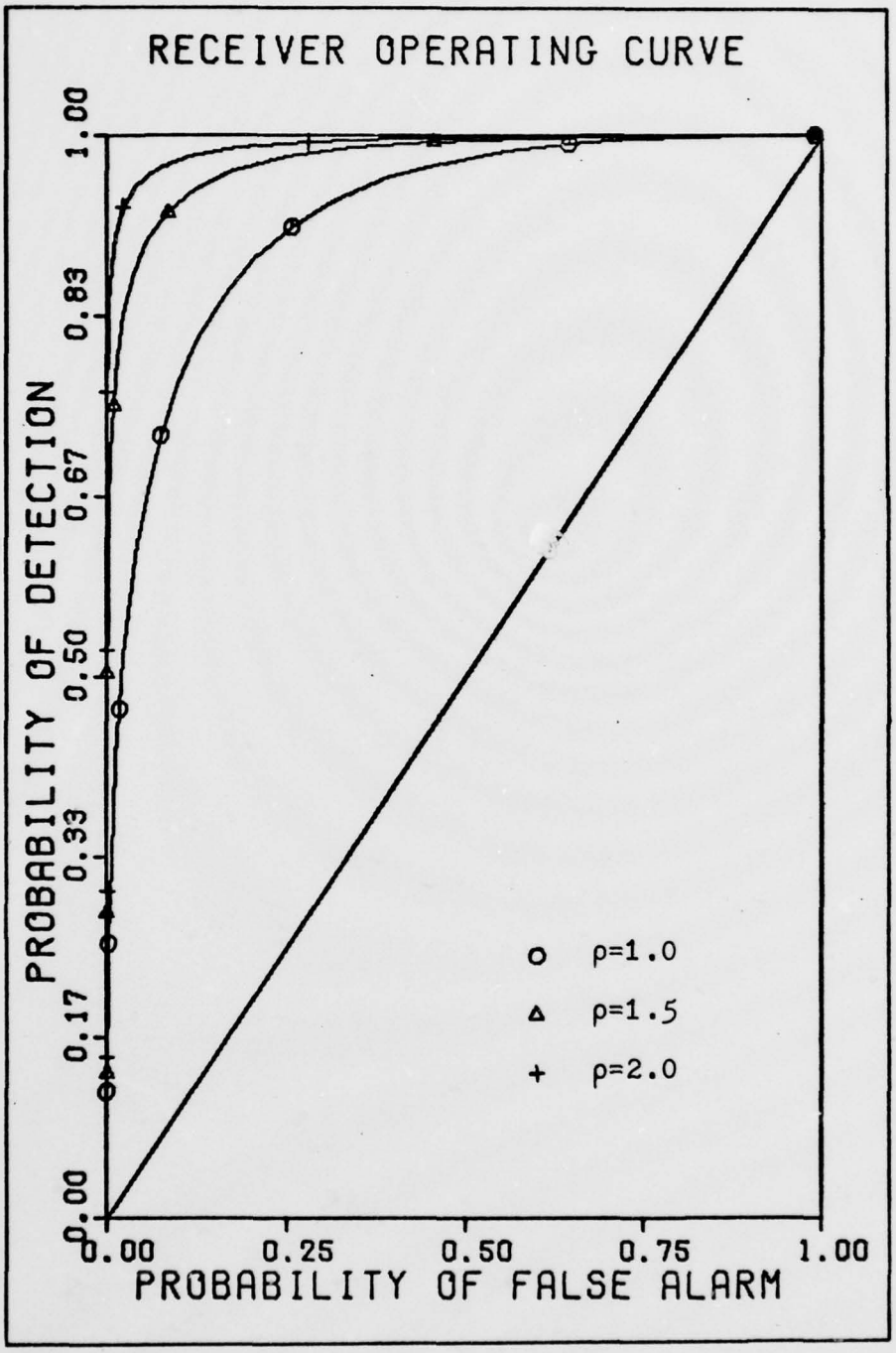

Fig. 27. Linear Processor ROC, Change in Variance

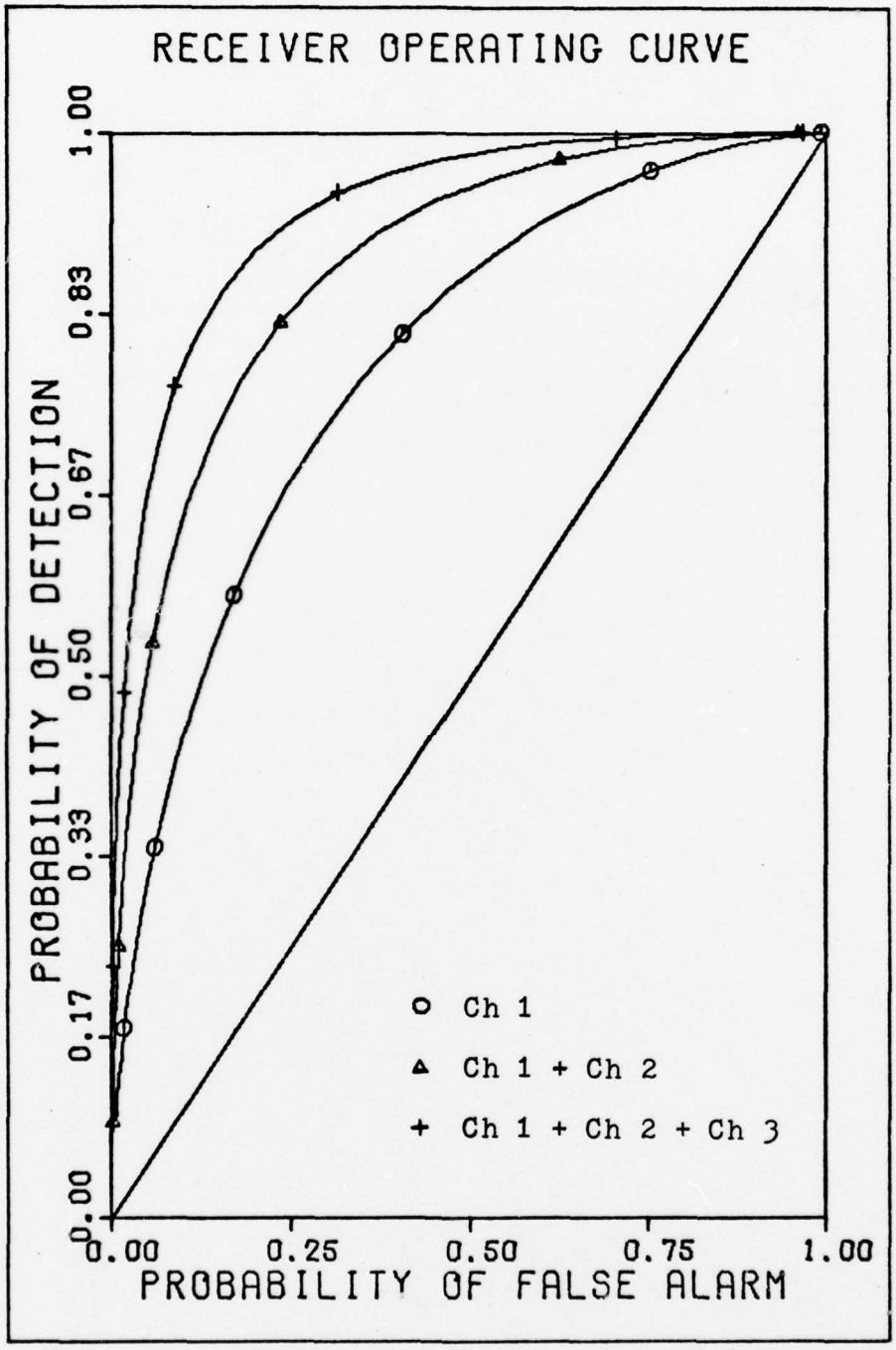

Fig. 28. Multichannel Linear Processor ROCs

$$H_0: f_z(z) = \frac{1}{|2K_i\sigma_{i0}^2|} \exp\left[-\frac{z}{2K_i\sigma_{i0}^2} - \frac{m_{i0}}{2\sigma_{i0}^2}\right] I_o\left(\sqrt{\frac{zm_{i0}}{K_i\sigma_{i0}^4}}\right) \quad (52)$$

$$H_1: f_z(z) = \frac{1}{|2K_i\sigma_{i1}^2|} \exp\left[-\frac{z}{2K_i\sigma_{i1}^2} - \frac{m_{i1}}{2\sigma_{i1}^2}\right] I_o\left(\sqrt{\frac{zm_{i1}}{K_i\sigma_{i1}^4}}\right) \quad (53)$$

where $K_i = (m_{i1}/\sigma_{i1}^4 - m_{i0}/\sigma_{i0}^4)$

These density functions can be expressed in terms of the parameters η_0, η_1, and ρ previously defined. Since the processor structure is similar to that of the linear approximate processor, differing only in the value of K_i, performance curves for the ad-hoc linear processor were generated by using the program listed in Appendix D with only slight modification. The resulting performance curves for the ad-hoc linear processor #1 for changes in mean and variance are shown in Figures 29 and 30. For identical parameters, the performance of the ad-hoc linear processor #1 is identical to the performance observed for both the non-linear and linear approximate processors.

Similarly, the single channel conditional processor output density functions for the ad-hoc linear processor #2 were derived from the processor algorithm given by Eq (26). The density functions for the ad-hoc linear processor #2 are of the same form as Eqs (52) and (53) except that K_i is now defined by

$$K_i = (m_{i1}/\sigma_{i1}^2 - m_{i0}/\sigma_{i0}^2)$$

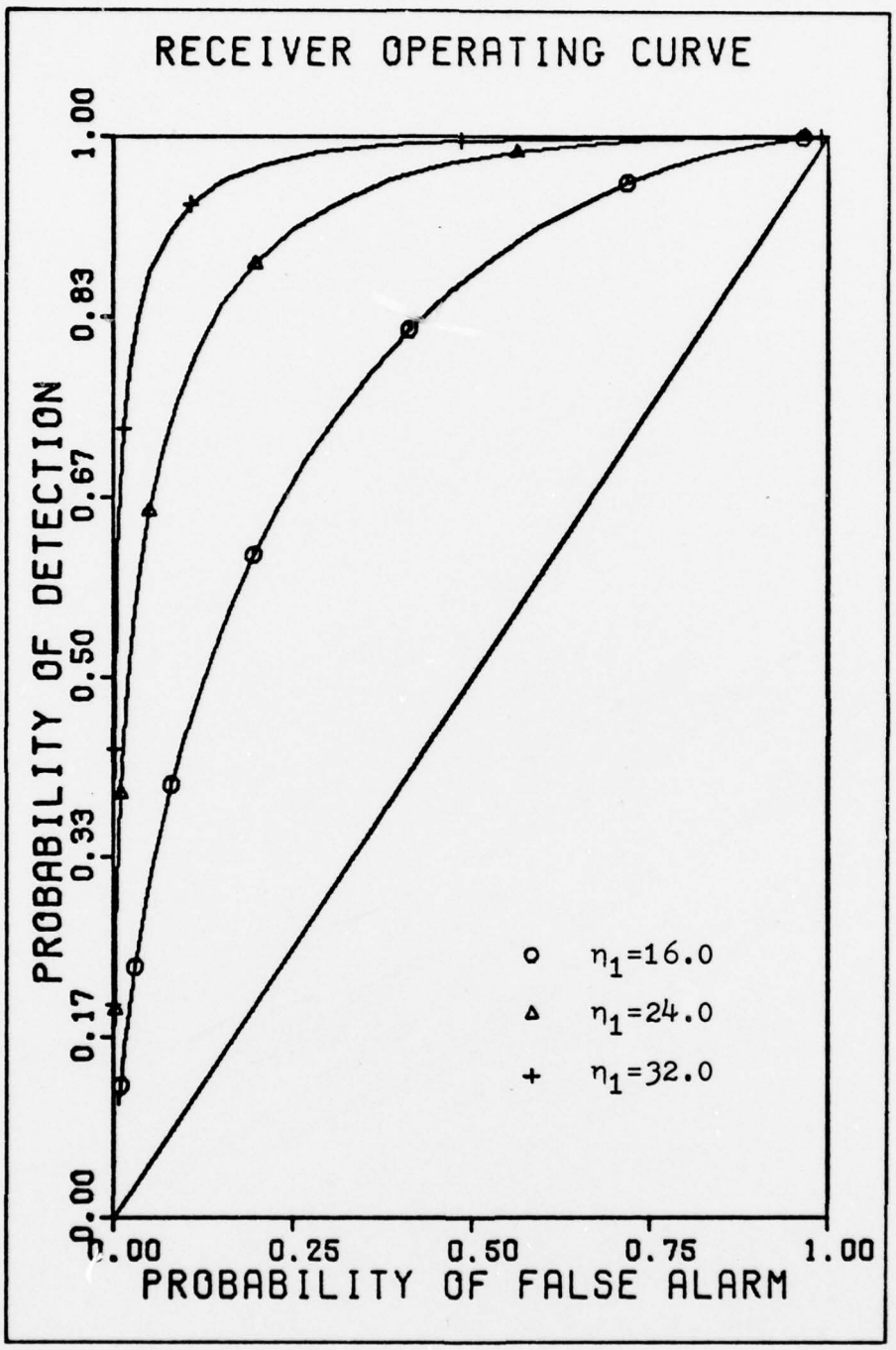

Fig. 29. Ad-hoc Processor #1 ROC, Change in Mean

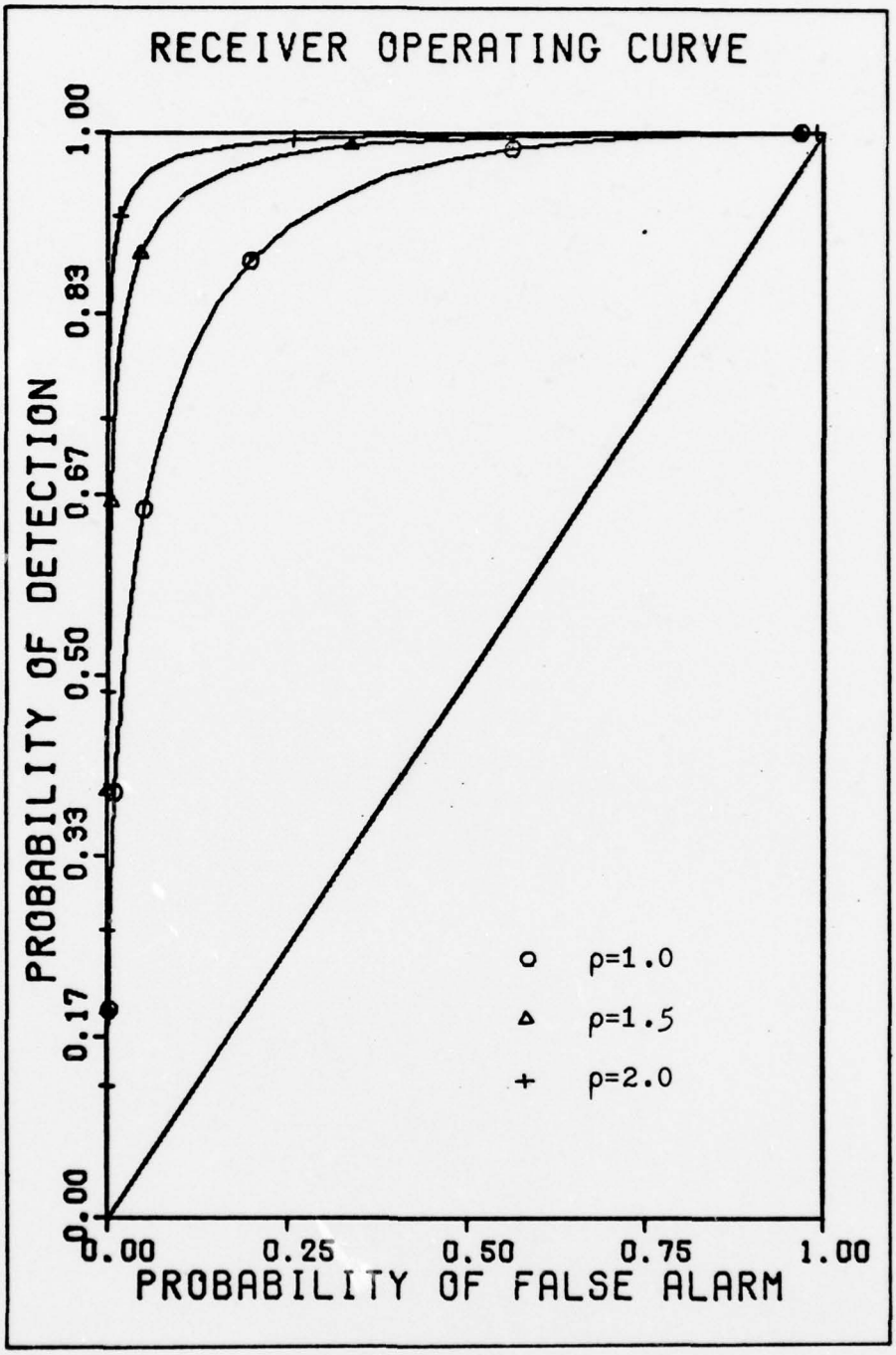

Fig. 30. Ad-hoc Processor #1 ROC, Change in Variance

These density functions can be expressed in terms of the parameters m_{i0}, m_{i1}, and ρ. For the purpose of performance calculations the value of m_{i0} was arbitrarily chosen to be 2.5 . To make the performance calculations for the ad-hoc linear processor #2 consistent with those for the other processors, m_{i1} was determined by the following equation:

$$m_{i1} = m_{i0}\rho \frac{\eta_1}{\eta_0} \tag{54}$$

where η_0, η_1, and ρ are the channel parameters listed in Tables II and III. As before, the program listed in Appendix D was modified to generate the ROC's for this processor. The resulting performance curves for the ad-hoc linear processor #2 for changes in mean and variance are shown in Figures 31 and 32. For identical parameters, the performance of this processor is also identical to the performance observed for both the non-linear and linear approximate processors.

Performance Parameter Dependence

In an effort to determine the manner in which receiver performance depends upon the parameters η_0, η_1, and ρ, functions of these parameters were tested against previous results.

The first function tested was $\eta_1-\eta_0$. For the parameters listed in Table II, this function has the values 8.0, 16.0, and 24.0 . To test the dependence of receiver performance upon this function, η_0 was set equal to 0.0 and η_1 set equal to 8.0, 16.0, and 24.0 . The resulting performance curves

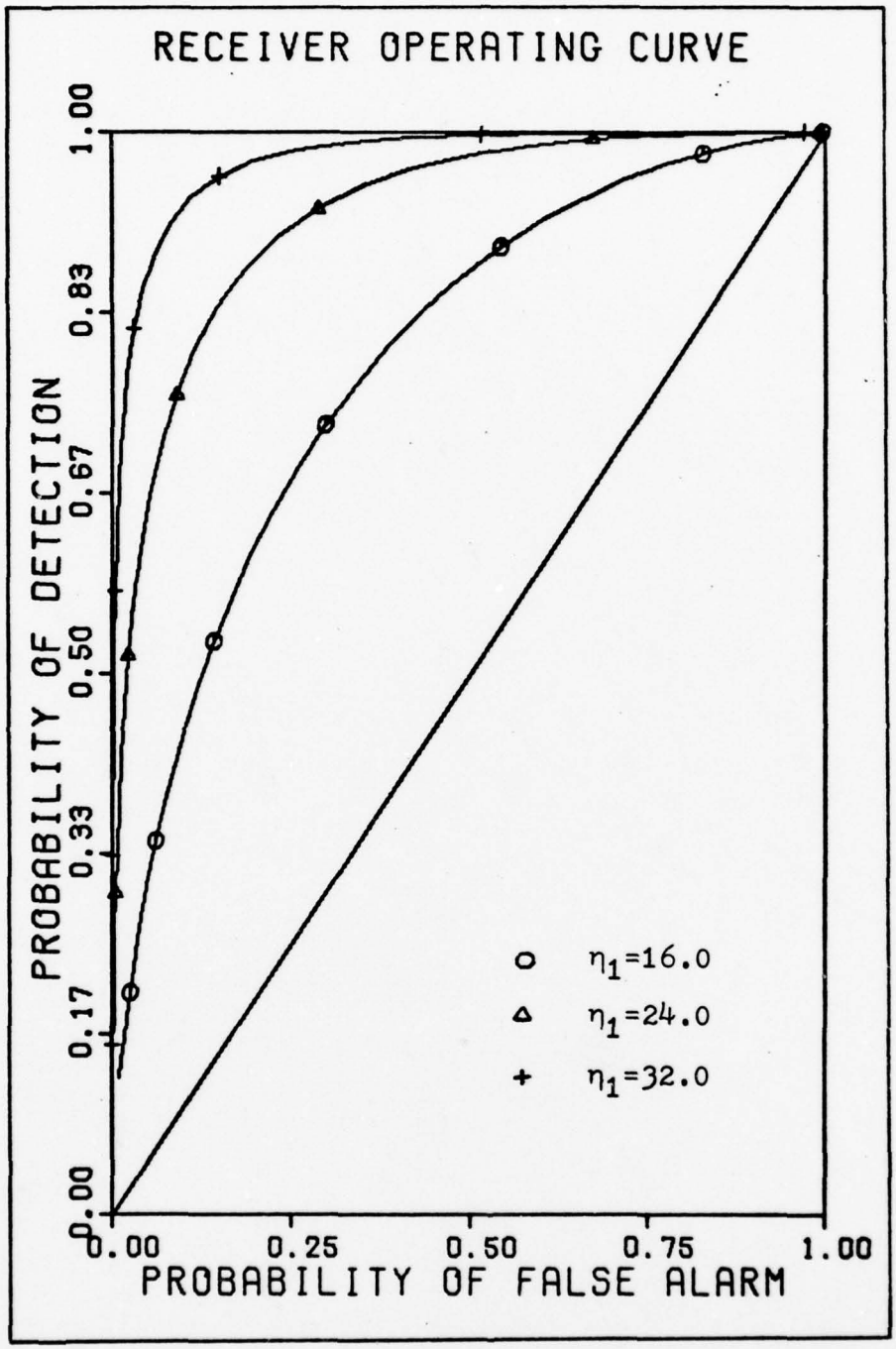

Fig. 31. Ad-hoc Processor #2 ROC, Change in Mean

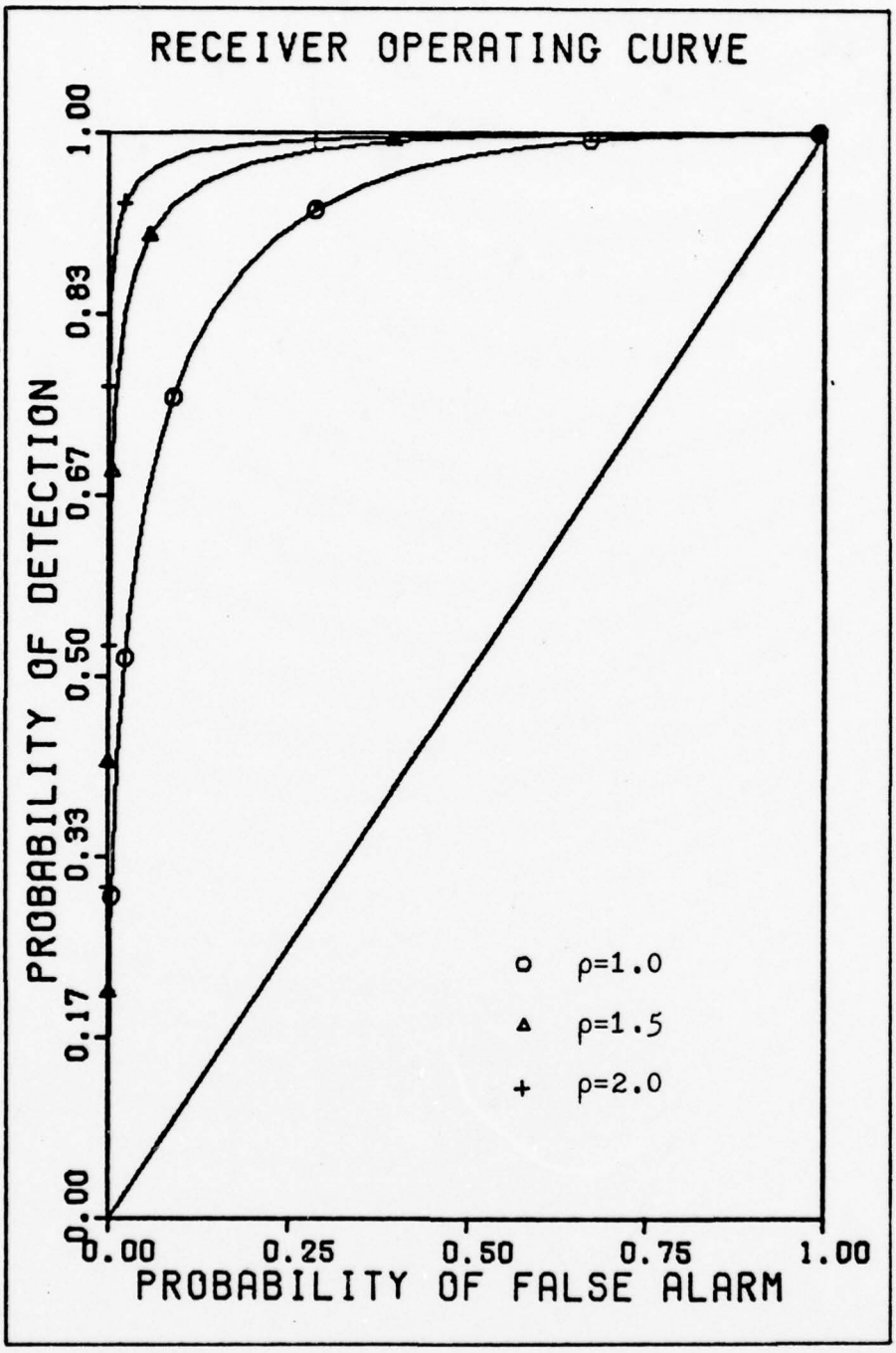

Fig. 32. Ad-hoc Processor #2 ROC, Change in Variance

for the non-linear approximate processor are shown in Figure 33. Comparing performance with that of Figure 15, it is obvious that receiver performance does not depend upon the difference between the hypothesis mean to variance ratios.

The next function tested after analyzing the previous results was $\sqrt{\eta_1} - \sqrt{\eta_0}$. For the parameters listed in Table II, this function has the values 1.17, 2.07, and 2.82 . To test the dependence of receiver performance upon this function, η_0 was set equal to 6.0 and η_1 set to 13.112, 20.43, and 27.856 . The resulting performance curves for the non-linear approximate processor are shown in Figure 34. Comparing these performance curves with those of Figure 15, it is apparent that performance is identical. One may conclude from this result that receiver performance depends upon the difference between the square roots of the hypothesis mean to variance ratios. This differs from the Gaussian signal case where receiver performance depends upon the difference between the hypothesis mean to standard deviation ratios, $m_{i1}/\sigma_{i1} - m_{i0}/\sigma_{i0}$. Determination of receiver performance dependence upon functions also involving ρ were unsuccessful.

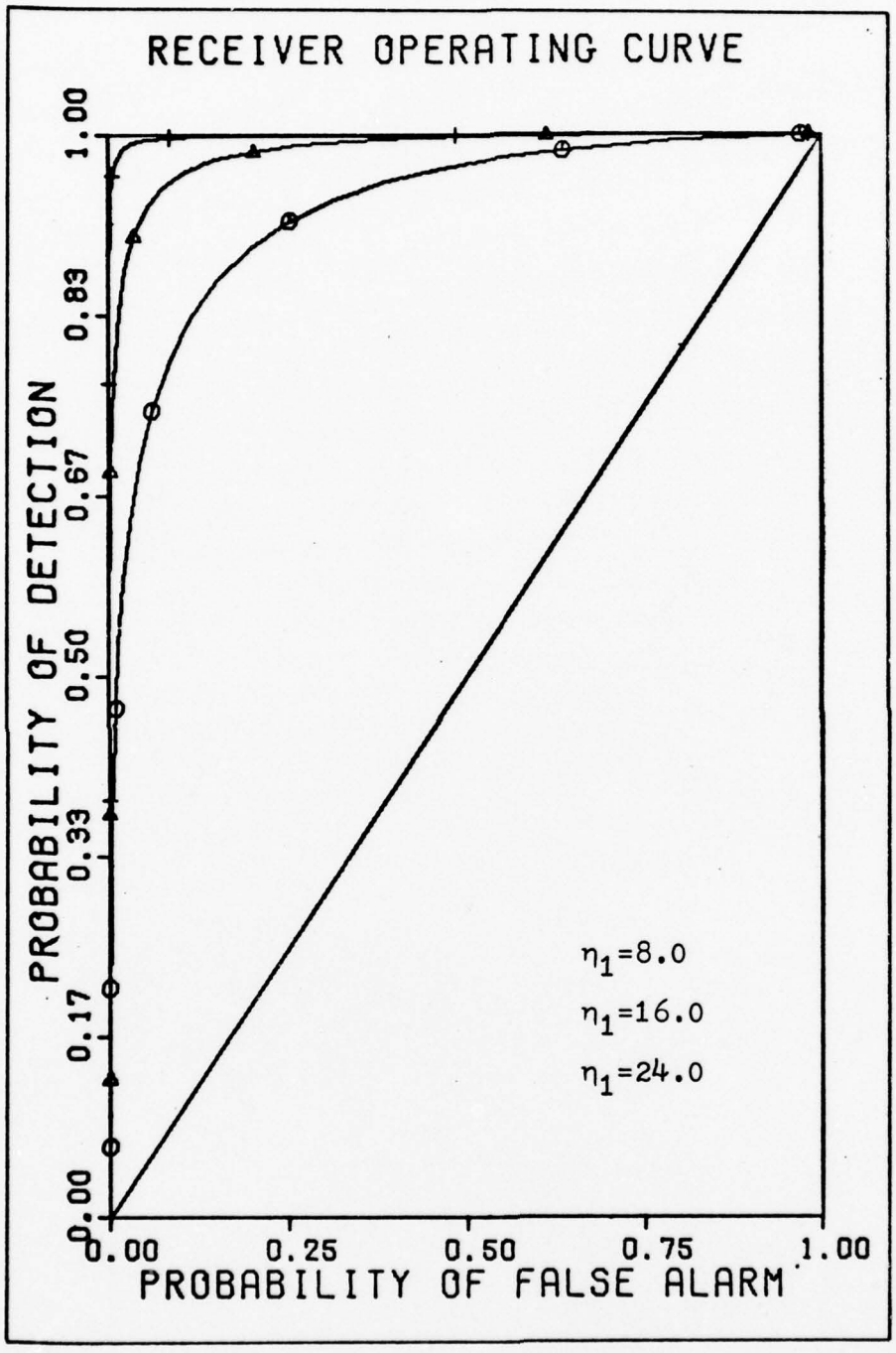

Fig. 33. Functional Receiver Performance Dependence, η_1-η_0

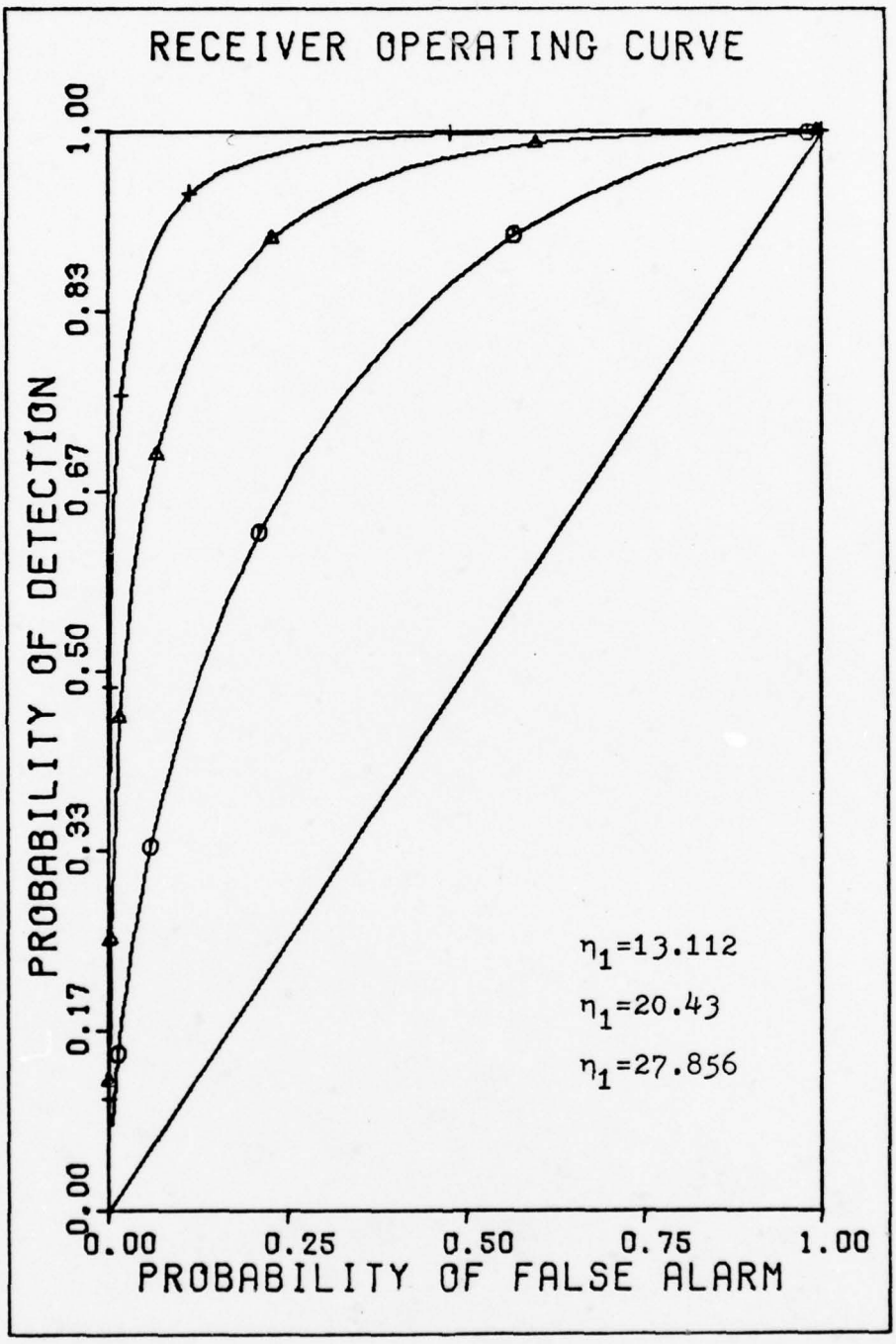

Fig. 34. Functional Receiver Performance Dependence, $\sqrt{\eta_1}-\sqrt{\eta_0}$

V. Conclusions and Recommendations

The results of this thesis indicate a number of conclusions and also suggest a number of areas for further study.

Conclusions

The following conclusions are made by this study:

The non-central chi-square statistical detector output model appears to be valid. The model has a realistic physical basis in the complex Gaussian random process used to model the received infrared field and is further supported by available experimental infrared background statistical data.

Receiver performance equal to that of either the non-linear approximate processor or the linear approximate processor derived from the optimal signal processor can be obtained using a relatively simple ad-hoc linear reciever.

Receiver performance depends upon the difference between the square roots of the hypothesis mean to variance ratios $(\sqrt{m_{i1}/\sigma_{i1}^2} - \sqrt{m_{i0}/\sigma_{i0}^2})$ and the ratio of hypothesis variances $(\sigma_{i1}^2/\sigma_{i0}^2)$.

Receiver performance improves as the number of receiver channels and the number of looks increase.

Recommendations

The following are recommendations of areas for further study pertaining to multichannel infrared receiver performance:

While the statistical detector output model appears to be valid, raw experimental infrared background data should be

analyzed to validate the model for different types of backgrounds. This might be accomplished by analyzing the raw LMSC Background Measurements Program data or by original experiment.

Another area for futher study is to determine a statistical model for the infrared emissions of anti-aircraft missiles and to determine the effects of this model upon the overall signal statistics.

The attempts to obtain analytic performance expressions were frustrated by the complexity of the mathematics involved with the non-central chi-square probability density function. It may be possible to simplify the required mathematics and gain some insight into receiver performance dependence by using Gaussian approximations to the non-central chi-square pdf. Possible approximations to the non-central chi-square pdf are suggested in a University of Michigan technical report titled "Approximations to the Noncentral Chi Square Distributions with Applications to Signal Detection Models" (Ref 9).

While it has been determined that the four signal processor structures examined in this thesis have equal performance, it is not known how this performance compares with that of the optimal processor. It is possible to calculate optimal processor performance numerically by first computing the conditional detector output density functions and then process these density functions according to the optimal processor algorithm to obtain the conditional processor output density

functions. These pdf's can then be numerically integrated to obtain receiver operating curves comparable to those of the other processors.

Other areas for futher study might include temporal signal processing, adaptive receivers, and determination of parameter dependence for multichannel and multi-look receiver performance.

Bibliography

1. Campbell, George A. and R. M. Foster. Fourier Integrals for Practical Applications. New York: Van Nostrand Co., Inc., 1948.

2. Gallager, Robert G. Information Theory and Reliable Communication. New York: John Wiley and Sons, Inc., 1968.

3. Hoversten, E. V. "Optical Communication Theory." Laser Handbook. F. T. Arecchi and E. D. Schultz-Dubois, Eds. Amsterdam: North-Holland Pub. Co., 1972.

4. Itakura, Yasumasa., et al. "Statistical Properties of the Background Noise for the Atmospheric Windows in the Intermediate Infrared Region." Infrared Physics, 14: 17-29 (February 1974).

5. Kulgein, Norman G. Background Measurements Program. Special Technical Report LMSC-D502556. Palo Alto, California: Lockheed Missile and Space Co., May 1976.

6. Kulgein, Norman G. Background Measurements Program. Second Special Technical Report LMSC-D506988. Palo Alto, California: Lockheed Missile and Space Co., September 1976.

7. LMSC. Background Measurements Program. Second Semiannual Technical Report LMSC-D501944. Palo Alto, California: Lockheed Missile and Space Co., April 1976.

8. LMSC. Background Measurements Program. Third Semiannual Technical Report LMSC-D506926. Palo Alto, California: Lockheed Missile and Space Co., September 1976.

9. Lamphiear, D. E. and T. G. Birdsall. Approximations to the Noncentral Chi Square Distributions with Applications to Signal Detection Models. University of Michigan technical report 101. Ann Arbor: University of Michigan, May 1960.

10. Papoulis, A. Probability, Random Variables, and Stochastic Processes. New York: McGraw-Hill, Inc., 1965.

11. Robinson, S. and J. Gobien. "Processing of Multi-Spectral Optical Sensor Signals." Proceedings of the IEEE 1977 National Aerospace and Electronics Conference: 580-587 (1977).

12. Van Trees, Harry L. Detection, Estimation, and Modulation Theory: Part I. New York: John Wiley and Sons, Inc., 1968.

13. Van Trees, Harry L. Detection, Estimation, and Modulation Theory: Part III. New York: John Wiley and Sons, Inc., 1971.

Appendix A

The combined relative frequency plots for filters 4, 5, and 6 are illustrated in Figures A-1, A-2, and A-3. These plots closely approximate the experimental histograms obtained by LMSC for the corresponding filter. Figures A-4 and A-5 are plots of the estimated pdf parameters as a function of filter bandwidth. There appears to be a nearly linear relationship between density parameters and filter bandwidth, with deviations resulting from parameter estimation error. For Figures A-4 and A-5, the left edge of each filter is fixed at 4.39 μm in all cases.

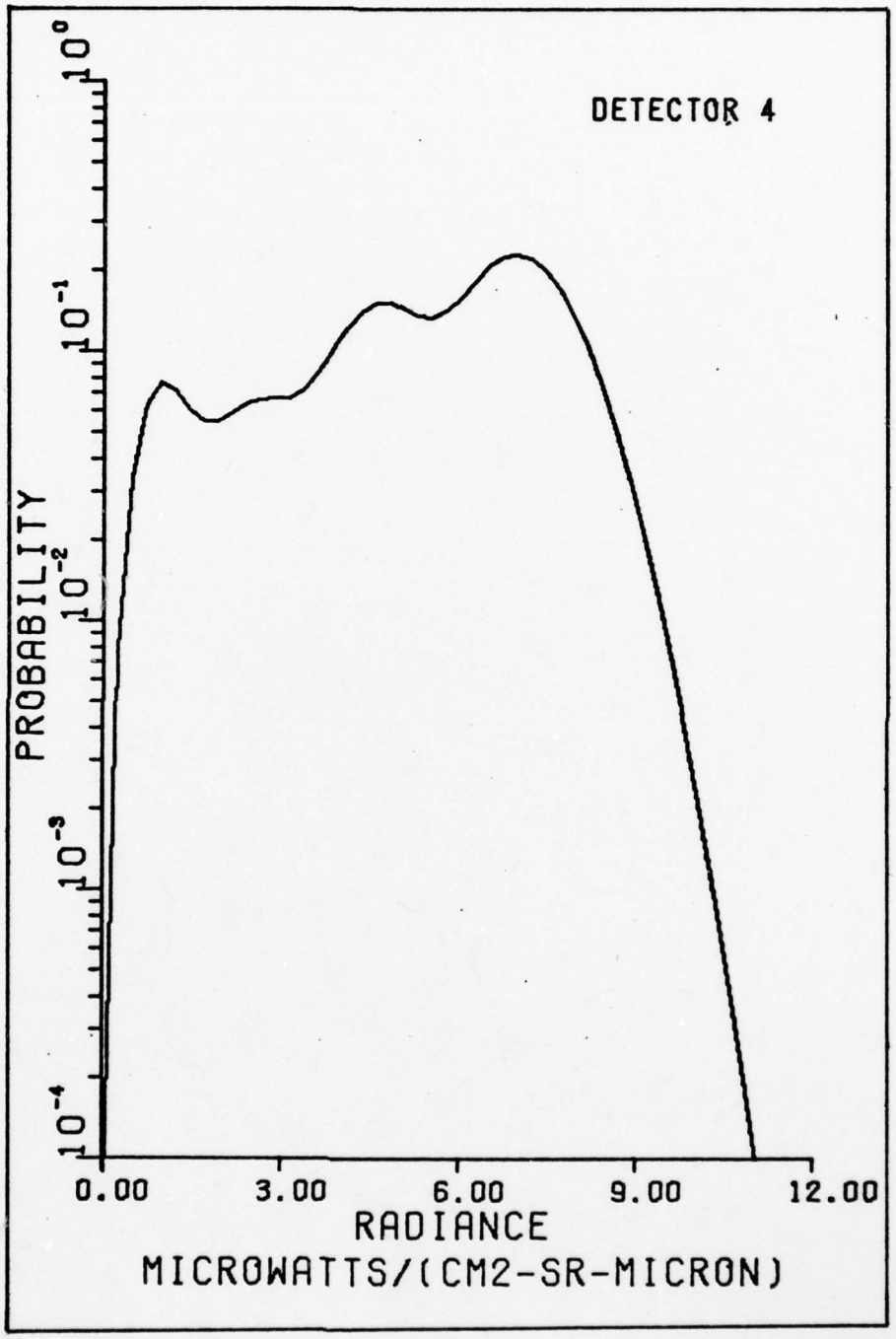

Fig. A-1. Relative Frequency Plot, Filter 4

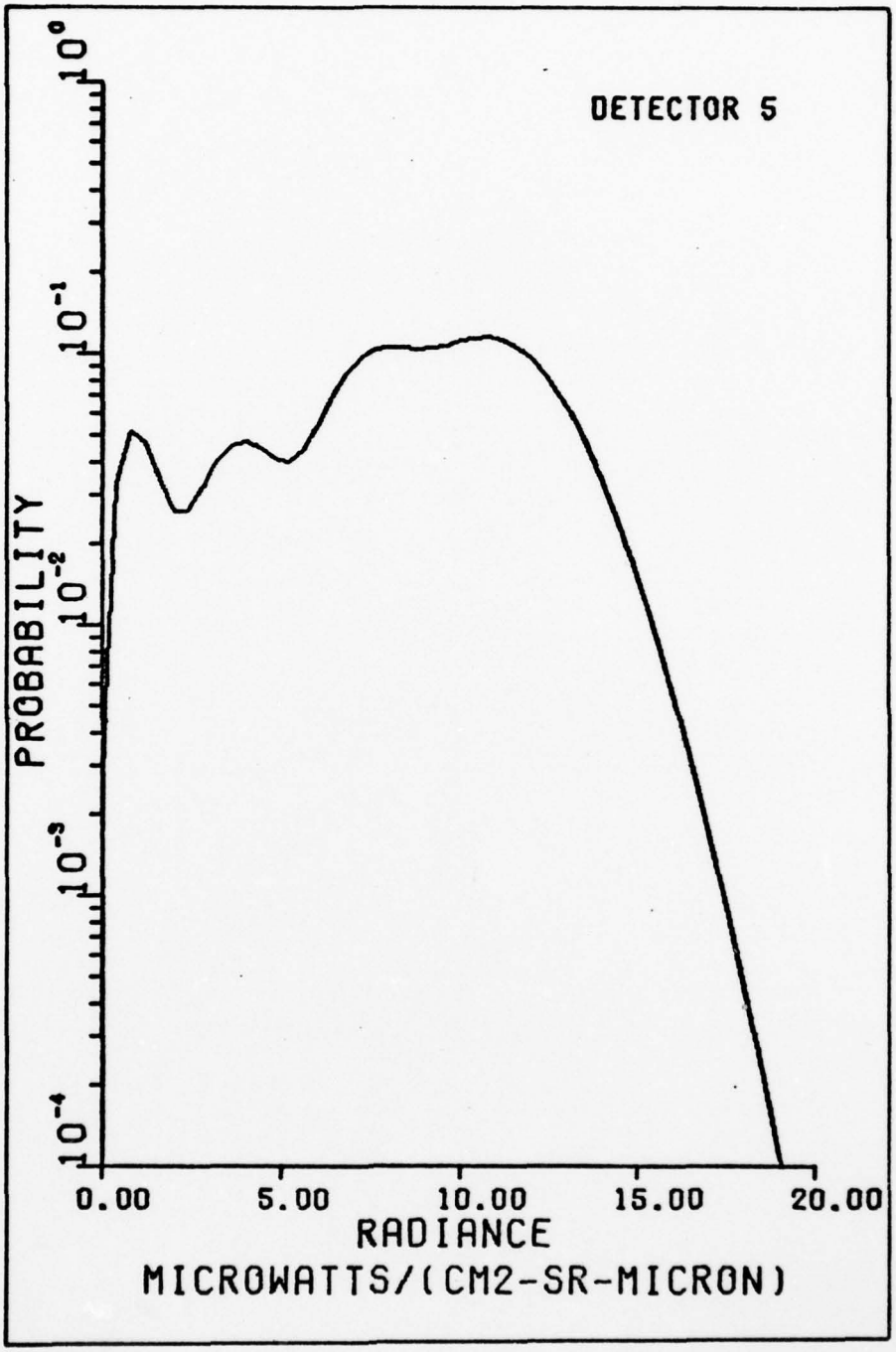

Fig. A-2. Relative Frequency Plot, Filter 5

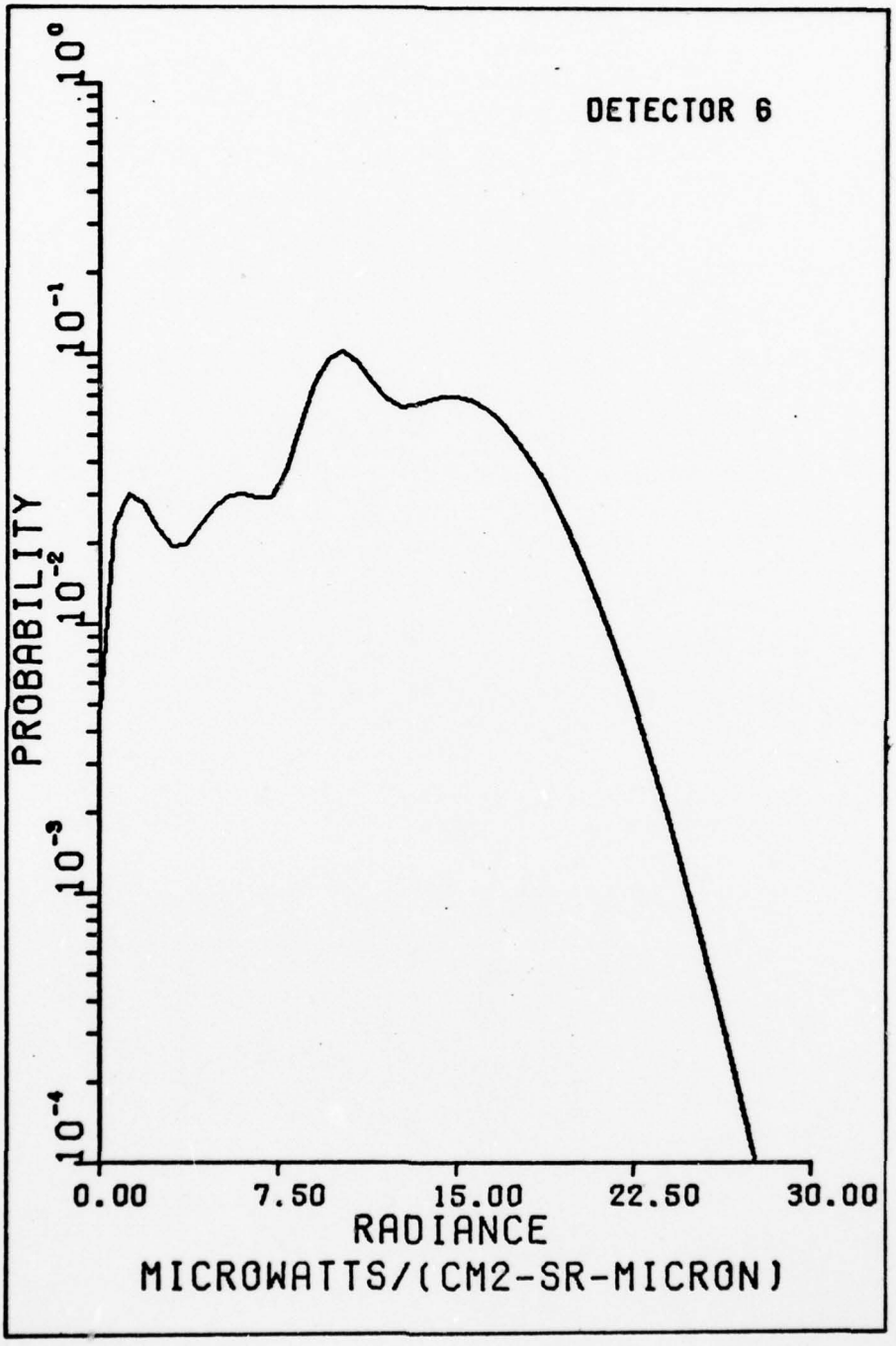

Fig. A-3. Relative Frequency Plot, Filter 6

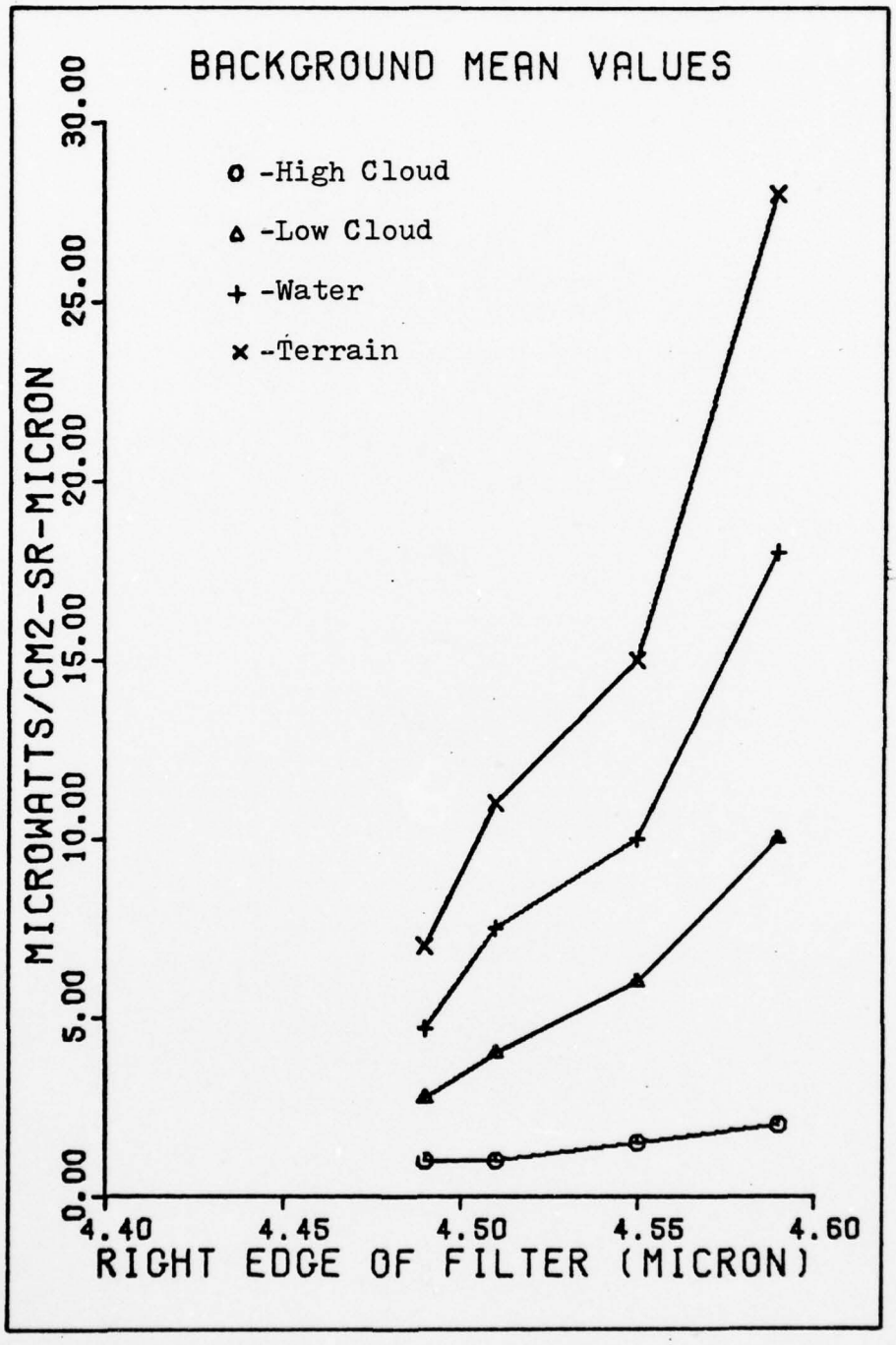

Fig. A-4. Background Mean Values

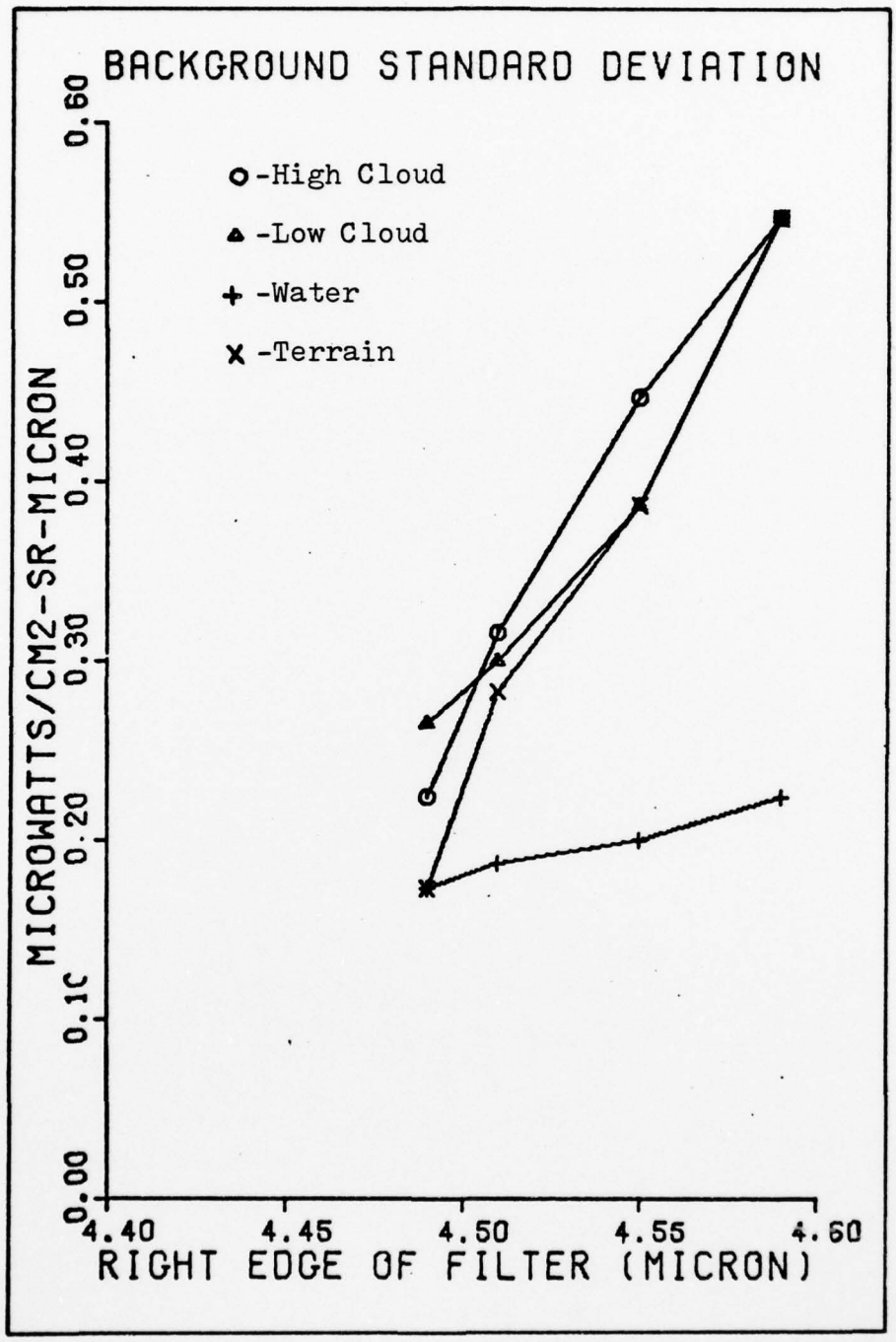

Fig. A-5. Background Standard Deviation

Appendix B

The following program listing is typical of the FORTRAN programs used to generate receiver performance curves for the non-linear approximate processor.

```
      PROGRAM GRAPH (INPUT,OUTPUT,PLOT)
      INTEGER POINT
      DIMENSION Y(602),D0(602),D1(602)
      DIMENSION PFA(40),PD(40)
      DATA FAMIN,DMIN,FAD,DD/0.0,0.0,0.25,0.16667/
      CALL PLOT(0.,-3.0,-3)
      CALL PLOT(0.,2.5,-3)
      CALL PLOT(0.0,6.0,3)
      CALL PLOT(4.0,6.0,2)
      CALL PLOT(4.0,0.0,2)
      CALL PLOT(4.0,6.0,3)
      CALL PLOT(0.0,0.0,2)
      CALL AXIS(0.,0.,26HPROBABILITY OF FALSE ALARM,-26,4.0,
     +0.0,FAMIN,FAD)
      CALL AXIS(0.,0.,24HPROBABILITY OF DETECTION,24,6.0,90.,
     +DMIN,DD)
      CALL SYMBOL(0.25,6.4,0.14,24HRECEIVER OPERATING CURVE,
     +0.0,24)
*
*     POINT  = NUMBER OF DATA POINTS IN EACH DENSITY
*     INDEX J = NUMBER OF DATA SETS
*
      POINT=240
      ETA0=8.0
      ETA1=24.0
      RHO=1.0
*
*     COMPUTE H0 AND H1 DENSITIES FOR EQUAL VARIANCE
*
      DI0=2.0*((ETA1/RHO)-2.0*SQRT(ETA1*ETA0/RHO)+ETA0)
      CI0=SQRT(ETA0)/(SQRT(ETA1/RHO)-SQRT(ETA0))
      DI1=RHO*DI0
      CI1=SQRT(ETA1)/(SQRT(ETA1)-SQRT(ETA0*RHO))
      IF(CI0.LT.0.0) CI0=ABS(CI0)
      IF(CI1.LT.0.0) CI1=ABS(CI1)
      DO 50 I=1,POINT
      Y(I)=0.1*(FLOAT(I-1))
      D0(I)=XCHINL(Y(I),ETA0,CI0,DI0)
      D1(I)=XCHINL(Y(I),ETA1,CI1,DI1)
   50 CONTINUE
*
*     CALCULATE ROC POINTS
*
      N=0
      DO 75 M=30,138,4
      N=N+1
      PFA(N)=GRAL(D0,M,POINT)
      PD(N)=GRAL(D1,M,POINT)
   75 CONTINUE
```

```
*
*     PLOT THE RECEIVER OPERATION CURVE (ROC) : PD VS PFA
*
      PFA(N+1)=PD(N+1)=0.0
      PFA(N+2)=0.25
      PD(N+2)=0.16667
      CALL LINE(PFA,PD,N,1,5,1)
*
*     CONTINUE FOR DENSITIES WITH UNEQUAL VARIANCE
*
      READ*,POINT
      DO 300 J=2,3
      READ*,ETA0,ETA1,RHO
*
*     COMPUTE H0 AND H1 DENSITIES
*
      A=SQRT(ETA1)-SQRT(ETA0*RHO)
      B=SQRT(ETA1/RHO)-SQRT(ETA0)
      C=1.0-(1.0/RHO)
      D=RHO-1.0
      E=(ETA1/RHO)+ETA0-(2.0*SQRT(ETA0*ETA1/RHO))
      F=ETA1+(RHO*ETA0)-(2.0*SQRT(ETA0*ETA1*RHO))
      G=2.0*E/C
      DO 100 I=1,POINT
      Y(I)=0.1*FLOAT(I-1)
      D0(I)=XNL(Y(I),ETA0,RHO,A,C,F,G,B,E)
      D1(I)=XNL(Y(I),ETA1,RHO,A,D,F,G,A,F)
  100 CONTINUE
      CALL SCALE(D0,4.0,POINT,1)
      CALL SCALE(D1,4.0,POINT,1)
      THR=D0(POINT+2)
*
*     FIND THE STARTING POINT OF H0 DENSITY,INDEX K
*
      DO 110 I=1,POINT
      IF(D0(I).GT.THR) GO TO 120
  110 CONTINUE
  120 K=(INT(FLOAT(I)/2.0))*2
*
*     FIND END POINT OF H1 DENSITY, INDEX L
*
      THR=D1(POINT+2)
      DO 130 I=1,POINT
      IF(D1(I).GT.THR) GO TO 140
  130 CONTINUE
  140 DO 150 L=I,POINT
      IF(D1(L).LT.THR) GO TO 160
  150 CONTINUE
  160 L=(INT(FLOAT(L)/2.0))*2
```

```
*
*     THIS SECTION DIVIDES THE DIFFERENCE BETWEEN THE CHOSEN
*     BEGINNING AND END POINTS OF THE DENSITIES BY 30 TO GET
*     THE LOOP INCREMENT INDEX, I, SO AS TO CALCULATE 30 ROC
*     POINTS OVER THE SIGNIFICANT PORTIONS OF THE DENSITIES
*
      I=INT(FLOAT(L-K)/30.+0.5)
      IF(I.EQ.0) I=1
      PRINT*,"ROC PARAMETERS  ",K,L,I
      PRINT*," "
      N=0
      DO 200 M=K,L,I
      N=N+1
      PFA(N)=GRAL(D0,M,POINT)
      PD(N)=GRAL(D1,M,POINT)
  200 CONTINUE
      PFA(N+1)=PD(N+1)=0.0
      PFA(N+2)=0.25
      PD(N+2)=0.15667
*
*   PLOT THE RECEIVER OPERATION CURVE (ROC) : PD VS PFA
*
      CALL LINE(PFA,PD,N,1,5,J)
  300 CONTINUE
      CALL PLOTE(N)
      STOP
      END


*
*     THIS FUNCTION COMPUTES THE OUTPUT DENSITY FOR THE NON-
*     LINEAR PROCESSOR WHEN THE VARIANCES ARE NOT EQUAL FOR
*     THE TWO HYPOTHESES, IE. RHO IS GREATER THAN ONE.
*
      FUNCTION XNL(Y,ETA,R,AA,BB,CC,DD,EE,FF)
      DOUBLE V
      V=(Y+(2.*DD)-2.*SQRT(Y*DD+DD*DD))/BB
      V=-(V+(ETA/2.0))
      X=(1./BB)-(AA/(BB*SQRT((Y*(R-1.)/2.0)+CC)))
      X=ABS(X)
      Z1=X*DEXP(V)
      Z2=2.0*SQRT(ETA)/BB
      Z2=Z2*(SQRT((Y*BB/2.0)+FF)-EE)
      Z2=FI0(Z2)
      XNL=Z1*Z2
      RETURN
      END
```

```
*
*     THIS FUNCTION COMPUTES A POINT ON THE NON-LINEAR
*     PROCESSOR OUTPUT DENSITY WHEN THE VARIANCES ARE EQUAL
*
      FUNCTION XCHINL(Y,ETA,CI,DI)
      DOUBLE V
      V=-((Y**2)/DI+ETA/2.0)
      Z1=2.0*DEXP(V)*ABS(Y)/DI
      Z2=FI0(Y*CI)
      XCHINL=Z1*Z2
      RETURN
      END


*
*     THIS FUNCTION COMPUTES THE MODIFIED BESSEL FUNCTION OF
*     THE FIRST KIND OF ORDER ZERO
*
      FUNCTION FI0(X)
      DIMENSION XL(6),XH(8)
      DOUBLE W
      DATA XL/3.5156229,3.0899424,1.2067492,0.2659732,0.0360768,
     10.0045813/,XH/0.01328592,0.00225319,-0.00157565,0.00916281,
     2-0.02057706,0.02635537,-0.01647633,0.00392377/
      W=X
      XA=ABS(X)
      IF (XA.GT.0.0001) GO TO 10
      FI0=1.0
      RETURN
   10 IF (X.GT.0) GO TO 20
      X=XA
   20 T=X/3.75
      IF (T.GT.1.0) GO TO 40
      FI0=1.0
      DO 30 J=1,6
      FI0=FI0+XL(J)*(T**(2*J))
   30 CONTINUE
      RETURN
   40 FI0=0.39894228
      TI=1.0/T
      DO 50 J=1,8
      FI0=FI0+XH(J)*(TI**J)
   50 CONTINUE
      FI0=FI0*DEXP(W)*(1.0/SQRT(X))
      RETURN
      END
```

```
*
*     THIS FUNCTION COMPUTES THE INTEGRAL OF THE FUNCTION
*     CONTAINED IN THE ARRAY A USING A SIMPLE RECTANGULAR
*     SUMMATION ALGORITHM
*
      FUNCTION GRAL (A,J,K)
      DIMENSION A(K)
      M=K-2
      GRAL=0.0
      DO 100 I=J,M,2
      GRAL=GRAL+A(I)+A(I+2)
  100 CONTINUE
      GRAL=0.1*GRAL
      RETURN
      END
```

AD-A052 937 AIR FORCE INST OF TECH WRIGHT-PATTERSON AFB OHIO SCH--ETC F/G 17/5
MULTICHANNEL INFRARED RECEIVER PERFORMANCE.(U)
DEC 77 S J DUNNING

UNCLASSIFIED AFIT/GE/EE/77-15 NL

2 OF 2
AD
A052937

END
DATE
FILMED
5-78
DDC

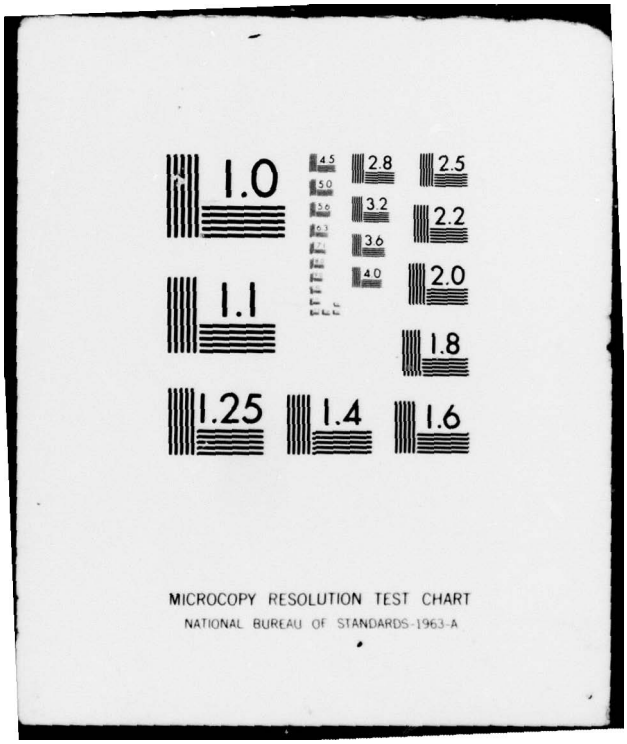
1.0
1.1
1.25
1.4
1.6
1.8
2.0
2.2
2.5
2.8
3.2
3.6
4.0
4.5
5.0
5.6
6.3
7.1
MICROCOPY RESOLUTION TEST CHART
NATIONAL BUREAU OF STANDARDS-1963-A

Appendix C

The following program listing is typical of the FORTRAN programs used to generate multichannel receiver performance curves for the non-linear and linear approximate processors.

```
      PROGRAM GRAPH (INPUT,OUTPUT,PLOT)
      INTEGER POINT
      COMPLEX A(512),B(512),C(512),D(512)
      DIMENSION Y(514),D0(514),D1(514)
      DIMENSION PFA(50),PD(50)
      DATA FAMIN,DMIN,FAD,DD/0.0,0.0,0.25,0.16667/
      CALL PLOT(0.,-3.0,-3)
      CALL PLOT(0.,2.5,-3)
      CALL PLOT(0.0,6.0,3)
      CALL PLOT(4.0,6.0,2)
      CALL PLOT(4.0,0.0,2)
      CALL PLOT(4.0,6.0,3)
      CALL PLOT(0.0,0.0,2)
      CALL AXIS(0.,0.,26HPROBABILITY OF FALSE ALARM,-26,4.0,
     +0.0,FAMIN,FAD)
      CALL AXIS(0.,0.,24HPROBABILITY OF DETECTION,24,6.0,90.,
     +DMIN,DD)
      CALL SYMBOL(0.25,6.4,0.14,24HRECEIVER OPERATING CURVE,
     +0.0,24)
*
*     POINT  = NUMBER OF DATA POINTS IN EACH DENSITY
*     INDEX J = NUMBER OF DATA SETS
*     IFFT = NUMBER OF FFT POINTS
*     NFFT = LOG2(IFFT)
*     NCHAN = NUMBER OF CHANNELS
*     DELTA = DIFFERENCE BETWEEN DENSITY POINTS
*
      DO 300 J=1,3
      READ*,POINT,IFFT,NFFT,NCHAN
*
*     INITIALIZE COMPLEX MULTIPLIER
*
      DO 10 I=1,IFFT
      B(I)=(1.0,0.0)
      D(I)=(1.0,0.0)
   10 CONTINUE
      DELTA=0.1
      DO 50 JJ=1,NCHAN
      READ*,ETA0,ETA1,RHO
*
*     COMPUTE CHANNEL DENSITIES
*
      DI0=2.0*((ETA1/RHO)-2.0*SQRT(ETA1*ETA0/RHO)+ETA0)
      CI0=SQRT(ETA0)/(SQRT(ETA1/RHO)-SQRT(ETA0))
      DI1=RHO*DI0
      CI1=SQRT(ETA1)/(SQRT(ETA1)-SQRT(ETA0*RHO))
      DO 20 I=1,POINT
      Y(I)=DELTA*FLOAT(I-1)
      A(I)=XCHINL(Y(I),ETA0,CI0,DI0)
      C(I)=XCHINL(Y(I),ETA1,CI1,DI1)
   20 CONTINUE
```

```
*
*     ZERO FILL
*
      KK=POINT+1
      DO 30 I=KK,IFFT
      Y(I)=DELTA*FLOAT(I-1)
      A(I)=(0.0,0.0)
      C(I)=(0.0,0.0)
   30 CONTINUE
*
*     TAKE FFT OF DENSITIES
*
      CALL FFT(A,NFFT,IFFT,-1)
      CALL FFT(C,NFFT,IFFT,-1)
*
*     PERFORM CONVOLUTION BY MULTIPLYING TRANSFORMS
*
      DO 40 I=1,IFFT
      B(I)=A(I)*B(I)
      D(I)=C(I)*D(I)
   40 CONTINUE
*
*     RETURN FOR NEXT CHANNEL
*
   50 CONTINUE
*
*     TAKE INVERSE TRANSFORM TO GET JOINT DENSITIES
*
      CALL FFT(B,NFFT,IFFT,+1)
      CALL FFT(D,NFFT,IFFT,+1)
*
*     SCALE AND SET TO REAL VALUES
*
*     T SCALES DATA TO ACCOUNT FOR DIFFERENCES IN THE DELTAS
*     SINCE THE FFT ALGORITHM ASSUMES A DELTA OF 1
*
      T=DELTA**NCHAN
      DO 60 I=1,IFFT
      D0(I)=T*B(I)/IFFT
      D1(I)=T*D(I)/IFFT
   60 CONTINUE
*
*     COMPUTE ROC FOR MULTICHANNEL PROCESSOR
*     DENSITY IS NOW COMPOSED OF IFFT POINTS
*
      POINT=IFFT
      CALL SCALE(D0,4.0,POINT,1)
      CALL SCALE(D1,4.0,POINT,1)
      THR=D0(POINT+2)
```

```
*
*     FIND THE STARTING POINT OF H0 DENSITY,INDEX K
*
      DO 110 I=1,POINT
      IF(D0(I).GT.THR) GO TO 120
  110 CONTINUE
  120 K=(INT(FLOAT(I)/2.0))*2
      IF(K.LE.0) K=1
*
*     FIND END POINT OF H1 DENSITY, INDEX L
*
      THR=D1(POINT+2)
      DO 130 I=1,POINT
      IF(D1(I).GT.THR) GO TO 140
  130 CONTINUE
  140 DO 150 L=I,POINT
      IF(D1(L).LT.THR) GO TO 160
  150 CONTINUE
  160 L=(INT(FLOAT(L)/2.0))*2
*
*     THIS SECTION DIVIDES THE DIFFERENCE BETWEEN THE CHOSEN
*     BEGINNING AND END POINTS OF THE DENSITIES BY 30 TO GET
*     THE LOOP INCREMENT INDEX, I, SO AS TO CALCULATE 30 ROC
*     POINTS OVER THE SIGNIFICANT PORTIONS OF THE DENSITIES
*
      I=INT(FLOAT(L-K)/30.+0.5)
      IF(I.EQ.0) I=1
      PRINT*,"ROC PARAMETERS  ",K,L,I
      PRINT*," "
      N=0
      DO 200 M=K,L,I
      N=N+1
      PFA(N)=GRAL(D0,M,POINT)
      PD(N)=GRAL(D1,M,POINT)
  200 CONTINUE
      PFA(N+1)=PD(N+1)=0.0
      PFA(N+2)=0.25
      PD(N+2)=0.16667
*
*   PLOT THE RECEIVER OPERATION CURVE (ROC) : PD VS PFA
*
      CALL LINE(PFA,PD,N,1,5,J)
  300 CONTINUE
      CALL PLOTE(N)
      STOP
      END
```

```
*
*     FAST FOURIER TRANSFORM SUBROUTINE
*
      SUBROUTINE FFT(A,M,N,IS)
*
*        A = COMPLEX INPUT ARRAY OF SAMPLES
*        M = LOG2(N)
*        N = 2 ** M =NUMBER OF SAMPLES
*       IS = -1, FORWARD TRANSFORM
*          = +1, INVERSE TRANSFORM (UNNORMALIZED)
*
      COMPLEX A,U,W,T
      DIMENSION A(N)
      DATA PI/3.14159265/
      NV2=N/2
      NM1=N-1
      J=1
      DO 30 I=1,NM1
      IF(I.GE.J) GO TO 10
      T=A(J)
      A(J)=A(I)
      A(I)=T
   10 K=NV2
   20 IF(K.GE.J) GO TO 30
      J=J-K
      K=K/2
      GO TO 20
   30 J=J+K
      DO 80 L=1,M
      LE=2**L
      LE1=LE/2
      U=CMPLX(1.0,0.)
      IF(IS) 40,50,50
   40 W=CMPLX(COS(PI/LE1),-SIN(PI/LE1))
      GO TO 60
   50 W=CMPLX(COS(PI/LE1),SIN(PI/LE1))
   60 DO 80 J=1,LE1
      DO 70 I=J,N,LE
      IP=I+LE1
      T=A(IP)*U
      A(IP)=A(I)-T
   70 A(I)=A(I)+T
   80 U=U*W
      RETURN
      END
```

Appendix D

The following program listing is typical of the FORTRAN programs used to generate receiver performance curves for the linear approximate processor. Subroutines not listed here are listed in Appendices B and C. This program was also used to generate receiver performance curves for the two ad-hoc linear processors after modification of the processor output density function calculation subroutine.

```
      PROGRAM GRAPH (INPUT,OUTPUT,PLOT)
      INTEGER POINT
      DIMENSION Y(602),D0(602),D1(602)
      DIMENSION PFA(40),PD(40)
      DATA FAMIN,DMIN,FAD,DD/0.0,0.0,0.25,0.16667/
*
*     POINT  = NUMBER OF DATA POINTS IN EACH DENSITY
*     INDEX J = NUMBER OF DATA SETS
*
      READ*,POINT
      CALL PLOT(0.,-3.0,-3)
      CALL PLOT(0.,2.5,-3)
      CALL PLOT(0.0,6.0,3)
      CALL PLOT(4.0,6.0,2)
      CALL PLOT(4.0,0.0,2)
      CALL PLOT(4.0,6.0,3)
      CALL PLOT(0.0,0.0,2)
      CALL AXIS(0.,0.,26HPROBABILITY OF FALSE ALARM,-26,4.0,
     +0.0,FAMIN,FAD)
      CALL AXIS(0.,0.,24HPROBABILITY OF DETECTION,24,6.0,90.,
     +DMIN,DD)
      CALL SYMBOL(0.25,6.4,0.14,24HRECEIVER OPERATING CURVE,
     +0.0,24)
      DO 300 J=1,3
      READ*,ETA0,ETA1,RHO
*
*     COMPUTE H0 AND H1 DENSITIES
*
      DI0=1.0-(1.0/RHO)+((ETA1/RHO)-ETA0)/2.0
      DI1=(RHO-1.0)+(ETA1-(RHO*ETA0))/2.0
      PRINT*," DI0= ",DI0,"  DI1= ",DI1
      PRINT*," "
      IF (DI0.LT.0.0) DI0=ABS(DI0)
      IF (DI1.LT.0.0) DI1=ABS(DI1)
      DO 100 I=1,POINT
      Y(I)=FLOAT(I)-1.
      D0(I)=XCHI(Y(I),ETA0,DI0)
      D1(I)=XCHI(Y(I),ETA1,DI1)
  100 CONTINUE
      CALL SCALE(D0,4.0,POINT,1)
      CALL SCALE(D1,4.0,POINT,1)
      THR=D0(POINT+2)
*
*     FIND THE STARTING POINT OF H0 DENSITY,INDEX K
*
      DO 110 I=1,POINT
      IF(D0(I).GT.THR) GO TO 120
  110 CONTINUE
  120 K=(INT(FLOAT(I)/2.0))*2
      IF(K.LE.0) K=1
```

```
*
*     FIND END POINT OF H1 DENSITY, INDEX L
*
      THR=D1(POINT+2)
      DO 130 I=1,POINT
      IF(D1(I).GT.THR) GO TO 140
  130 CONTINUE
  140 DO 150 L=I,POINT
      IF(D1(L).LT.THR) GO TO 160
  150 CONTINUE
  160 L=(INT(FLOAT(L)/2.0))*2
*
*     THIS SECTION DIVIDES THE DIFFERENCE BETWEEN THE CHOSEN
*     BEGINNING AND END POINTS OF THE DENSITIES BY 30 TO GET
*     THE LOOP INCREMENT INDEX, I, SO AS TO CALCULATE 30 ROC
*     POINTS OVER THE SIGNIFICANT PORTIONS OF THE DENSITIES
*
      I=INT(FLOAT(L-K)/30.+0.5)
      IF(I.EQ.0) I=1
      PRINT*,"ROC PARAMETERS  ",K,L,I
      PRINT*," "
      N=0
      DO 200 M=K,L,I
      N=N+1
      PFA(N)=GRAL(D0,M,POINT)
      PD(N)=GRAL(D1,M,POINT)
  200 CONTINUE
      PFA(N+1)=PD(N+1)=0.0
      PFA(N+2)=0.25
      PD(N+2)=0.16667
*
*    PLOT THE RECEIVER OPERATION CURVE (ROC) : PD VS PFA
*
      CALL LINE(PFA,PD,N,1,5,J)
  300 CONTINUE
      CALL PLOTE(N)
      STOP
      END
*
*     THIS FUNCTION COMPUTES A POINT ON THE LINEAR PROCESSOR
*     OUTPUT DENSITY
*
      FUNCTION XCHI(Y,ETA,DI)
      DOUBLE V
      V=-(Y/DI+ETA/2.0)
      Z1=(1.0/ABS(DI))*DEXP(V)
      Z2=FI0(SQRT((2.0*Y*ETA)/DI))
      XCHI=Z1*Z2
      RETURN
      END
```

Appendix E

Equal Receiver Performance Analysis

This appendix demonstrates analytically that the non-linear approximate processor and the linear approximate processor have equal performance. For simplicity, a single channel processor with equal conditional variances is assumed.

Using Eqs (34), (35), and (36) the performance parameters probability of detection and probability of false alarm can be defined for the non-linear approximate processor. These parameters are given by

$$P_D = \int_0^w \frac{z}{K^2\sigma^2} \exp\left[-\frac{z^2}{2K^2\sigma^2} - \frac{m_1}{2\sigma^2}\right] I_o\left[\frac{z\sqrt{m_1}}{K\sigma^2}\right] dz \qquad (55)$$

$$P_{FA} = \int_w^\infty \frac{z}{K^2\sigma^2} \exp\left[-\frac{z^2}{2K^2\sigma^2} - \frac{m_0}{2\sigma^2}\right] I_o\left[\frac{z\sqrt{m_0}}{K\sigma^2}\right] dz \qquad (56)$$

where $K = c - e = \sqrt{m_1}-\sqrt{m_0}/\sigma^2$ and w is the threshold.

Similarly, using Eqs (34), (35), and (38) performance parameters for the linear approximate processor are given by

$$P_D = \int_0^{w'} \frac{1}{2|K'|\sigma^2} \exp\left[-\frac{z}{2K'\sigma^2} - \frac{m_1}{2\sigma^2}\right] I_o\left[\sqrt{\frac{zm_1}{K'\sigma^4}}\right] dz \qquad (57)$$

$$P_{FA} = \int_{w'}^\infty \frac{1}{2|K'|\sigma^2} \exp\left[-\frac{z}{2K'\sigma^2} - \frac{m_0}{2\sigma^2}\right] I_o\left[\sqrt{\frac{zm_0}{K'\sigma^4}}\right] dz \qquad (58)$$

where $K' = c^2 - e^2/4 = m_1 - m_0/4\sigma^4$ and w' is the threshold.

If the variable transformation given by

$$z = \frac{m_1 - m_0}{4(\sqrt{m_1} - \sqrt{m_0})^2} x^2 \qquad (59)$$

is applied to the expression for P_D for the linear approximate processor given by Eq (57) one obtains

$$P_D = \int_0^t \frac{x}{K^2\sigma^2} \exp\left[- \frac{x^2}{2K^2\sigma^2} - \frac{m_1}{2\sigma^2} \right] I_o\left[\frac{x\sqrt{m_1}}{K\sigma^2} \right] dx \qquad (60)$$

where t is the transformed threshold; $t = 2(\sqrt{m_1} - \sqrt{m_0})\sqrt{\frac{w'}{m_1 - m_0}}$
Comparing this expression with the non-linear approximate processor expression for P_D given by Eq (55), it is observed that the two integrals are of the same form and are equal when $w = t = 2(\sqrt{m_1} - \sqrt{m_0})\sqrt{w'/(m_1 - m_0)}$.

Applying the transformation given by Eq (59) to the expression for P_{FA} for the linear approximate processor yields

$$P_{FA} = \int_t^\infty \frac{x}{K^2\sigma^2} \exp\left[- \frac{x^2}{2K^2\sigma^2} - \frac{m_0}{2\sigma^2} \right] I_o\left[\frac{x\sqrt{m_0}}{K\sigma^2} \right] dx \qquad (61)$$

where t is the transformed threshold defined above. This expression is of the same form as the non-linear approximate processor expression for P_{FA} given by Eq (56). These expressions for P_{FA} are equal when w = t, the identical result

obtained above for probability of detection.

Since there is a one-to-one correspondence between w' and t, corresponding thresholds would generate identical receiver operating points for both the non-linear approximate processor and the linear approximate processor. Because individual operating points are identical, identical receiver operating curves would be generated for both processors over the entire range of thresholds. This verifies the results of the numerical analysis presented in Chapter IV. While not proven here, the numerical results indicate that equal receiver performance between processors can also be expected for the more general case of unequal conditional variances, although the necessary variable transformation is much more complex than the transformation presented here.

VITA

Stephen J. Dunning was born in Denver, Colorado on November 17, 1949. He graduated from high school in Durham, North Carolina in 1967. He received a B.S.E.E. degree from North Carolina State University in 1971 and was commissioned as a second lieutenant in the United States Air Force. After attending technical training at Keesler AFB, Mississippi, he was assigned to the Stategic Air Command (SAC), Offutt AFB, Nebraska as a Communications-Electronics Engineer where he helped set up a SAC Communications Systems Engineering Team. In June 1976, Captain Dunning entered the Air Force Institute of Technology Graduate Electrical Engineering program at Wright-Patterson AFB, Ohio.

Permanent address: 1309 Huntwood Lane
Cary, North Carolina 27511

UNCLASSIFIED
SECURITY CLASSIFICATION OF THIS PAGE (When Data Entered)

REPORT DOCUMENTATION PAGE		READ INSTRUCTIONS BEFORE COMPLETING FORM
1. REPORT NUMBER AFIT/GE/EE/77-15	2. GOVT ACCESSION NO.	3. RECIPIENT'S CATALOG NUMBER
4. TITLE (and Subtitle) MULTICHANNEL INFRARED RECEIVER PERFORMANCE		5. TYPE OF REPORT & PERIOD COVERED MS Thesis 6. PERFORMING ORG. REPORT NUMBER
7. AUTHOR(s) Stephen J. Dunning		8. CONTRACT OR GRANT NUMBER(s)
9. PERFORMING ORGANIZATION NAME AND ADDRESS Air Force Institute of Technology(AFIT-EN) Wright-Patterson AFB, Ohio 45433		10. PROGRAM ELEMENT, PROJECT, TASK AREA & WORK UNIT NUMBERS
11. CONTROLLING OFFICE NAME AND ADDRESS Expendables and Optics Branch (ASD/ENADC) Aeronautical Systems Division Wright-Patterson AFB, Ohio 45433		12. REPORT DATE December, 1977 13. NUMBER OF PAGES 108
14. MONITORING AGENCY NAME & ADDRESS(if different from Controlling Office)		15. SECURITY CLASS. (of this report) Unclassified 15a. DECLASSIFICATION/DOWNGRADING SCHEDULE

16. DISTRIBUTION STATEMENT (of this Report)

Approved for public release; distribution unlimited

17. DISTRIBUTION STATEMENT (of the abstract entered in Block 20, if different from Report)

18. SUPPLEMENTARY NOTES

Approved for public release; IAW AFR 190-17

JERRAL F. GUESS, Captain, USAF
Director of Information

19. KEY WORDS (Continue on reverse side if necessary and identify by block number)

Infrared Receiver
Infrared Background
Infrared Signal Processing
Threat Warning Receiver

20. ABSTRACT (Continue on reverse side if necessary and identify by block number)

The use of passive electro-optical sensors in military systems has received increased emphasis in recent years. In particular, passive infrared sensors could be used in an infrared airborne threat warning receiver. The performance of an optical receiver designed to detect a threat by taking advantage of the spectral signature of the threat is presented. The receiver is based upon a statistical model which represents the infrared field as a Gaussian random process whose moments depend upon the threat and

DD FORM 1 JAN 73 1473 EDITION OF 1 NOV 65 IS OBSOLETE

UNCLASSIFIED
SECURITY CLASSIFICATION OF THIS PAGE (When Data Entered)

background characteristics. The optimal Bayes/Neyman-Pearson receiver structure for an M spectral channel, N sequential look scanning receiver is presented and two practical suboptimal receiver structures are developed and compared with two ad-hoc linear processor structures.

The results indicate that the approximate suboptimal receiver structures and the two ad-hoc linear receiver structures have identical performance. The results also show that receiver performance depends upon the difference between the square roots of the hypothesis dependent mean to variance ratios and the ratio of variances, and that receiver performance improves as the number of receiver channels and/or the number of looks increase.